

**ANALYSIS AND RTDS IMPLEMENTATION OF
STATCOM FOR POWER SYSTEM STABILITY ENHANCEMENT**

BY
FAHAD SALEH MOHAMMAD AL-ISMAIL

A Thesis Presented to the
DEANSHIP OF GRADUATE STUDIES

KING FAHD UNIVERSITY OF PETROLEUM & MINERALS
DHAHRAN, SAUDI ARABIA

In Partial Fulfillment of the
Requirements for the Degree of

MASTER OF SCIENCE
In
ELECTRICAL ENGINEERING

FEBRUARY 2013

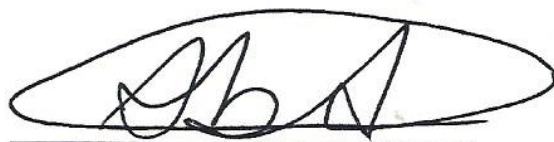
KING FAHD UNIVERSITY OF PETROLEUM AND MINERALS

DHAHRAN 31261, SAUDI ARABIA

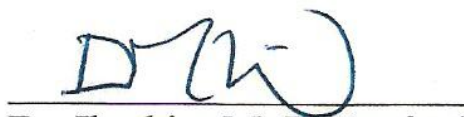
DEANSHIP OF GRADUATE STUDIES

This thesis, written by **FAHAD SALEH MOHAMMAD AL-ISMAIL** under the direction of his thesis advisor and approved by his thesis committee, has been presented to and accepted by the Dean of Graduate Studies, in partial fulfillment of the requirements for the degree of **MASTER OF SCIENCE IN ELECTRICAL ENGINEERING**.

Thesis Committee




Dr. Mohammad A. Abido (Advisor)



Dr. Ibrahim M. El-Amin (Member)



Dr. A. H. Abdur-Rahim (Member)



Dr. Ali Al-Shaikhi
Department Chairman



Dr. Salam A. Zummo
Dean of Graduate Studies



23/2/13

Date

© Fahad Saleh Mohammad AL-Ismail

December 2012

بسم الله الرحمن الرحيم

In the name of Allah, Most Beneficent, Most Merciful

قال الله تعالى:

{كُلُّ نَفْسٍ ذَائِقَةُ الْمَوْتِ وَإِنَّمَا تُوَفَّقُونَ أُجُورَكُمْ يَوْمَ الْقِيَامَةِ فَمَنْ زُحْزِحَ عَنِ النَّارِ وَأُدْخِلَ الْجَنَّةَ فَقَدْ فَازَ وَمَا الْحَيَاةُ الدُّنْيَا إِلَّا مَتَاعُ الْغُرُورِ} صدق الله العظيم

آل عمران 185

Every soul will taste of death. And ye will be paid on the Day of Resurrection only that which ye have fairly earned. Whoso is removed from the Fire and is made to enter paradise, he indeed is triumphant. The life of this world is but comfort of illusion

Al-Emran185

To the loving memory of my beloved father, Saleh Mohammad AL-Ismael, who Allah has chosen to be next to Him, who brought me up in the best ways. His wise teachings, warm feelings and continuous support were very influential on my personality and success. He always advise me to seek knowledge, and I hope that in future I would be exactly as he dreamed.

O Allah, forgive him and have mercy on him, keep him safe and sound and forgive him, honour his rest and ease his entrance; wash him with water and snow and hail, and cleanse him of sin as a white garment is cleansed of dirt. O Allah, give him a home better than his home and a family better than his family. O Allah, admit him to Paradise and protect him from the torment of the grave and the torment of Hell-fire; make his grave spacious and fill it with light.

Ameen.

To his happy soul, I dedicate this thesis.

ACKNOWLEDGMENTS

**In the name of Allah, the Most Gracious, the Most Merciful
All praise and thanks to Almighty Allah for His countless blessings**

Acknowledgement is due to King Fahd University of Petroleum & Minerals whose research facilities and continuing support make this accomplishment possible.

I would like to convey my deep thanks and appreciation to my advisor, Dr. Mohammad A. Abido, whose experience, knowledge and persistence provide me a valuable assistance to accomplish my thesis. I appreciate his patience and endurance. Dr. Abido supported me throughout my courses work, built my confidence, encouraged me to a challenging thesis topic, and guided me technically with his experience.

I would also like to thank my thesis committee members Dr. Ibrahim M. El-Amin and Dr. A. H. Abdur-Rahim for their guidance, constructive and positive feedback.

Very special thanks are due to Dr. Mohammad H. Shwehdi, for his eloquent, total support and invaluable advising.

My appreciation is extended to Dr. Mohamed Ali Hassan and Mr. Saleh Mohammad Bamasak for their involvement and for the valuable technical support they always offer.

My sincerest gratitude, special thanks and total devotion for the most dear to me:

My beloved mother, "Um-Fahad", for her love, and constant encouragement who always worried about my studies and my life conditions. Your prayers and moral support will always boot my progress.

My brother Mohammad and my sisters Munerah, Nourah, Dalal, Shimaa, Aseel, Seba and Hissah. I am always grateful to you for your kind care and your interest in my success, you really deserve my warm thanks for your encouragements and love.

My sincere love and deepest appreciation goes to:

My wife, Fatimah, without whose love, endurance, constant support, patience, care and understanding I could never have made it through these studies. Thanks for your strong emotional support which make my life pleasant even in the hardest times and more meaningful.

TABLE OF CONTENTS

ACKNOWLEDGMENTS	III
TABLE OF CONTENTS	IV
LIST OF TABLES	VII
LIST OF FIGURES	VIII
THESIS ABSTRACT	XVI
خلاصة الرسالة	XVII
CHAPTER 1 INTRODUCTION.....	1
1.1 OVERVIEW	1
1.2 MOTIVATION.....	3
1.3 THESIS OBJECTIVE	4
1.4 THESIS CONTRIBUTION	5
1.5 THESIS ORGANIZATION	6
CHAPTER 2 LITERATURE REVIEW.....	7
2.1 POWER SYSTEM STABILIZER (PSS)	7
2.2 FACTS DEVICES	11
2.2.1 First Generation FACTS Devices.....	13
2.2.1. (a) Static Var Compensator (SVC).....	13
2.2.1. (b) Thyristor-Controlled Series Capacitor (TCSC).....	16
2.2.1. (c) Thyristor-Controlled Phase Shifter (TCPS).....	18
2.2.2 Second Generation FACTS Devices:	20
2.2.2. (a) STATic synchronous COMpensator (STATCOM).....	20
2.2.2. (b) Static Synchronous Series Compensator (SSSC)	23
2.2.2. (c) Unified Power Flow Controller (UPFC).....	24
2.3 STATCOM MODELING FOR STABILITY STUDIES	27
2.4 CONTROLLING DESIGN APPROACHES USED IN STATCOM.....	29
CHAPTER 3 POWER SYSTEM MODEL.....	32
3.1 GENERATOR.....	32
3.2 EXCITER AND PSS	33
3.3 STATCOM -BASED STABILIZERS	34

6.1.4 The STATCOM Model and its Controllers.	78
CHAPTER 7	RTDS EXPERIMENTAL RESULTS81
7.1 ROTOR SPEED DEVIATION RESPONSE FOR DIFFERENT LOADING	
CONDITIONS UNDER SEVERAL DISTURBANCES.	82
7.1.1 Nominal Loading	82
7.1.2 Heavy Loading.....	84
7.1.3 Light Loading	86
7.2 GENERATOR TERMINAL VOLTAGE FOR DIFFERENT LOADING CONDITIONS	
UNDER SEVERAL DISTURBANCES	88
7.2.1 Nominal Loading	88
7.2.2 Heavy Loading.....	90
7.2.3 Light Loading	92
7.3 DC VOLTAGE FOR DIFFERENT LOADING CONDITIONS UNDER SEVERAL	
DISTURBANCES	94
7.3.1 Nominal Loading	94
7.3.2 Heavy Loading.....	96
7.3.3 Light Loading	98
7.4 GENERATOR POWER FOR DIFFERENT LOADING CONDITIONS UNDER	
SEVERAL DISTURBANCES.....	100
7.4.1 Nominal Loading	100
7.4.2 Heavy Loading.....	102
7.4.3 Light Loading	104
7.5 COMPARISON BETWEEN SIMULATED AND RTDS IMPLEMENTED RESULTS	
.....	106
CHAPTER 8	CONCLUSION111
8.1 CONCLUSION.....	111
8.2 FUTURE WORK	112
APPENDICES	114
BIBLIOGRAPHY	130
LIST OF PUBLICATIONS	145
VITAE	146

LIST OF TABLES

Table 1 Partial list of a utility scaled STATCOM.	28
Table 2 Optimal Parameter Settings of C-Based & Φ -Based for Individual and Coordinated Design at Nominal Loading.....	51
Table 3 System's eigenvalues of nominal loading condition, for C -based and Φ -based stabilizers, individual and coordinated design.....	52
Table 4 Optimal Parameter Settings of C-Based & Φ -Based for Individual and Coordinated Design at Heavy Loading.	54
Table 5 System eigenvalues of heavy loading condition, for C -based and Φ -based stabilizers, individual and coordinated design.	54
Table 6 Optimal parameter settings of C-based & Φ -based for individual and coordinated design at light loading.	56
Table 7 System eigenvalues of light loading condition, for C -based and Φ -based stabilizers, individual and coordinated design.	56
Table 8 The Generator General Model Configuration.....	128
Table 9 IEEE Type st1 Excitation System Model Data.....	128
Table 10 Transmission Line Parameters Data.	129
Table 11 The STATCOM Rating.	129

LIST OF FIGURES

Fig. 2-1 Classification of flexible AC transmission system (FACTS).	13
Fig. 2-2 SVC Configuration.....	16
Fig. 2-3 Transmission line with a TCSC Configuration.	16
Fig. 2-4 Schematic diagram of TCPS.	18
Fig. 2-5 Schematic diagram of SSSC.	23
Fig. 2-6 Schematic diagram of UPFC.....	25
Fig. 3-1 Single machine infinite bus system with a STATCOM.....	32
Fig. 3-2 IEEE Type-ST1 excitation system with a Lead-Lag PSS.....	34
Fig. 3-3 STATCOM PI controller for AC voltage with a lead-lag damping controller.	36
Fig. 3-4 STATCOM PI controller for DC voltage with a lead-lag damping controller.	36
Fig. 4-1 Minimum singular value with STATCOM stabilizer at $Q = -0.4$ pu for different input signals "C & Φ ".	42
Fig. 4-2 Minimum singular value with STATCOM stabilizer at $Q = 0$ pu for different input signals "C & Φ ".	42
Fig. 4-3 Minimum singular value with STATCOM stabilizer at $Q = +0.4$ pu for different input signals "C & Φ ".	43
Fig. 4-4 Crossover operation procedure.....	47
Fig. 4-5 Differential Evolution flowchart.	49
Fig. 5-1 Convergence of objective function in nominal loading condition for different controllers approaches.	51
Fig. 5-2 Convergence of objective function in heavy loading condition for different controllers approaches.	53
Fig. 5-3 Convergence of objective function in light loading condition for different controllers approaches.	55
Fig. 5-4 Rotor angle response for 6-cycle fault with nominal loading C & Φ , individual and coordinated design.	58
Fig. 5-5 Rotor speed response for 6-cycle fault with nominal loading C & Φ , individual and coordinated design.	58
Fig. 5-6 DC voltage response for 6-cycle fault with nominal loading C & Φ , individual and coordinated design.	59
Fig. 5-7 VSC angle response for 6-cycle fault with nominal loading C & Φ , individual and coordinated design.	59
Fig. 5-8 VSC magnitude response for 6-cycle fault with nominal loading C & Φ , individual and coordinated design.	60
Fig. 5-9 Generator power response for 6-cycle fault with nominal loading C & Φ , individual and coordinated design.	60
Fig. 5-10 Generator terminal voltage response for 6-cycle fault with nominal loading C & Φ , individual and coordinated design.	61

Fig. 5-11 STATCOM bus voltage response for 6-cycle fault with nominal loading C & Φ , individual and coordinated design.	61
Fig. 5-12 Rotor angle response for 6-cycle fault with heavy loading C & Φ , individual and coordinated design.	62
Fig. 5-13 Rotor speed response for 6-cycle fault with heavy loading C & Φ , individual and coordinated design.	63
Fig. 5-14 DC voltage response for 6-cycle fault with heavy loading C & Φ , individual and coordinated design.	63
Fig. 5-15 VSC angle response for 6-cycle fault with heavy loading C & Φ , individual and coordinated design.	64
Fig. 5-16 VSC magnitude response for 6-cycle fault with heavy loading C & Φ , individual and coordinated design.	64
Fig. 5-17 Generator power response for 6-cycle fault with heavy loading C & Φ , individual and coordinated design.	65
Fig. 5-18 Generator terminal voltage response for 6-cycle fault with heavy loading C & Φ , individual and coordinated design.	65
Fig. 5-19 STATCOM bus voltage response for 6-cycle fault with heavy loading C & Φ , individual and coordinated design.	66
Fig. 5-20 Rotor angle response for 6-cycle fault with light loading C & Φ , individual and coordinated design.	67
Fig. 5-21 Rotor speed response for 6-cycle fault with light loading C & Φ , individual and coordinated design.	68
Fig. 5-22 DC voltage response for 6-cycle fault with light loading C & Φ , individual and coordinated design.	68
Fig. 5-23 VSC angle response for 6-cycle fault with light loading C & Φ , individual and coordinated design.	69
Fig. 5-24 VSC magnitude response for 6-cycle fault with light loading C & Φ , individual and coordinated design.	69
Fig. 5-25 Generator power response for 6-cycle fault with heavy loading C & Φ , individual and coordinated design.	70
Fig. 5-26 Generator terminal voltage response for 6-cycle fault with light loading C & Φ , individual and coordinated design.	70
Fig. 5-27 STATCOM bus voltage response for 6-cycle fault with light loading C & Φ , individual and coordinated design.	71
Fig. 6-1 Schematic diagram of single machine infinite bus system with STATCOM.	75
Fig. 6-2 Synchronous machine model with transformer in RSCAD.	76
Fig. 6-3 IEEE Type ST1 Excitation System Model.	77
Fig. 6-4 The system's transmission line diagram.	77
Fig. 6-5 Modeling of STATCOM with its VSC in Small Time Step including pulse and triangle wave generators.	78
Fig. 6-6 The STATCOM Voltage and Current Regulation Controller.	79
Fig. 6-7 Phase Locked Loop (PLL) block model.	79

Fig. 6-8 Modulating Signal Generation - DQ to ABC transformation of the STATCOM bus voltage signals in RTDS.	80
Fig. 7-1 Rotor speed response for 1- Φ fault - nominal loading.	82
Fig. 7-2 Rotor speed response for 2- Φ fault - nominal loading.	83
Fig. 7-3 Rotor speed response for 3- Φ fault - nominal loading.	83
Fig. 7-4 Rotor speed response for 1- Φ fault - heavy loading.	84
Fig. 7-5 Rotor speed response for 2- Φ fault - heavy loading.	85
Fig. 7-6 Rotor speed response for 3- Φ fault - heavy loading.	85
Fig. 7-7 Rotor speed response for 1- Φ fault - light loading.	86
Fig. 7-8 Rotor speed response for 2- Φ fault - light loading.	87
Fig. 7-9 Rotor speed response for 3- Φ fault - light loading.	87
Fig. 7-10 Generator terminal voltage response for 1- Φ fault - nominal loading.	88
Fig. 7-11 Generator terminal voltage response for 2- Φ fault - nominal loading.	89
Fig. 7-12 Generator terminal voltage response for 3- Φ fault - nominal loading.	89
Fig. 7-13 Generator terminal voltage response for 1- Φ fault - heavy loading.	90
Fig. 7-14 Generator terminal voltage response for 2- Φ fault - heavy loading.	91
Fig. 7-15 Generator terminal voltage response for 3- Φ fault - heavy loading.	91
Fig. 7-16 Generator terminal voltage response for 1- Φ fault - light loading.	92
Fig. 7-17 Generator terminal voltage response for 2- Φ fault - light loading.	93
Fig. 7-18 Generator terminal voltage response for 3- Φ fault - light loading.	93
Fig. 7-19 DC voltage response for 1- Φ fault - nominal loading.	94
Fig. 7-20 DC voltage response for 2- Φ fault - nominal loading.	95
Fig. 7-21 DC voltage response for 3- Φ fault - nominal loading.	95
Fig. 7-22 DC voltage response for 1- Φ fault - heavy loading.	96
Fig. 7-23 DC voltage response for 2- Φ fault - heavy loading.	97
Fig. 7-24 DC voltage response for 3- Φ fault - heavy loading.	97
Fig. 7-25 DC voltage response for 1- Φ fault - light loading.	98
Fig. 7-26 DC voltage response for 2- Φ fault - light loading.	99
Fig. 7-27 DC voltage response for 3- Φ fault - light loading.	99
Fig. 7-28 Generator power response for 1- Φ fault - nominal loading.	100
Fig. 7-29 Generator power response for 2- Φ fault - nominal loading.	101
Fig. 7-30 Generator power response for 3- Φ fault - nominal loading.	101
Fig. 7-31 Generator power response for 1- Φ fault - heavy loading.	102
Fig. 7-32 Generator power response for 2- Φ fault - heavy loading.	103
Fig. 7-33 Generator power response for 3- Φ fault - heavy loading.	103
Fig. 7-34 Generator power response for 1- Φ fault - light loading.	104
Fig. 7-35 Generator power response for 2- Φ fault - light loading.	105
Fig. 7-36 Generator power response for 3- Φ fault - light loading.	105
Fig. 7-37 Comparison between simulated and RTDS implemented results due to 6-cycle fault in a c-based controller designed system - Nominal Loading.	106
Fig. 7-38 Comparison between simulated and RTDS implemented results due to 6-cycle fault in a C-based controller designed system - Heavy Loading.	107

Fig. 7-39 Comparison between simulated and RTDS implemented results due to 6-cycle fault in a C-based controller designed system - Light Loading.	107
Fig. 7-40 Comparison between simulated and RTDS implemented results due to 6-cycle fault in a Φ -based controller designed system - Nominal Loading.....	108
Fig. 7-41 Comparison between simulated and RTDS implemented results due to 6-cycle fault in a Φ -based controller designed system - Heavy Loading.	108
Fig. 7-42 Comparison between simulated and RTDS implemented results due to 6-cycle fault in a Φ -based controller designed system - Light Loading.	109
Fig. 7-43 Comparison between simulated and RTDS implemented results due to 6-cycle fault in a Φ &C Coordinated-based controller designed system - Nominal Loading.	109
Fig. 7-44 Comparison between simulated and RTDS implemented results due to 6-cycle fault in a Φ &C Coordinated-based controller designed system - Heavy Loading.....	110
Fig. 7-45 Comparison between simulated and RTDS implemented results due to 6-cycle fault in a Φ &C Coordinated-based controller designed system - Light Loading.	110

NOMENCLATURE

Abbreviations

<i>SMIB</i>	Single machine infinite bus
<i>FACTS</i>	Flexible AC transmission systems
<i>STATCOM</i>	Static synchronous compensators
<i>VSC</i>	Voltage source converter
<i>PWM</i>	Pulse width modulation
<i>GPC</i>	Gigabyte processing card
<i>PSS</i>	Power system stabilizer
<i>CPSS</i>	Conventional power system stabilizer
<i>PI-PSS</i>	Proportional-integral power system stabilizer
<i>PID-PSS</i>	Proportional integral derivative power system stabilizer
<i>EPRI</i>	The Electric Power Research Institute
<i>SVC</i>	Static Var compensator
<i>TCSC</i>	Thyristor-controlled series capacitor
<i>TCPS</i>	Thyristor-controlled phase shifter
<i>SSSC</i>	Static synchronous series compensator
<i>UPFC</i>	Unified power flow controller
<i>IPFC</i>	Interline power flow controller
<i>SPS</i>	Static phase shifter
<i>QFT</i>	quantitative feedback theory
<i>LMI</i>	Linear matrix inequalities

<i>IGCT</i>	Integrated Gate-Commutated Thyristor
<i>GTO</i>	Gate turn-off
<i>ANFIS</i>	adaptive fuzzy inference system
<i>POD</i>	power oscillations damping
<i>GA</i>	Genetic Algorithm
<i>PSO</i>	Particle swarm optimizer
<i>SVD</i>	Singular value decomposition
<i>pu</i>	Per unit
<i>Pf</i>	Power factor
<i>DE</i>	Differential Evolution
<i>CCT</i>	Critical clearing time
<i>RTDS</i>	Real Time Digital Simulation
<i>HVDC</i>	High voltage direct current
<i>DSP</i>	Digital signal processors
<i>IRC</i>	Inter rack communication
<i>WIF</i>	Workstation inter face
<i>3PC</i>	Triple processor card
<i>GPC</i>	Giga processor card
<i>TPC</i>	Tandem processor card
<i>THD</i>	Total harmonic distortion
<i>CHIL</i>	Control hardware in loop

Symbols

Y_L	Load impedance
g, b	Load Inductance and susceptance
Z_1, X_1, R_1	Transmission line first section impedance, reactance, and resistance
Z_2, X_2, R_2	Transmission second section line impedance, reactance, and resistance
P_m, P_e	Mechanical input power and electrical output power of the generator
M, H	Machine inertia coefficient and inertia constant
D	Machine damping coefficient
i_d, i_q	d- and q-axis armature current
V_d, V_q	d- and q-axis terminal voltage
T'_{do}	Open-circuit field time constant
x_d, x'_d	d-axis reactance and d-axis transient reactances
x_q, x'_q	Generator q-axis reactance
v or V	Generator terminal voltage
E_q, E_{fd}	Generator internal and field voltages
V^{ref}	Reference voltage
V_b	Infinite bus voltage
K_A, T_A	Gain and time constant of the excitation system
u_{PSS}	PSS control signal
V_m	STATCOM bus voltage

x_t	STATCOM transformer reactance
i_{sd} , i_{sq}	d- and q-axis of the STATCOM current
J	Objective functions

Greek Symbols

δ	Rotor angle
ω	Rotor speed
ω_b	Synchronous speed
Φ	Thyristor firing angle
ζ	Damping ratio
σ	Damping factor

THESIS ABSTRACT

Name FAHAD SALEH MOHAMMED AL-ISMAIL
Title ANALYSIS AND RTDS IMPLEMENTATION OF
STATCOM FOR POWER SYSTEM STABILITY
ENHANCEMENT
Degree MASTER OF SCIENCE
Major Field ELECTRICAL ENGINEERING
Date of Degree DECEMBER

The objective of this thesis is to design, analyze and implement a STATCOM based stabilizers to enhance damping of low frequency oscillations. The effectiveness of STATCOM gain and phase modulation channels to enhance the damping characteristics is investigated. The coordination among the internal AC and DC voltage controllers and the proposed damping controllers on each channel is designed. Differential Evolution as an intelligent optimization technique is considered to design the STATCOM supplementary damping controllers. The implementation of STATCOM based stabilizers on Real Time Digital Simulator (RTDS) is carried out. The RTDS experimental setup of a power system with STATCOM is verified. The power system considered is tested through nonlinear time domain simulations to examine the validity of the proposed approach to damp low frequency oscillations. Comparisons with similar results reported in literature are demonstrated.

Keywords: Power System Stabilizer, PSS, FACTS, STATCOM, DE, RTDS.

MASTER OF SCIENCE DEGREE

KING FAHD UNIVERSITY OF PETROLEUM & MINERALS, DHAHRAN

DECEMBER 2012

خلاصة الرسالة

الاسم	فهد صالح محمد السماعيل
عنوان الرسالة	تحليل و تطبيق جهاز STATCOM في جهاز المحاكاة الرقمي في الوقت الحقيقي لرفع كفاءة ثبات نظام القوى الكهربائية
الدرجة	الماجستير في العلوم
التخصص	الهندسة الكهربائية
تاريخ التخرج	ديسمبر 2012م

يهدف هذا البحث إلى تصميم و تحليل و دراسة كفاءة أنظمة التحكم المتزامن لمضبط شبكة الطاقة الكهربائية مع المضبطات المستندة على جهاز STATCOM لغرض تحسين إهتزازات نظام الطاقة. و يدرس البحث نظام طاقة مجهز بجهاز STATCOM و يصنف هذا الجهاز على أنه من الجيل الثاني للأنظمة المرنة لنقل التيار المتردد. كذلك يدرس البحث جدوى إستخدام عدة مصادر للإشارات المستخدمة في التحكم بالنظام المقترح كلا على حدة أو من خلال الدمج بينهما للحصول على النتائج المرجوة. لتقدير مدى قدرة هذه المضبطات المختلفة على زيادة خمد الإهتزازات الكهروميكانيكية, يتم تطبيق طريقة تحليل القيم المنفردة. كما صيغة مسألة تصميم المضبطات بشكل مسألة الحل الأمثل. بحيث تستخدم طريقة التطور التفاضلي للبحث عن أفضل قيم لمكونات كل مضبط بشكل متزامن. للتحقق من كفاءة التصميم المقترح يجرى المحاكاة الزمنية اللاخطية لإشارات الشبكة و كذلك عن طريق التجربة العملية بإستخدام جهاز المحاكاة الرقمية في الوقت الحقيقي.

درجة الماجستير في العلوم

جامعة الملك فهد للبترول و المعادن، الظهران

ديسمبر 2012

CHAPTER 1 INTRODUCTION

1.1 Overview

Over the last few years, power transmission systems have expanded in size and complexity with a huge number of interconnections, thousands of substations and hundreds of generators[1]. Moreover, the role of long distance and large power transmission lines become more important due to the continuing increasing in the electrical power demand, even though, the constructions of new transmission lines are becoming so critical in term of power system stability. Recently, great accomplishments have been achieved in terms of power electronics technologies which encouraged the inventions of more efficient power systems. The main reason is the ability of power electronics devices to deal with power system dynamics and control power flow in transmission lines.

On the basis of the above background, many flexible ac transmission system (FACTS) technologies have been developed[2]. Furthermore, as a typical FACTS device, static synchronous compensators (STATCOM) have been developed and put into operation to enhance the system robustness and to improve its operation .

Several distinct models have been proposed to represent STATCOM in static and dynamic analysis. In[3], STATCOM is modeled as parallel connected current source; where in the controllable parameter is assumed to be current magnitude. In[4] the STATCOM model is suitable to study the performance of STATCOM under unbalanced distorted system voltage. Different models for transient stability and steady state stability analysis of the power system with STATCOM are presented in [5]. However, the models were based on the assumptions that

voltages and currents are sinusoidal, balanced and operate near fundamental frequency, hence could not be applied to systems under the impact of large disturbance that have voltage and/or current with high harmonic content. A comparative study is carried out for dynamic operation of different models of STATCOM and their performance[6].

New developments in the Real Time Digital Simulator (RTDS®) Simulator with particular focus on the simulation of multilevel VSCs using PWM control are presented in [7]. The work conducted clearly shows that the RTDS Simulator can be relied upon to accurately test VSC firing pulse controls using PWM frequencies in the range of 1500 Hz. The RTDS main network is solved with a typical time-step size of about 50 μ s. Recently, RTDS added the capability of simulating power electronic switches used in Voltage Source Converters (VSC) on GPC (Gigabyte Processing Card) with significantly smaller time steps from 1.4 to 2.5 μ s. In [8], the author proposes a third order dynamic model of the power system to incorporate STATCOM in the system to study its damping properties.

Validating a five-level STATCOM model implemented in the RTDS small time-step environment is presented in [9]. A simulation performed on the RTDS hardware is controlled from RSCAD/Runtime [10]. A technique explored by Hui and Christopoulos, whereby the Dommel network conductance does not need to be decomposed or inverted during the simulation, was implemented [11][12]. K. L. Lian presented a method based on Time Averaging to simulate the voltage source converter in RTDS [13] .

In this thesis, the synchronous machine model, STATCOM based stabilizer model with its control scheme is presented. STATCOM is implemented on RTDS. The modeling of STATCOM is done in small time-step, which could be used any power hardware-in-loop test. Simulation

studies are carried out with the RTDS simulation. The dynamic behavior of the system was obtained for fault disturbance.

1.2 Motivation

STATCOM has been developed and put into operation to maintain voltage and to improve the power swing damping by the auxiliary control which will control the real and reactive power goes in and out of the STATCOM. In other words, a STATCOM can be used to enhance the power quality provided to consumers by decreasing voltage flicker and mitigate small voltage sags. Also, it has been shown that a STATCOM with a new controller can be used to handle unbalanced voltages in distribution power systems [14].

As an example of insertion of STATCOM into a power system, a STATCOM is currently installed at Inuyama in Japan and the Sullivan Substation of the Tennessee Valley Authority (TVA) for transmission line compensation[15]. The active power injection/absorption control function has better performance for the power swing damping and can improve the transient stability. But STATCOM itself cannot control the active power injection/absorption to power system. A STATCOM with energy storage system can control both the reactive and the active power injection/absorption, thus providing more flexible power system operation [16]. In a nutshell, STATCOM became very useful solution for several problems that are being faced by both the utility as well as the industries, its advantages could be summarized as follow:

- Maintain voltage level within the acceptable range.
- Improve the transient stability of the power system by enhancing the power swing damping using reactive and active power control.

- Increasing power transfer capability.
- Power factor correction.
- Unsymmetrical load balancing.
- Minimizing line losses.

1.3 Thesis Objective

The objective of this thesis is to analyze and to implement in real time the STATCOM based stabilizer for power system stability enhancement. This study includes coordination design between PSS and STATCOM-based controllers. The procedure to achieve the thesis objective is as follows:

1. For a the system equipped with PSS and STATCOM the linearized models were developed.
2. Singular Value Decomposition (SVD) analysis is employed as a controllability measure of the different control signals on the system.
3. The design problem of PSS and STATCOM controllers are formulated as an optimization problem to search for optimal controller's parameters by maximizes the minimum damping ratio of all complex eigenvalues.
4. Eigenvalue analysis is carried out to assess the effectiveness of the proposed stabilizers on enhancing the EM mode stability.
5. Coordination design of PSS and STATCOM controllers is carried out by considering more than one stabilizer in the design process.
6. The design process is extended to make the controller robust by considering a wide range of operation conditions during the design.

7. The eigenvalue analysis and the nonlinear time-domain simulation used throughout the thesis to certify the effectiveness of the proposed controllers. The controllers are simulated and experimentally tested under different operating conditions to examine the impact of the proposed scheme on the power system stability.

1.4 Thesis Contribution

To solve the problem described in the previous section, the thesis introduces a novel approach to design a STATCOM based stabilizer controller by making the following contributions:

1. Modeling and simulation of a power system equipped with an optimally designed power system stabilizer.
2. Integrate the power system model and the STATCOM model.
3. Develop and implement differential evolution algorithm (DE) for STATCOM based stabilizer controller design.
4. Build the experimental setup using RTDS.
5. Implement the proposed control strategy on RTDS.
6. Validate the simulation results with the experimental ones.

1.5 Thesis Organization

This thesis is organized as follows: in Chapter 2, introduction and basic operating principles of FACTS devices and mainly STATCOM are introduced with their power oscillation damping (POD) controller structure.

Chapter 3 concentrates on the power system linear and non-linear models of a SMIB system model equipped with PSS, and STATCOM.

Chapter 4 presents the proposed approaches which are used in the controllers design process. These approaches or tools are differential evolution algorithm, controllability measurement using singular value decomposition (SVD) and modal analysis. Furthermore, the problem formulation is outlined in this chapter.

The eigenvalue analysis and nonlinear simulation of a SMIB equipped with STATCOM are presented in chapter 5.

Chapter 6 demonstrates the RTDS experimental implementation, whereas the results for proposed approach are in Chapter 7. Conclusions and future work are discussed in chapter 8.

CHAPTER 2 Literature Review

This chapter presents a comprehensive literature research on PSS and FACTS devices. its modeling, applications and their ability to damp low frequency oscillations are demonstrated. Furthermore, the approaches which are used to control these devices are illustrated and a brief comparison between their performance and characteristics are verified.

2.1 Power System Stabilizer (PSS)

Large electric power systems are complex nonlinear systems and often exhibit low frequency electromechanical oscillations due to insufficient damping caused by adverse operating. These oscillations with small magnitude and low frequency often persist for long periods of time and in some cases they even present limitations on power transfer capability [17]. In analyzing and controlling the power system's stability, two distinct types of system oscillations are recognized. One is associated with generators at a generating station swinging with respect to the rest of the power system. Such oscillations are referred to as "intra-area mode" oscillations. The second type is associated with swinging of many machines in an area of the system against machines in other areas. This is referred to as "inter-area mode" oscillations. Power system stabilizers (PSS) are used to generate supplementary control signals for the excitation system in order to damp both types of oscillations.

PSS was proposed in the 1950's to damp low-frequency oscillations. It is known now as the conventional PSS (CPSS) and it is based on the linear model of the power system at some operating point. It typically consists of a reset block and a phase compensator, usually a lead-lag

block. The reset block is designed as a high pass filter so that the PSS is functional only if the input signal has a transient change.

The desired damping ratio can be achieved by tuning this compensator's phase and gain based on a linearized model of the power system [18][19]. Rotor speed is often used as an input signal for PSS. As the rotor speed deviates from its synchronous speed, PSS introduces a damping electrical torque in this rotor to offset this change[20].

CPSS works well if the system is operating within a certain range of operating conditions. However, power systems operate over a wide range and random load variations affect their performance. Therefore, CPSS parameters need to be retuned manually to different values at different operating conditions.

An adaptive PSS, anticipated in [21] simplifies tuning procedure using a self-optimizing pole shifting control strategy. Gain-scheduled control is used to set PSS parameters at a number of operating points and then interpolate these parameters between the operating points. PSS parameters were also optimized using intelligent techniques such as genetic algorithm[22], evolutionary programming [23], simulated annealing [24] and particle swarm optimization [25]. These optimization techniques are model-based since they need the power system mathematical model. Frequency-domain analysis, such as eigenvalue analysis, is usually used in the case of linearized systems. A nonlinear approach based on synergetic control theory was presented in [26] to design PSS. It uses simplified nonlinear model of the power system to decrease computation time.

Kundur et al. in [27] have presented a comprehensive analysis of the effects of the different CPSS parameters on the overall dynamic performance of the power system. It is shown that the appropriate selection of CPSS parameters results in satisfactory performance during system

upsets. In addition, Gibbard [28] demonstrated that the CPSS provide satisfactory damping performance over a wide range of system loading conditions. Robust design of CPSSs in multi machine power systems using genetic algorithm is presented in [29] where several loading conditions are considered in the design process. Although PSSs provide supplementary feedback stabilizing signals, they suffer a drawback of being liable to cause great variations in the voltage profile and they may even result in leading power factor operation under severe disturbances.

DeMello and Concordia in 1969 [30] presented the concepts of synchronous machine stability as affected by excitation control. They established an understanding of the stabilizing requirements for static excitation systems. Their work developed insights into effects of excitation systems and requirement of supplementary stabilizing action for such systems based on the concept of damping and synchronizing torques.

Klein et al. in [31][32] presented the simulation studies into the effects of stabilizers on inter-area and local modes of oscillations in interconnected power systems. It was shown that the PSS location and the voltage characteristics of the system loads are significant factor in the ability of a PSS to increase the damping of inter-area oscillations. Nowadays, the conventional lead-lag power system stabilizer is widely used by the power system utility [33].

Other types of PSS such as proportional-integral power system stabilizer (PI-PSS) and proportional-integral-derivative power system stabilizer (PID-PSS) have also been proposed [34][35].

Although, power system stabilizers have been extensively used to increase the system damping for low frequency oscillations. However, there have been problems experienced with PSS over the years of operation. Some of these were due to the limited capability of PSS, in damping only local and not inter-area modes of oscillations. In addition, PSS can cause great variations in the

voltage profile under severe disturbances and it may even results in leading power factor operation and losing system stability [36]. This situation has necessitated a review of the traditional power system concepts and practices to achieve a larger stability margin, greater operating flexibility, and better utilization of existing power systems.

2.2 FACTS Devices

Series capacitor, shunt capacitor, and phase shifter are different approaches to increase the power system load ability. In past decades, all these devices were controlled mechanically and were, therefore, relatively slow. They are very useful in a steady state operation of power systems but from a dynamical point of view, their time response is too slow to effectively damp transient oscillations. If mechanically controlled systems were made to respond faster, power system security would be significantly improved, allowing the full utilization of system capability while maintaining adequate levels of stability. This concept and advances in the field of power electronics led to a new approach introduced by the Electric Power Research Institute (EPRI) in the late 1980. Called Flexible AC Transmission Systems or simply FACTS. Generally, the main objectives of FACTS are to increase the useable transmission capacity of lines and control power flow over designated transmission routes[37].

Hingorani and Gyugyi [37] and Hingorani [38][39] proposed the concept of FACTS. Edris in [40] proposed terms and definitions for different FACTS controllers. Flexible AC Transmission System (FACTS) is an alternating current transmission system incorporating power electronic-based and other static controllers to enhance controllability and increase power transfer capability [37]. FACTS devices have become very important applications of power electronics in controlling power flow by controlling any of the AC transmission system parameters, that are voltage magnitude, phase and load impedance [41].

FACTS devices were the solution to the difficulties arising with the geographically irregular growing power demand. FACTS met the transmission system requirement to use the existing power facilities without decreasing system availability and security. In addition, the use of FACTS provides voltage support to prevent voltage collapses when the electricity network is

under heavy loading. The main objectives of FACTS are to increase transmission capacity of lines and to control the power flow over chosen transmission routes [42]. As supplementary functions, damping the inter-area modes and enhancing power system stability using FACTS controllers have been extensively studied and investigated. Generally, it is not cost-effective to install FACTS devices for the sole purpose of power system stability enhancement.

A FACT offers the possibility of meeting many recent power demands. FACTS devices are routinely employed in order to enhance the power transfer capability of the otherwise under-utilized parts of the interconnected network [43]. To install FACTS devices in realistic system, it is necessary to study the power network to choose the best locations for them for power stability improvement and voltage regulation during dynamic disturbances [44].

There are two generations for realization of power electronics-based FACTS controllers: the first generation employs conventional thyristor-switched capacitors and reactors, and quadrature tap-changing transformers, the second generation employs gate turn-off (GTO) thyristor-switched converters as voltage source converters (VSC). The first generation has resulted in the Static Var Compensator (SVC), the Thyristor- Controlled Series Capacitor (TCSC), and the Thyristor- Controlled Phase Shifter (TCPS) [45]. The second generation has produced the Static Synchronous Compensator (STATCOM), the Static Synchronous Series Compensator (SSSC), the Unified Power Flow Controller (UPFC), and the Interline Power Flow Controller (IPFC) [46]. The two groups of FACTS controllers have distinctly different operating and performance characteristics.

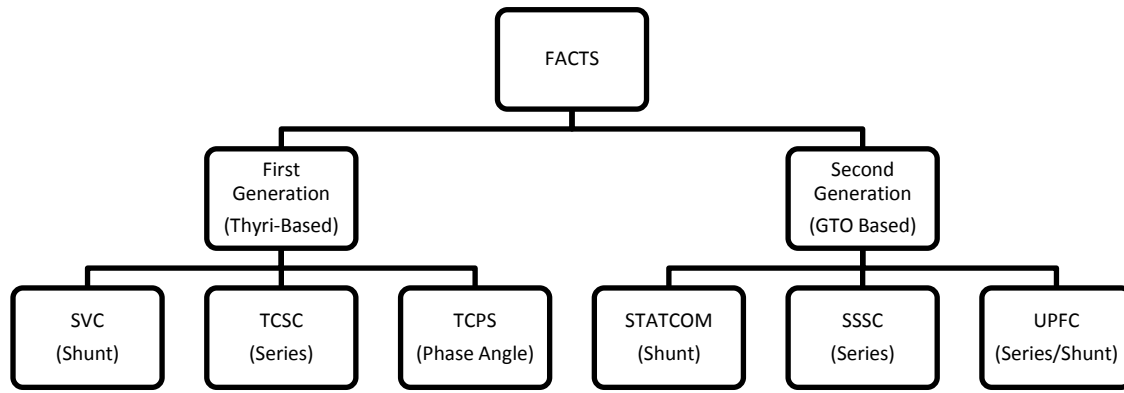


Fig. 2-1 Classification of flexible AC transmission system (FACTS).

2.2.1 First Generation FACTS Devices

Developments in the field of high voltage power electronics have made possible the practical realization of FACTS controllers. By the 1970s, the voltage and current rating of Thyristor had been increased significantly making them suitable for applications in high voltage power systems [38][47]. This made construction of modern Static Var Compensators (SVC), Thyristor Controlled/Switched Series Capacitors (TCSC/TSSC), and Thyristor Controlled Phase Shifter Regulators (TCPS). A fundamental feature of the thyristor based switching controllers is that the speed of response of passive power system components such as a capacitor or a reactor is enhanced, but their compensation capacity is still solely determined by the size of the reactive component.

2.2.1. (a) Static Var Compensator (SVC)

Hammad [48] presented a fundamental analysis of the application of SVC for enhancing the power systems stability. Then, the low frequency oscillation damping enhancement via SVC has been analyzed [49][50]. It is shown that the SVC enhances the system damping of local as well as inter area oscillation modes. Self-tuning and model reference adaptive stabilizers for SVC control have been also proposed and designed [51][52]. Robust SVC controllers based on H_∞ , structured singular value μ , and quantitative feedback theory QFT has been presented to enhance

system damping [53][54]. However, the importance and difficulties in the selection of weighting functions of H_∞ optimization problem have been reported. In addition, the additive and/or multiplicative uncertainty representation cannot treat situations where a nominal stable system becomes unstable after being perturbed [55].

Moreover, the pole-zero cancellation phenomenon associated with this approach produces closed loop poles whose damping is directly dependent on the open loop system (nominal system) [56]. Genetic algorithms and fuzzy logic based approaches have been proposed for SVC control [57][58][52][59][60][61][62][63]. The superiority of these approaches over the conventional methods is confirmed through time domain simulations.

Messina and Barocio [64] studied the nonlinear modal interaction in stressed power systems with multiple SVC voltage support. It was observed that SVC controls can significantly influence nonlinear system behavior especially under high-stress operating conditions and increased SVC gains.

Wang and Swift [65] developed a novel unified Phillips-Heffron model for a power system equipped with a SVC, a TCSC and a TCPS. Several approaches based on modern control theory have been applied to TCSC controller design [66][67][68][69][70][71][72][73][74]. Chen et al. [68] presented a state feedback controller for TCSC by using a pole placement technique.

Chang and Chow [69] developed a time optimal control strategy for the TCSC where a performance index of time was minimized. A fuzzy logic controller for a TCSC was proposed in [70]. Heuristic optimization techniques have been implemented to search for the optimum TCSC based stabilizer parameters for the purpose of enhancing SMIB system stability [71][72][73].

In addition, different control scheme for a TCSC were proposed such as variable structure controller [74], bilinear generalized predictive controller [75], and H_∞ -based controller [76]. A considerable attention has been directed to realization of various TCPS schemes [77].

Baker et al. [78] developed a control algorithm for SPS using stochastic optimal control theory. Edris [79] proposed a simple control algorithm based on equal area criterion. Furthermore, Jiang et al. [80] proposed an SPS control technique based on nonlinear variable structure control theory. In the literature, SVCs have been applied successfully to improve the transient stability of a synchronous machine [81].

Wang and Swift [50] used damping torque coefficients approach to investigate the SVC damping control of a SMIB system on the basis of Phillips-Heffron model. It was shown that the SVC damping control provides the power system with negative damping when it operates at a lower load condition than the dead point, the point at which SVC control produces zero damping effect. Robust SVC controllers based on H_∞ , structured singular value μ , and quantitative feedback theory QFT also have been presented to enhance system damping [49][82][50][83][84].

M. Noroozian et al. [85][86][87] examined the enhancement of multi-machine power system stability by use TCSCs and SVCs. SVC was found to be more effective for controlling power swings at higher levels of power transfer; when it design to damp the inter-area modes, it might excite the local modes, and its damping effect dependent on load characteristics. While TCSC is not sensitive to the load characteristic and when it is designed to damp the inter-area modes, it does not excite the local modes.

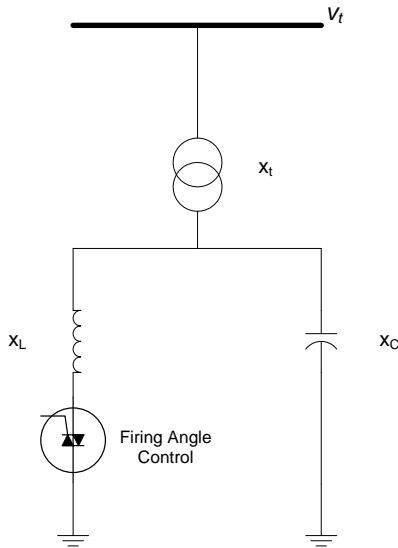


Fig. 2-2 SVC Configuration.

2.2.1. (b) Thyristor-Controlled Series Capacitor (TCSC)

Thyristor-Controlled Series Compensator (TCSC) is a line impedance controller. It can be used to damp oscillations. It uses thyristor-switched capacitors or a fixed capacitor with a parallel thyristor-controlled reactor as shown in Fig. 2-3. In the first case, the number of series capacitor banks is varied by turning their thyristor switches on and off to obtain the degree of series compensation needed. In the second case, the current in the reactor is adjusted to reach the desired degree of series compensation. TCSC can be very effective in preventing loop flows of power.

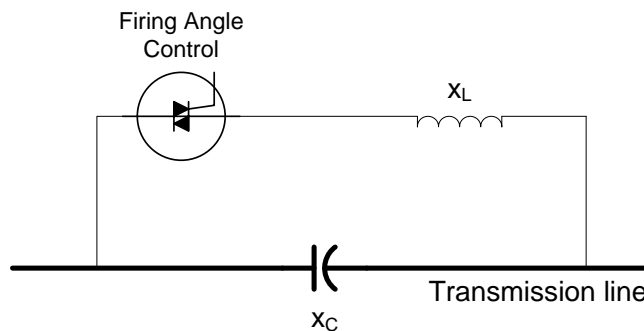


Fig. 2-3 Transmission line with a TCSC Configuration.

Chen et al. [68] presented a state feedback controller for TCSC by using a pole placement technique. However, the controller requires all system states which reduces its applicability. Chang and Chow [69] developed a time optimal control strategy for the TCSC where a performance index of time was minimized.

A fuzzy logic controller for a TCSC was proposed in [70]. The impedance of the TCSC was adjusted based on machine rotor angle and the magnitude of the speed deviation. In addition, different control schemes for a TCSC were proposed such as variable structure controller [74][88], bilinear generalized predictive controller [75], and H_∞ -based controller [76]. The neural networks [89] have been proposed for TCSC-based stabilizer design. The parameters of the stabilizers are determined by genetic algorithm (GA) [90]. The damping characteristics of the designed stabilizers have been demonstrated through simulation results on a multi-machine power system.

Wang et al.[71] presented a robust nonlinear coordinated control approach to excitation and TCSC for transient stability enhancement. The excitation controller and TCSC controller have been designed separately using a direct feedback linearization technique. Lee and Moon [91] presented a hybrid linearization method in which the algebraic and the numerical linearization technique were combined.

Sidhartha Panda [92] presented the modeling and optimizing the parameters for a TCSC controller for transient stability improvement of a multi-machine power system. First, the location of the TCSC controller is obtained from the point of view of transient stability improvement. Then, a simple transfer function model of TCSC controller for stability improvement is developed and the parameters of the proposed controller are optimally tuned. The minimization of the rotor angle deviation following a severe disturbance is formulated as an

optimization problem and the optimal TCSC controller parameters are obtained by means of genetic algorithm. The performance of the TCSC controller is tested over a 3-machines 9-bus power system, for the most severe situation in terms of critical fault clearing time. Nonlinear simulation results show the effectiveness of TCSC controller in enhancing the critical fault clearing time of the system and damping power system oscillations.

2.2.1. (c) Thyristor-Controlled Phase Shifter (TCPS)

The basic function of a phase shifter is to provide means to control the power flow in a transmission line. This can be accomplished by modifying the voltage phase angle by inserting a variable quadrature voltage in series with the transmission line. The phase of the output voltage can be varied relative to that of the input voltage by simply varying the magnitude of the series quadrature voltage. The structure of a thyristor controlled phase shifter is shown in Fig. 2-4.

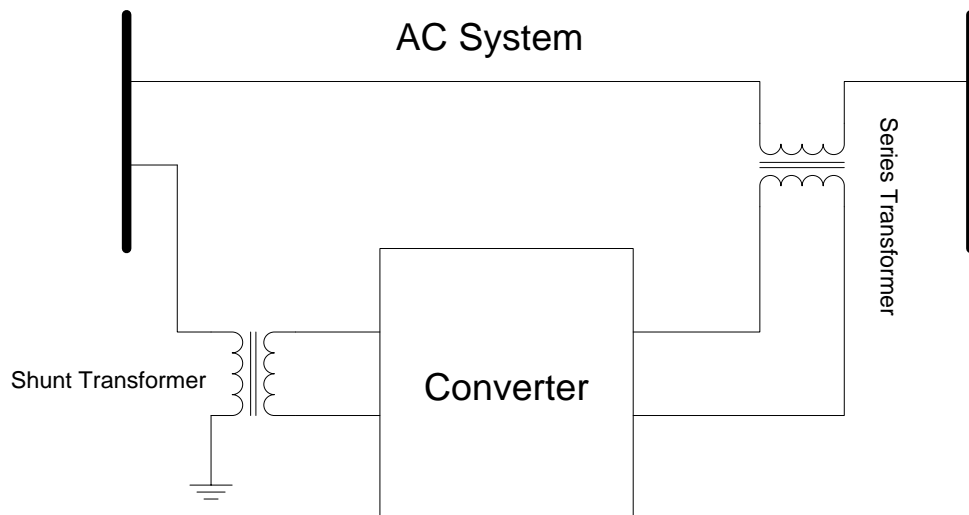


Fig. 2-4 Schematic diagram of TCPS.

A considerable attention has been directed to realization of various TCPS schemes [93][94]. However, a relatively little work in TCPS control aspects has been reported in the literature.

Baker et al. [78] developed a control algorithm for TCPS using stochastic optimal control theory. Edris [79] proposed a simple control algorithm based on the equal area criterion.

Jiang et al. [80] proposed a TCPS control technique based on nonlinear variable structure control theory. In their control scheme the phase shift angle is determined as a nonlinear function of rotor angle and speed. However, in real-life power system with a large number of generators, the rotor angle of a single generator measured with respect to the system reference will not be very meaningful. Tan and Wang [81] proposed a direct feedback linearization technique to linearize and decouple the power system model to design the excitation and TCPS controllers.

2.2.2 Second Generation FACTS Devices:

2.2.2. (a) STATic synchronous COMpensator (STATCOM)

STATCOM is a shunt-connected FACTS controller, which can be utilized to control the voltage at the point of connection [95][96][97]. It senses the AC system terminal voltage and compensate for the voltage difference across the coupling transformer connecting it to the AC system by exchanging active and reactive power. If the output voltage is greater than the AC voltage, it supplies power to the AC system and if the output voltage is less than the AC voltage, it absorbs power from the AC system. Besides controlling the voltage, the function of the STATCOM can be extended to include damping of low power system electromechanical oscillations.

Wang H.F developed the linearized Phillips-Heffron models of a single-machine and multi-machine power systems with STATCOM to design a STATCOM stabilizer to improve the power system oscillation stability. The influence of the DC and AC voltage controllers of the STATCOM on electromechanical oscillations damping in power systems has been investigated also by Wang H.F. in 2000 [98][99]. It has been shown that the DC and AC voltage controllers have a negative effect on the damping torque. The tuning and the performance evaluation of a damping controller for the STATCOM have been presented by Padiyar and Swayam in 2003 [100].

A detailed eigenvalue analysis of a four-machine power system has been performed to study the effectiveness of the developed control law and the location of the damping controller. In (Wang 2003) [101].

A study case of negative interactions between STATCOM AC and DC voltage control has been reported. It has been shown that multiple control functions of the STATCOM have to be

implemented by a single multivariable controller. A damping controller design for the STATCOM with multiple operating points has been proposed [102].

A two-step based LMI (Linear Matrix Inequalities) approach for output feedback damping control design for the system with multiple operating points has been presented for single machine and multi-machine power systems. A nonlinear programming model has been developed to coordinate the design of the power system stabilizer and the STATCOM damping controller [103].

The study has been performed using eigenvalue analysis and non-linear simulation of 10-generator New England test power system. An optimal neurofuzzy controller for the STATCOM has been designed to improve the transient stability of a 12-bus power system [104]. A heuristic dynamic programming-based approach has been utilized to train the controller and allow it to provide nonlinear optimal control at various operating conditions of the 12-bus power system.

The optimal location of the STATCOM in a four-machine power system and its coordinated design with power system stabilizers for power system stability improvement has been studied by Panda and Narayana in 2008 [105]. The location of the STATCOM has been formulated as an optimization problem to improve transient stability and particle swarm optimization has been used to search for its optimal location. In addition, the optimal parameters of the STATCOM have been determined.

The building block for STATCOM is a six-pulse voltage-sourced DC to AC inverter (VSI). The output voltage waveforms of this block have high harmonic contents. To reduce these harmonics, a number of six-pulse VSI's are combined to generate a balanced three-phase voltage whose amplitude and phase are controllable by power electronic devices such as Gate Turn-Off (GTO) thyristor and Integrated Gate-Commutated Thyristor (IGCT) .

STATCOM can be used to obtain desired reactive power compensation and regulate the bus voltage. It can dramatically increase the stability of electric power grid and decrease disturbance to the rest of the electric power grid [46]. Regulating the reactive and active power transferred by STATCOM to the network controls the power flow in the line and the DC link voltage inside STATCOM. Compared to the old style reactive power support methods using capacitor banks and thyristors, STATCOM can offer much higher dynamic performance. These benefits are well-recognized [106].

Compared to SVC and other conventional reactive power compensators, STATCOM has several advantages. STATCOM has a dynamic performance far exceeding the other var compensators. The overall system response time of STATCOM can reach 10 ms and sometimes less than that. STATCOM can maintain full capacitive output current even at low system voltage. Thus, it is more effective than SVC in improving transient stability. Also, STATCOM has a smaller installation space, about half of that for SVC . STATCOM controllers are generally Pulse Width Modulated (PWM) controllers that are used to control the output voltage of STATCOM to supply or absorb reactive power [107].

A genetic algorithm technique was used to design STATCOM controllers. Other intelligent techniques were also used, such as particle swarm optimization in and fuzzy logic in [107].

2.2.2. (b) Static Synchronous Series Compensator (SSSC)

Static Synchronous Series Compensator (SSSC) is a series connected line impedance controller composed of voltage source inverter coupled with a transformer. It can vary the effective reactance of the transmission line by injecting a variable-magnitude voltage in series with it. Hence, it inserts more inductive or capacitive reactance to increase or decrease the effective reactance of the line to obtain the required level of compensation [108].

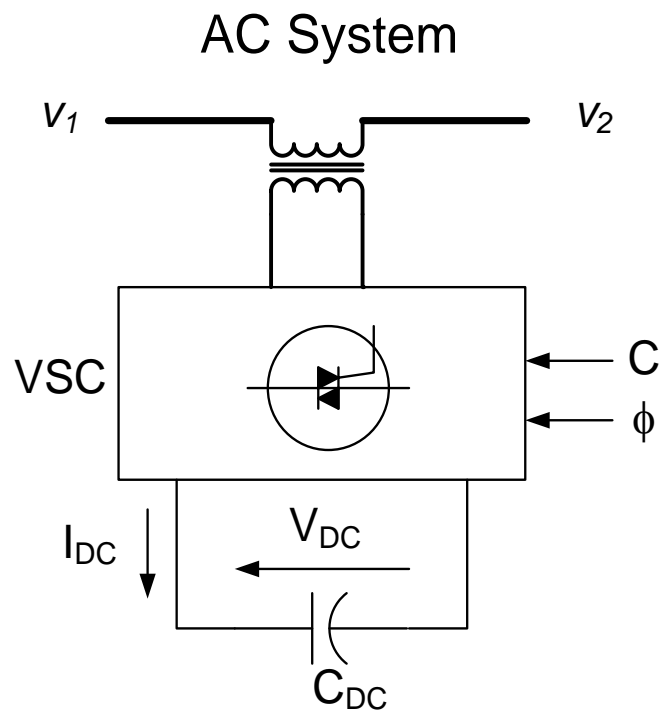


Fig. 2-5 Schematic diagram of SSSC.

2.2.2. (c) Unified Power Flow Controller (UPFC)

Unified Power Flow Controller (UPFC), a multifunctional Flexible AC Transmission system (FACTS) Controller opens up new opportunities for controlling power and enhancing the usable capacity of present, as well as new and upgraded lines. A UPFC supplementary damping controller has been presented in the UPFC control system for damping the electromechanical mode oscillations[109].

UPFC can control voltage magnitude, phase and line impedance, damp power system oscillations and improve transient stability [110]. It can be looked at as a combination of shunt STATCOM and series SSSC operated from a common DC storage capacitor. This allows it to independently exchange both active and reactive power. As shown in Fig. 2-6 UPFC functions like a shunt compensator, series compensator and phase shifter and can maintain controllable active and reactive power in the transmission line to adapt almost instantaneously to load demands and system operating conditions [109].

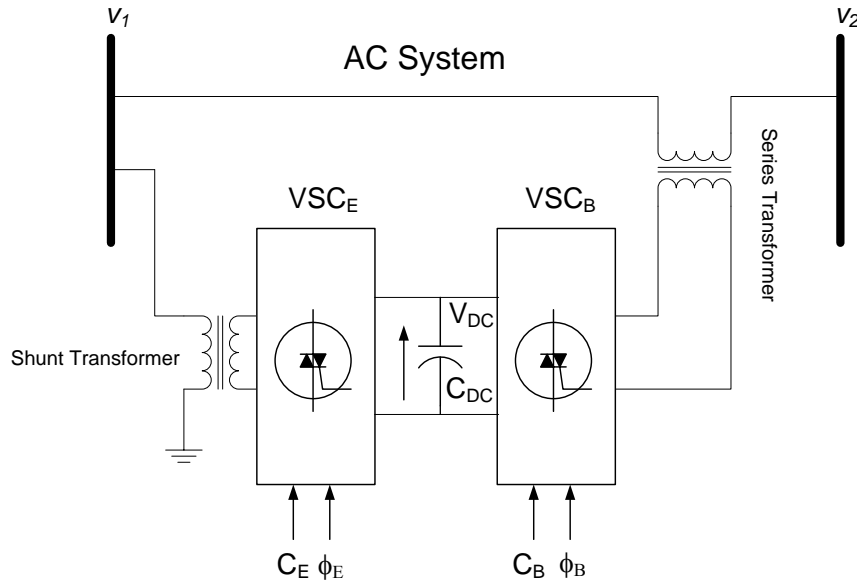


Fig. 2-6 Schematic diagram of UPFC.

In [111][112] systematic designs of four alternative UPFC damping controllers are presented. However, these UPFC damping controller gains are designed on the basis of nominal operating conditions and remain independent of system operating conditions and line loadings. Also the controller gains and hence the control structure is different for the various choices of UPFC control signals. Since damping of low frequency oscillations may be one of the secondary functions of the multifunctional UPFC based on its other major control assignments, the widely varying control structure with respect to the choice of control signals makes the real time implementation inflexible.

In[112] developed adaptive fuzzy inference system (ANFIS) based UPFC supplementary damping controller to superimpose the damping function on the control signal of UPFC for damping of power system electromechanical oscillations [113].

The adaptive fuzzy controller is obtained by embedding the fuzzy inference system into the framework of adaptive networks. The proposed ANFIS based damping controller performance is examined for the four choices of UPFC control signals based on modulating index and voltage

phase angle of UPFC series and shunt converters by simulations on a linearised Philips-Hefron model of a power system with UPFC [114].

The effectiveness of this controller is supported by the results observed in simulations, which show the ability of the controller in damping oscillations over a wide range of loading conditions and system parameters with the four choices of alternative UPFC control signals when compared to constant gain damping controllers designed using phase compensation technique at selected operating point. Integrating this approach to a multi-machine power system and through non-linear simulation the robustness of the proposed controller is validated [115].

Fawzi A [116] presented the damping torque and synchronizing torque contributed by STATCOM, based on Pulse Width Modulation (PWM), in radial power system considering two different damping schemes: (1) the traditional damping scheme; and (2) a proposed damping scheme. Eigenvalue analysis is used to study the influence of the parameters of the Proportional and Integral (PI) of the DC voltage controller and AC voltage controller, real power, and reactive power as well as the damping controller gain of the STATCOM on the damping torque and synchronizing torque. Using a method developed in the literature, which depends on the time responses of the rotor speed, rotor angle and electrical torque, the damping torque and synchronizing torque coefficients are estimated and compared for different loading conditions and control parameters of STATCOM to confirm the results obtained from the eigenvalue analysis. Non-linear simulations of the STATCOM compensated radial power system using PSCAD are performed to validate the outcomes from the eigenvalue analysis and estimation of damping torque and synchronizing torque coefficients.

Kanojia and Chandrakar [117] designed a power system installed with a STATCOM and demonstrates the application of the linearised Phillips-heffron model in analyzing the damping effect of the STATCOM to improve power system oscillation stability. The proposed PI

controller is designed to coordinate two control inputs: Voltage of the injection bus and capacitor voltage of the STATCOM, to improve the Dynamic stability of a SMIB system .The power oscillations damping (POD) control and power system stabilizer (PSS) and their coordinated action with proposed controllers are tested. The simulation result shows that the proposed damping controllers provide satisfactory performance in terms of improvements of dynamic stability of the system.

Kazuhiro Kobayashi et al. [14] proposes a linearized block diagram of a power system with an energy storage type STATCOM (ESTATCOM) and the control schemes for the ESTATCOM. The ESTATCOM, which controls both reactive and active power injection/ absorption, has a more significant effect on the oscillation damping compared to that controlling only the reactive power injection/absorption. From the active and reactive power responses of the compensator to oscillations for an ESTATCOM, it was found that the necessary energy storage capacity to improve the power swing damping is not so large, thus the additional cost for the energy storage system is expected to be small.

2.3 STATCOM Modeling for Stability Studies

Since the first STATCOM installation, there is an ever growing interest in STATCOM modeling due to its many advantages over conventional SVC controllers. In

Table 1 where a partial list of a utility scaled STATCOM it is clearly shown that there are several purposed motivated the utilities to install it and the rating of it is getting increased rapidly.

Table 1 Partial list of a utility scaled STATCOM [15].

SN	Year	MVAR	KV	Purpose	Place
1	1991	± 80	154	Power System stabilization	Inumaya, Japan
2	1992	± 50	500	Reactive power compensation	Nagona, Japan
3	1995	± 100	161	Voltage Regulation	Tennessee, USA
4	2001	± 225	400	Reactive power compensation	Winslow, England
5	2001	± 133	115	Reactive power compensation	Vermont, USA
6	2003	± 100	138	Reactive power compensation	California, USA
7	2011	± 640	500	Reactive power compensation	Dongguan, China

Several distinct models have been proposed to represent STATCOM in static and dynamic analysis. In[3] STATCOM is modeled as parallel connected current source; where in the controllable parameter is assumed to be current magnitude. In [4] the author proposes a per unit STATCOM model; which is suitable for study the performance of STATCOM under unbalanced distorted system voltage.

In [5] the authors proposed different models for transient stability and steady state stability analysis of the power system with STATCOM. However, the models were based on the assumptions that voltages and currents are sinusoidal, balanced and operate near fundamental frequency, hence could not be applied to systems under the impact of large disturbance that have voltage and/or current with high harmonic content.

A comparative study is carried out for dynamic operation of different models of STATCOM and their performance in [6]. In [8] the author proposes a third order dynamic model of the power system to incorporate STATCOM in the system to study its damping properties.

2.4 Controlling Design Approaches used in STATCOM

Many different control strategies such as Proportional-Integral (PI) controller, sliding mode controller [118] and nonlinear controller have been suggested to control STATCOM. Because of nonlinear operation of STATCOM, nonlinear controller is preferred over linear controller [119]. Moreover, in linear controller, four chosen sets of PI parameters may not be suitable for all ranges of operating points and finding these values are very time consuming and complex [120][121].

In nonlinear controller, the Generalized Averaged Method has been used to determine the nonlinear time invariant continuous model of the system [122][123][124]. This model has been used to present a nonlinear control based on exact linearization via feedback for STATCOM [125]. This method is particularly interesting because it transforms a nonlinear system into a linear one in terms of its input-output relationship.

In [122][123], only q axis current has been regulated, but it should be noted that unlike other shunt compensators, large energy storage device that have almost constant DC voltage, makes STATCOM more robust and it also enhances the response speed. Therefore, there are two control objectives implemented in STATCOM. First one is q-axes current and the second objective is capacitor voltage in DC link [126].

The q-axes current tracks its corresponding reference value perfectly, but the capacitor voltage (VDC) is not fixed on reference ideally because of presence of a PI controller between the reference of the d-axes current and VDC error. In other words, the performance indices (settling time, rise time and over shoot) have notable values. Thus, the optimized and exact determination of PI controller gains can lead to the reduction in system disturbances.

N. Farokhnia et al. [127], has presented two well-known optimization methods (e.g., GA [128][129] and PSO [130][131]) are applied to find optimized values of PI gains and compare with each other. The determined PI coefficients are implemented in the controller to demonstrate the improvement of the convergence speed, reduction of error, the overshoot in the capacitor voltage and other circuit parameters. The results are compared with trial and error method, too.

Previous researches present the establishment of the linearized Phillips–Heffron model of a power system installed with a STATCOM. It has not presented a systematic State Feedback Controller Design for a STATCOM using Quantum Particle Swarm Optimization Algorithm approach for designing the damping controllers. Further, no effort seems to have been made to identify the most suitable STATCOM control parameter, in order to arrive at a robust damping controller.

Intelligent controllers have the potential to overcome the above mentioned problems. Fuzzy-logic based controllers have, for example, been used for controlling a STATCOM [132]. The performance of such controllers can further be improved by adaptively updating their parameters. Also, although using the robust control methods [133], the uncertainties are directly introduced to the synthesis, but due to the large model order of power systems the order resulting controller will be very large in general, which is not feasible because of the computational economical difficulties in implementing. M.A. Abido in [134] introduces a special analysis and assessment of STATCOM-based damping stabilizers using real-coded genetic algorithm (RCGA) and presents a singular value decomposition (SVD)-based approach to assess and measure the controllability of the poorly damped electromechanical modes by STATCOM different control channels. In [135] the authors prove that effectiveness of using the coordination design between the PSS and the STATCOM in improving the dynamic of the system and

enhancing the damping of the low frequency oscillations, a PI controllers were used for AC voltage regulator, their controllers' parameters were optimized using RCGA.

The PSO approach, first introduced by Kennedy and Eberhart in 1995, is a population based stochastic algorithm [136]. Recently, the PSO technique is used for optimal tuning of the STATCOM based state feedback damping controller [137]. The PSO is a novel population based meta-heuristic, which utilize the swarm intelligence generated by the cooperation and competition between the particle in a swarm and has emerged as a useful tool for engineering optimization [138][139][140][141][142]. However, the main disadvantage is that the classical PSO algorithm is not guaranteed to be global convergent. In order to overcome this drawback and improve optimization synthesis developed a QPSO technique for optimal tuning of STATCOM based state feedback damping controller for enhancing of power systems low frequency oscillations damping [143].

In [143] author presented a design and evaluation of a state feedback controller for STATCOM installed in a single-machine infinite-bus power system (SMIB). The design problem of state feedback damping controller is formulated as an optimization problem according with the time domain based objective function which is solved by a Quantum Particle Swarm Optimization (QPSO) technique that has fewer parameters and stronger search capability than the classical particle swarm optimization (CPSO), as well as is easy to implement.

The effectiveness of the proposed controller is demonstrated through nonlinear time-domain simulation studies. The results analysis reveals that the designed QPSO based STATCOM damping controller has an excellent capability in damping low frequency oscillations in comparison with designed classical PSO based STATCOM controllers [143].

CHAPTER 3 Power System Model

3.1 Generator

The generator is equipped with a PSS and the system has a STATCOM installed somewhere at point m in transmission line as shown in Fig. 3-1. The generator has a local load of admittance $Y_L = g + jb$ and the transmission line has impedances of $Z_1 = R_1 + jX_1$ and $Z_2 = R_2 + jX_2$ for the first and the second sections respectively. The generator is represented by the third-order model comprising of the electromechanical swing equation and the generator internal voltage equation.

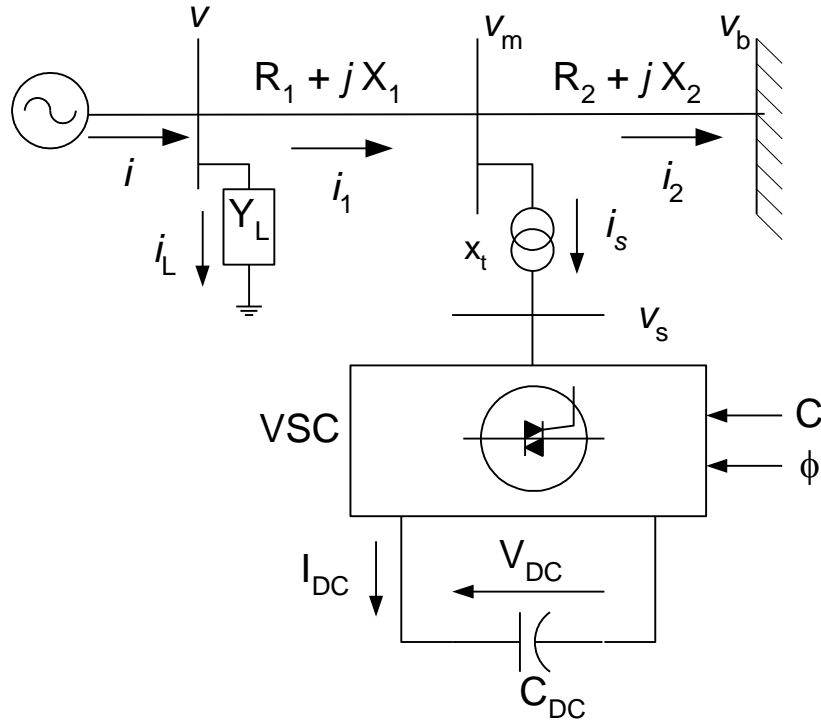


Fig. 3-1 Single machine infinite bus system with a STATCOM.

The swing equation is divided into the following equations

$$\dot{\delta} = \omega_b(\omega - 1) \quad (1)$$

$$\dot{\omega} = (P_m - P_e - D(\omega - 1)) / M \quad (2)$$

where, P_m and P_e are the input and output powers of the generator respectively; M and D are the inertia constant and damping coefficient respectively; δ and ω are the rotor angle and speed respectively. The output power of the generator can be expressed in terms of the d-axis and q-axis components of the armature current, i , and terminal voltage, v , as

$$P_e = v_d i_d + v_q i_q \quad (3)$$

The internal voltage, E'_q , equation is

$$\dot{E}'_q = (E_{fd} - (x_d - x'_d)i_d - E'_q) / T'_{do} \quad (4)$$

Here, E_{fd} is the field voltage; T'_{do} is the open circuit field time constant; x_d and x'_d are the d-axis reactance and the d-axis transient reactance of the generator respectively.

3.2 Exciter and PSS

The IEEE Type-ST1 excitation system shown in Fig. 3-2 is considered in this work. It can be described as

$$\dot{E}_{fd} = (K_A(V^{ref} - v + u_{PSS}) - E_{fd}) / T_A \quad (5)$$

where, K_A and T_A are the gain and time constant of the excitation system respectively; V^{ref} is the reference voltage. As explained in Fig. 3-2, a conventional lead-lag PSS is installed in the feedback loop to generate a stabilizing signal u_{PSS} . The terminal voltage v can be expressed as:

$$v = (v_d^2 + v_q^2)^{1/2} \quad (6)$$

$$v_d = x_q i_q \quad (7)$$

$$v_q = E_q' - x_d' i_d \quad (8)$$

where x_q is the q-axis reactance of the generator.

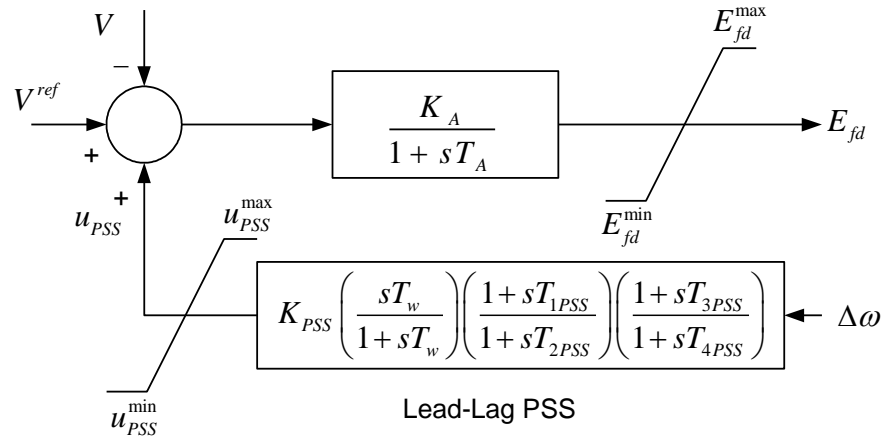


Fig. 3-2 IEEE Type-ST1 excitation system with a Lead-Lag PSS.

3.3 STATCOM -Based Stabilizers

As shown in Fig. 3-1, the STATCOM is connected to the transmission line through a step-down transformer with a leakage reactance of x_t . The STATCOM consists of a three-phase gate turn-off (GTO) – based voltage source converter (VSC) and a DC capacitor. The VSC generates a controllable AC voltage V_s given by

$$V_s = CV_{DC} \angle \phi \quad (9)$$

where $C = mk$, m is the modulation ratio defined by pulse width modulation (PWM), k is the ratio between the AC and DC voltage depending on the converter structure, V_{DC} is the DC

voltage, and ϕ is the phase defined by PWM. The magnitude and the phase of V_s can be controlled through m and ϕ respectively. By adjusting the STATCOM AC voltage V_s , the active and reactive power exchange between the STATCOM and the power system can be controlled through the difference between V_s and the STATCOM-bus voltage V_m . The DC voltage V_{DC} is governed by:

$$\dot{V}_{DC} = \frac{I_{DC}}{C_{DC}} = \frac{C}{C_{DC}} (i_{sd} \cos \phi + i_{sq} \sin \phi) \quad (10)$$

where C_{DC} is the DC capacitor value and I_{DC} is the capacitor current while i_{sd} and i_{sq} are the d and q components of the STATCOM current is respectively.

Fig. 3-3 illustrates the block diagram of STATCOM AC voltage PI controller with a lead-lag compensator while Fig. 3-4 illustrates the block diagram of STATCOM DC voltage PI controller with a lead-lag compensator. The proportional and integral gains are KP_{AC} , KI_{AC} and KP_{DC} , KI_{DC} for AC and DC voltages respectively. The STATCOM damping controllers are lead-lag structure where K_c and K_ϕ are the AC and DC voltage controller gains respectively, T_w is the washout time constant, and T_{1C} , T_{2C} , T_{3C} , T_{4C} , $T_{1\phi}$, $T_{2\phi}$, $T_{3\phi}$, and $T_{4\phi}$ are the controller time constants.

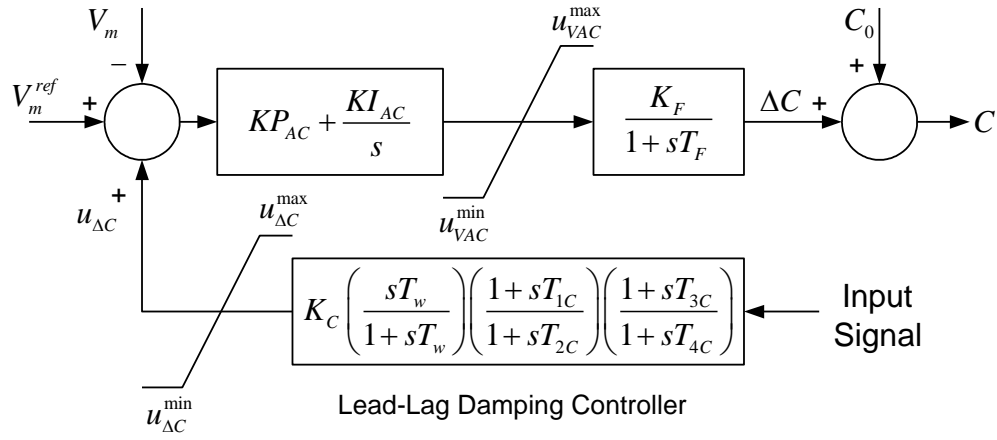


Fig. 3-3 STATCOM PI controller for AC voltage with a lead-lag damping controller.

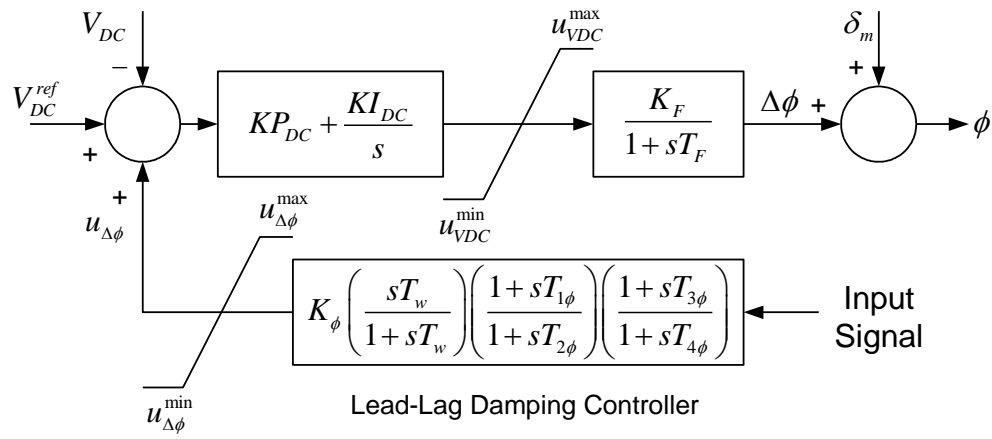


Fig. 3-4 STATCOM PI controller for DC voltage with a lead-lag damping controller.

3.4 Linearized power system model

The system which is described in to Fig. 3-1 is linearized as explained in Appendix B, which yields the following linearized power system model

$$\begin{bmatrix} \dot{\Delta\delta} \\ \dot{\Delta\omega} \\ \dot{\Delta E'_q} \\ \dot{\Delta E'_{fd}} \\ \dot{\Delta V_{DC}} \end{bmatrix} = \begin{bmatrix} 0 & 377 & 0 & 0 & 0 \\ -\frac{K_1}{M} & -\frac{D}{M} & -\frac{K_2}{M} & 0 & -\frac{K_{pDC}}{M} \\ -\frac{K_4}{T'_{do}} & 0 & -\frac{K_3}{T'_{do}} & \frac{1}{T'_{do}} & -\frac{K_{qDC}}{T'_{do}} \\ -\frac{K_A K_5}{T_A} & 0 & -\frac{K_A K_6}{T_A} & -\frac{1}{T_A} & -\frac{K_A K_{vDC}}{T_A} \\ K_7 & 0 & K_8 & 0 & K_{DC} \end{bmatrix} \begin{bmatrix} \Delta\delta \\ \Delta\omega \\ \Delta E'_q \\ \Delta E'_{fd} \\ \Delta V_{DC} \end{bmatrix} + \begin{bmatrix} 0 & 0 & 0 \\ 0 & -\frac{K_{pDC}}{M} & -\frac{K_{p\phi}}{M} \\ 0 & -\frac{K_{qDC}}{T'_{do}} & -\frac{K_{q\phi}}{T'_{do}} \\ \frac{K_A}{T_A} & -\frac{K_A K_{vDC}}{T_A} & \frac{K_A K_{v\phi}}{T_A} \\ 0 & K_{\Delta C} & K_{\Delta\phi} \end{bmatrix} \begin{bmatrix} u_{PSS} \\ \Delta C \\ \Delta\phi \end{bmatrix} \quad (11)$$

In short;

$$\dot{X} = AX + BU \quad (12)$$

Here, the state vector X is $[\Delta\delta, \Delta\omega, \Delta E'_q, \Delta E'_{fd}, \Delta V_{DC}]^T$ and the control vector U is $[u_{PSS}, \Delta C, \Delta\phi]^T$.

3.5 Problem Formulation

3.5.1 Stabilizer Structure

For the PSS and the STATCOM-based damping stabilizers, the commonly used lead-lag structure shown in Fig. 3-4 is chosen in this study. The transfer function of the stabilizer is

$$u = K \left(\frac{sT_w}{1+sT_w} \right) \left(\frac{1+sT_1}{1+sT_2} \right) \left(\frac{1+sT_3}{1+sT_4} \right) y \quad (13)$$

where u and y are the stabilizer output and input signals respectively, K is the stabilizer gain, T_w is the washout time constant, T_1 and, T_2 , T_3 , and T_4 are the stabilizer time constants. In this structure, T_w , T_2 , and T_4 are usually pre-specified. The controller gain K and time constants T_1 and T_3 are to be determined.

For the internal AC and DC voltage controllers of the STATCOM, the PI structure is used as shown in Fig. 3-3 and Fig. 3-4.

3.5.2 Objective Function

To increase the system damping to the electromechanical model, the objective function J which is defined in (14) is considered.

$$J = \max \{ \zeta \} \quad (14)$$

Where ζ is the minimum electromechanical mode damping ratio.

This objective function will recognize the minimum value of damping ratio among electromechanical modes of all loading condition considered in the design practice.

3.5.3 The Constraints

The problem constraints are the stabilizer optimized parameter bounds. Therefore, the design problem can be formulated as the following optimization problem.

$$\text{Maximize } J \quad (15)$$

Subject to

$$KP_{AC}^{\min} \leq KP_{AC} \leq KP_{AC}^{\max} \quad (16)$$

$$KI_{AC}^{\min} \leq KI_{AC} \leq KI_{AC}^{\max} \quad (17)$$

$$KP_{DC}^{\min} \leq KP_{DC} \leq KP_{DC}^{\max} \quad (18)$$

$$KI_{DC}^{\min} \leq KI_{DC} \leq KI_{DC}^{\max} \quad (19)$$

$$K_{PSS}^{\min} \leq K_{PSS} \leq K_{PSS}^{\max} \quad (20)$$

$$K_C^{\min} \leq K_C \leq K_C^{\max} \quad (21)$$

$$K_{\phi}^{\min} \leq K_{\phi} \leq K_{\phi}^{\max} \quad (22)$$

$$T_{1PSS}^{\min} \leq T_{1PSS} \leq T_{1PSS}^{\max} \quad (23)$$

$$T_{3PSS}^{\min} \leq T_{3PSS} \leq T_{3PSS}^{\max} \quad (24)$$

$$T_{1C}^{\min} \leq T_{1C} \leq T_{1C}^{\max} \quad (25)$$

$$T_{3C}^{\min} \leq T_{3C} \leq T_{3C}^{\max} \quad (26)$$

$$T_{1\phi}^{\min} \leq T_{1\phi} \leq T_{1\phi}^{\max} \quad (27)$$

$$T_{3\phi}^{\min} \leq T_{3\phi} \leq T_{3\phi}^{\max} \quad (28)$$

CHAPTER 4 Proposed Approach

4.1 Controllability Measure using Singular Value Decomposition (SVD)

To measure the controllability of the electromechanical mode by a given input signal to the proposed controller, the singular value decomposition (SVD) is engaged in this study.

Mathematically, if G is an $m \times n$ complex matrix then there exist unitary matrices W and V with dimensions of $m \times m$ and $n \times n$ respectively such that G can be written as

$$G = W \Sigma V^H \quad (29)$$

where

$$\Sigma = \begin{bmatrix} \Sigma_1 & 0 \\ 0 & 0 \end{bmatrix}, \quad \Sigma_1 = \text{diag}(\sigma_1, \dots, \sigma_r) \quad \text{with } \sigma_1 \geq \dots \geq \sigma_r \geq 0 \quad (30)$$

where $r = \min\{m, n\}$ and $\sigma_1, \dots, \sigma_r$ are the singular values of G .

The minimum singular value σ_r represents the distance of the matrix G from the all matrices with a rank of $r-1$. This property can be utilized to quantify modal controllability [144]. In this study, the matrix B in (12) can be written as $B = [b_1, b_2, b_3]$ where b_i is the column of matrix B corresponding to the i -th input. The minimum singular value, σ_{\min} , of the matrix $[\lambda I - A : b_i]$ indicates the capability of the i -th input to control the mode associated with the eigenvalue λ . As a matter of fact, the higher the σ_{\min} , the higher the controllability of this mode by the input

considered. Having been identified, the controllability of the electromechanical mode can be examined with all inputs in order to identify the most effective one to control that mode.

With each input signals of STATCOM-based stabilizer (ϕ & C) in the linearized model, the minimum singular value σ_{\min} has been estimated to measure the controllability of the electromechanical mode from that input. The minimum singular value has been predictably calculated for each STATCOM signal over a wide range of operating conditions. particularly, for a loading conditions specified by $P = [0.05 - 1.0]$ pu with a step of 0.05 pu and $Q = [-0.4 - 0.4]$ pu with a step of 0.4 pu, σ_{\min} has been estimated at each loading condition in the specified range, the system model is linearized, the electromechanical mode is identified, and the SVD-based controllability measure is implemented.

The capabilities of ϕ & C STATCOM signals to control the electromechanical modes over the specified range of operating conditions are given in Fig. 4-1, Fig. 4-2 & Fig. 4-3.

It can be seen that the controllability of the electromechanical mode with the ϕ and C increases with loading at lagging and leading power factor and slightly increasing at unity power factor.

However, the controllability of the electromechanical mode with the ϕ is higher.

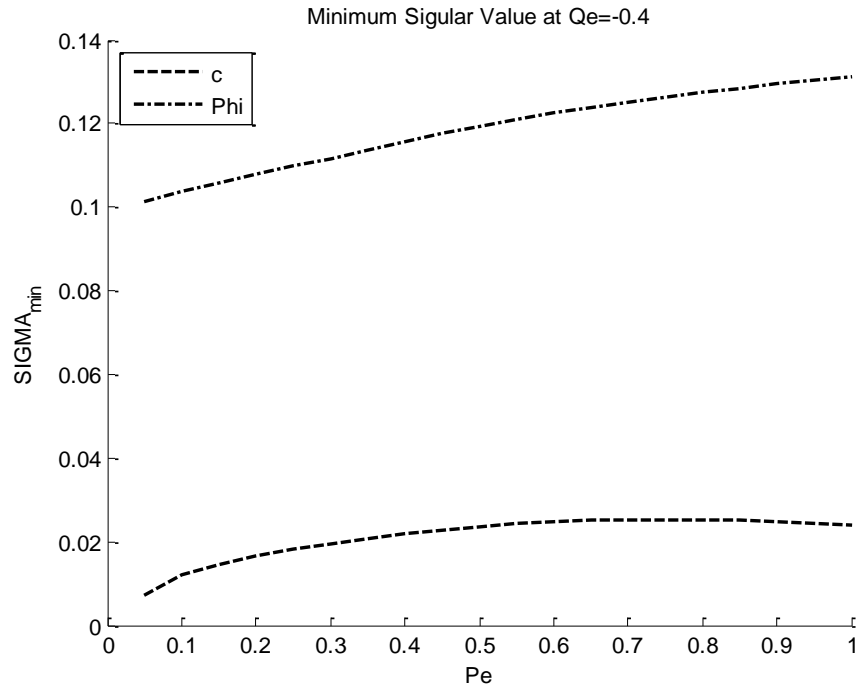


Fig. 4-1 Minimum singular value with STATCOM stabilizer at $Q = -0.4$ pu for different input signals "C & Phi".

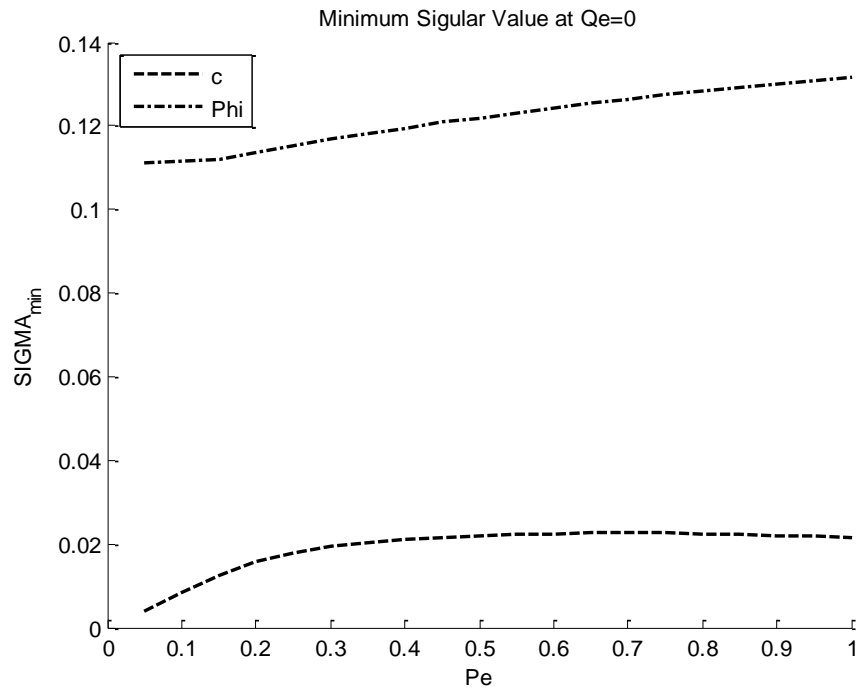


Fig. 4-2 Minimum singular value with STATCOM stabilizer at $Q = 0$ pu for different input signals "C & Phi".

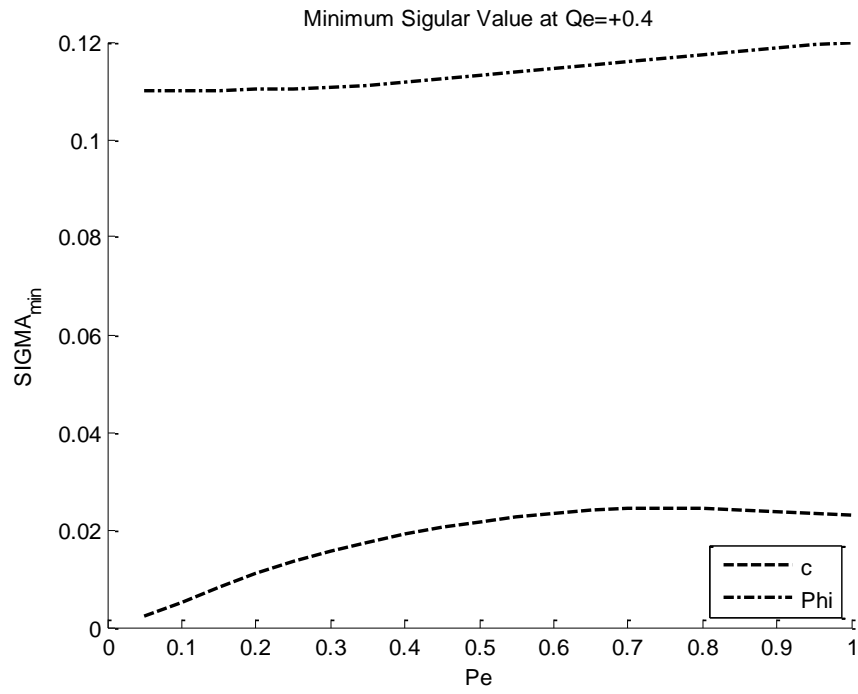


Fig. 4-3 Minimum singular value with STATCOM stabilizer at $Q = +0.4$ pu for different input signals "C &Phi".

4.2 Optimization Technique

4.2.1 Overview

Between 1994 to 1996, Rainer Storn and Kenneth Price introduced an optimization technique called “Differential Evolution” as a result of their joint work. During his work to solve a problem called "Chbychev Polynomial fitting problem", Ken has made an idea to use vector differences for perturbing the vector population. Then, both worked out this idea and made several improvements, until the DE was successfully formulated and introduced [145][146][147].

The DE is a population based optimization technique and is characterized by its simplicity, robustness, few control variables and fast convergence. Being an evolutionary algorithm, the DE technique is suited for solving non-linear and non-differentiable optimization problems. DE is a kind of searching technique and requires number (NP) of candidate solutions (X_n^i) to form the population G^i , where each solution consists of certain number of parameters x_{nj} depending on the problem dimension.

$$G^i = [X_1, X_2, \dots, X_{NP}] \quad i : \text{generation, NP population size}$$

$$X_n^i = [x_{n1}, x_{n2}, \dots, x_{nj}] \quad n : \text{problem dimension}$$

The main idea in any search technique relies in how to generate a variant (offspring) vector solution, on which the decision will be made, in order to choose the best (parent or variant). The strategy applied in this technique is to use the difference between randomly selected vectors to generate a new solution. For each solution in the original population, a trail solution is generated by performing process of mutation, recombination and selection operators. The old and new solutions are compared and the best solutions are emerged in the next generation.

Initially the DE was developed to solve single objective optimization problem. The DE was compared against the well known Particle Swarm Optimization technique [148], and the author has concluded that DE has better performance.

4.2.2 Optimization Procedure in DE For Single Objective Problem

The DE, as in any evolutionary technique, generally performs three steps: initialization, creating new trail generation and selection.

4.2.3 Initialization

As a preparation for the optimization process, the following requirements should be specified:

- D: problem dimension which defines the number of control variables. Also, the range of each control element should be defined. This range is required during the process.

Problem equality and inequality constraints, which will determine the feasibility of solutions.

- NP: population size
- Number of iterations
- F : mutation factor.
- CR: Crossover factor, which determine probability for offspring parameters for each control vector.

The first step in order to perform optimization using DE, is to generate an initial population composed of NP vectors (solutions). Each vector includes the values of the various control variables which represent a candidate solution to the problem. This is done by assigning random values for each parameter of solution x_i , within the range of the corresponding control variable.

$$x_{i,j} = x_{j,\min} + \text{random} \# (x_{j,\max} - x_{j,\min}) \quad i = 1, NP, j = 1, D$$

4.2.4 Evaluation and Finding The Best Solution

Once the initial population is formed, the objective value for each vector is calculated and then compared to get the best solution achieving the optimal objective. This value is stored externally and updated by comparison with all solutions in every generation.

4.2.5 Mutation

The mutation operation is considered as the first step towards the generation of new solutions. At this stage, for every solution (individual) in the population in generation i : $X_i^{(G)}$ $i=1, \dots, NP$, a mutant vector $V_i^{(G+1)}$ is generated using one of the following formulas:

$$V_i^{(G+1)} = X_{r1}^{(G)} + F(X_{r2}^{(G)} - X_{r3}^{(G)}) \quad (31)$$

$$V_i^{(G+1)} = X_{best}^{(G)} + F(X_{r1}^{(G)} - X_{r2}^{(G)}) \quad (32)$$

$$V_i^{(G+1)} = X_i^{(G)} + F(X_{best}^{(G)} - X_i^{(G)}) + F(X_{r1}^{(G)} - X_{r2}^{(G)}) \quad (33)$$

$$V_i^{(G+1)} = X_{r1}^{(G)} + F(X_{r2}^{(G)} - X_{r3}^{(G)}) + F(X_{r4}^{(G)} - X_{r5}^{(G)}) \quad (34)$$

Where: $X_{r1}^{(G)}$, $X_{r2}^{(G)}$, $X_{r3}^{(G)}$, $X_{r4}^{(G)}$, $X_{r5}^{(G)}$ are randomly selected solution vectors from the current generation (different from each other and the corresponding X_i) and $X_{Best}^{(G)}$ is the solution achieving best value. F is a mutation constant and it takes values between 1 and 0. The factor F plays a role in controlling the speed of convergence.

4.2.6 Crossover

To further perturb the generated solutions and enhance the diversity, a crossover operation is applied by the DE. In this step the parameters of the generated mutant vector and its corresponding vector i in the original population are copied to a trial solution according to a certain crossover factor $CR \in [1,0]$. For each parameter, a random number in the range $[1,0]$ is generated and compared with CR , and if its value is less than or equal to CR , the parameter value is taken from the mutant vector, otherwise, it will be taken from the parent. Crossover process is shown in Fig. 4-4. However, in case CR was defined to be zero, then all the parameters of the trial vector are copied from the parent vector X_i , except one value (randomly chosen) of the trial vector is set equal to the corresponding parameter in the mutant vector. On the other hand, if CR is set equal to one. Then, all parameters will be copied from the mutant vector, except one value (randomly chosen) of the trial vector is set equal to the corresponding parameter in the parent vector. The factor 'CR' plays a role in controlling the smoothness of the convergence. As CR becomes very small, it becomes very probable that the trial solutions would have characteristic of their parent vectors and therefore, slow the convergence.

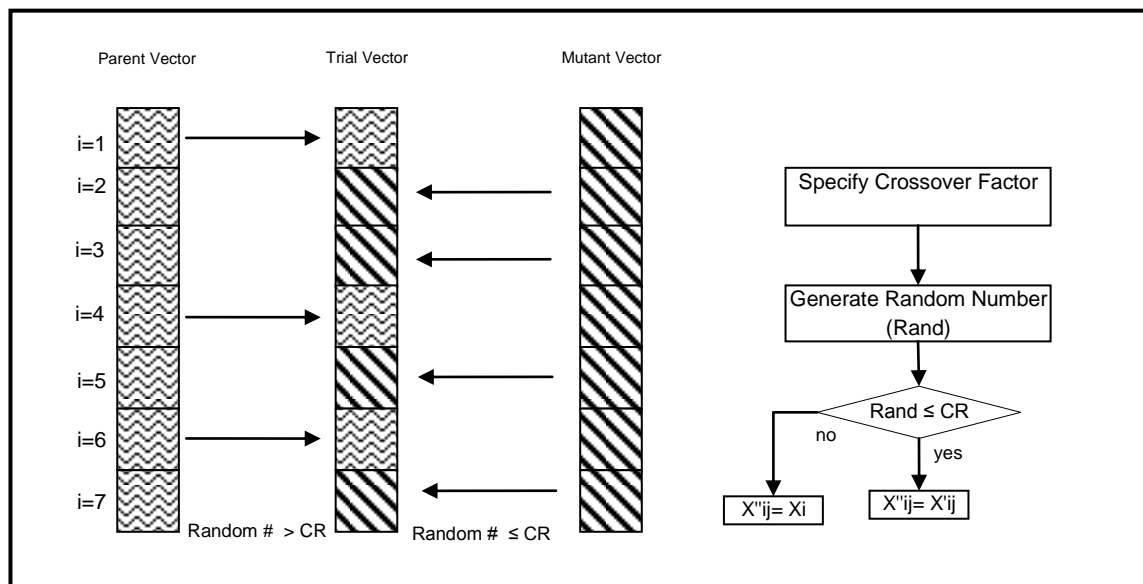


Fig. 4-4 Crossover operation procedure.

4.2.7 Selection

The last step toward generation of a new population is to compare the solutions in old population and their corresponding trial solutions and then select the better one. For this, the objective value corresponding to each trial solution is calculated and compared with the value of the parent. If the new solution performed better it replace the parent, otherwise the old solution is retained.

4.2.8 Stopping Criteria

Once, a new generation is produced, the problem updates the global best. The user defined criteria would also be checked. In most cases a maximum number of iterations is defined and selected as stopping criteria. In practice, the user can check the results and verify the change and can determine when to stop.

Fig. 4-5 shows a flow chart summarizing the procedure of DE as explained above.

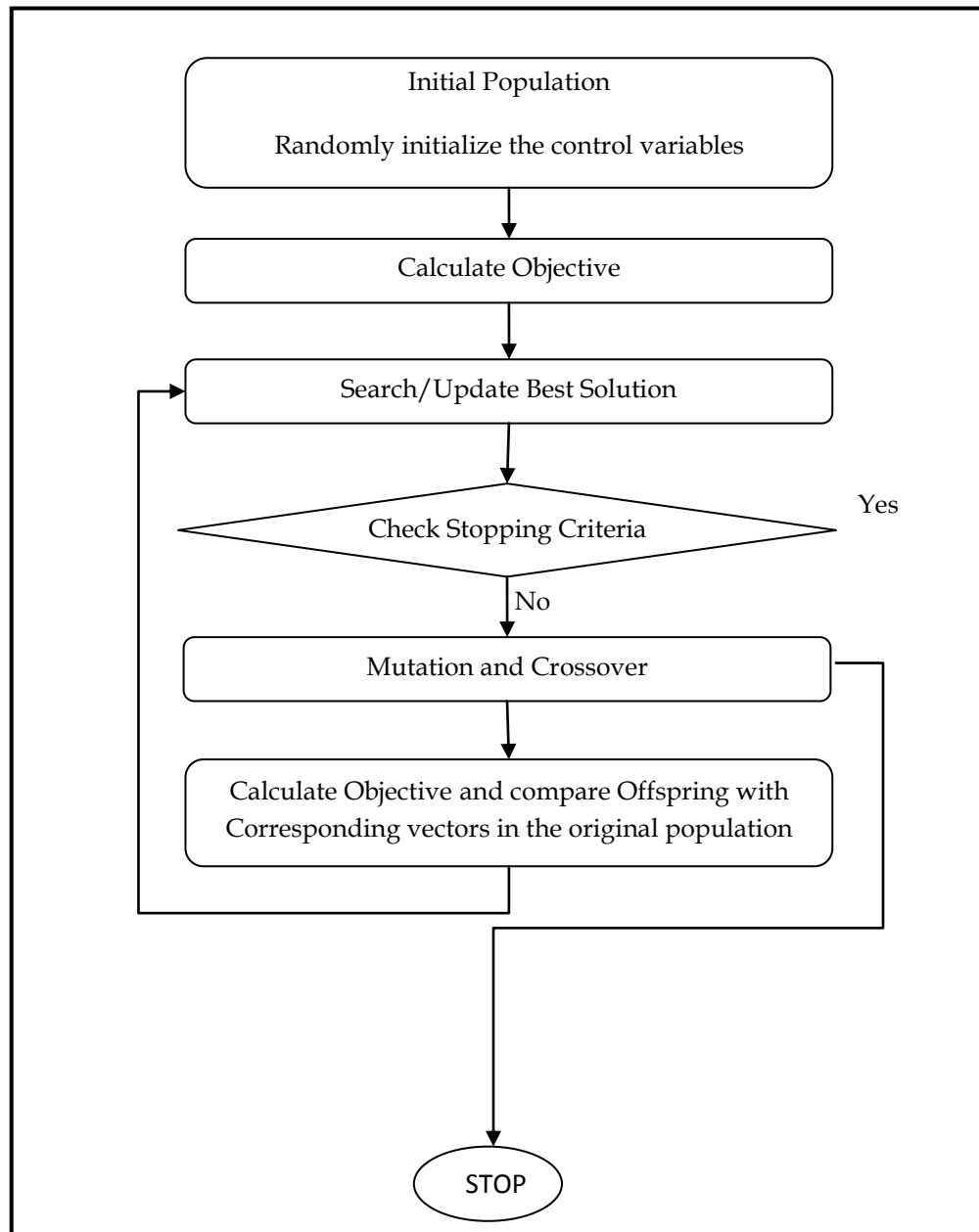


Fig. 4-5 Differential Evolution flowchart.

CHAPTER 5 ANALYSIS, DESIGN AND

SIMULATION RESULTS OF THE

STATCOM-BASED STABILIZER

In this chapter, the STATCOM internal AC and DC PI controllers are simulated in individual and coordination design with the damping controllers after finding their optimized parameters. Subsequently, they are tested under three different loading conditions which are nominal loading, heavy loading and light loading.

5.1 Optimization Results

5.1.1 Nominal Loading Condition ($P=1.0$, $Q=0.015$ & $V=1.0$)

The convergence rate of the objective function J for C -based, Φ -based and $C\&\Phi$ -coordinated based at a nominal loading condition are shown in Fig. 5-1. It can be seen that the damping characteristics of the coordinated design approach is better than those of the individual design one. The final settings of the optimized parameters for the proposed stabilizers and the System's eigenvalues of nominal loading condition, for C -based and Φ -based stabilizers, individual and coordinated design are given in Table 2 and Table 3 respectively.

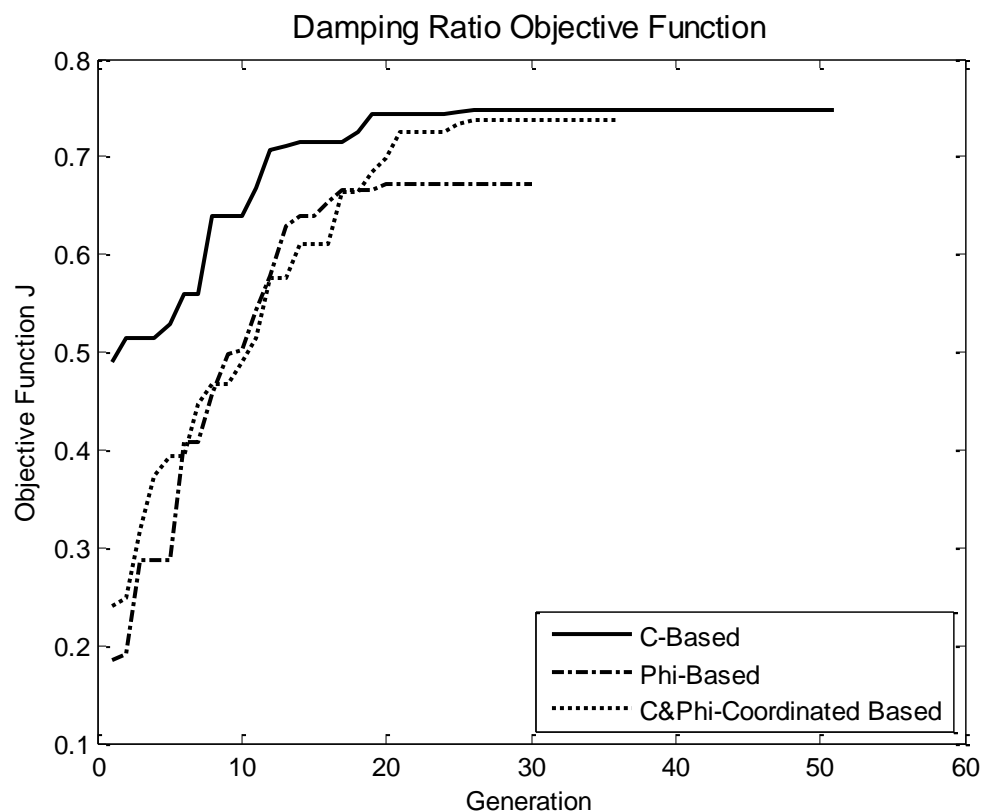


Fig. 5-1 Convergence of objective function in nominal loading condition for different controllers approaches.

Table 2 Optimal Parameter Settings of C-Based & Φ -Based for Individual and Coordinated Design at Nominal Loading

	Individual		Coordinated	
	C-based Controller	Φ -based Controller	C-based Controller	Φ -based Controller
Controller gain- K	94.4884	95.2861	97.7017	17.1744
T1	0.9954	0.9917	0.7657	0.1000
T2	0.7198	0.8612	0.5954	0.5177
T3	0.5777	0.1195	0.7896	0.1072
T4	0.3817	0.6266	0.4946	0.5632
KDCP	5.8488	1.9911		5.2617
KDCI	16.0402	4.0771		11.0592

Table 3 System's eigenvalues of nominal loading condition, for C -based and Φ -based stabilizers, individual and coordinated design

C-based controller	Φ-based controller	Coordinated [C & Φ]-based Controllers
-98.9998	-99.0730	-99.0719
-31.6478	-12.6985 \pm 11.2705i	-12.2147 \pm 11.1985i
-27.2783	-7.9670 \pm 7.0691i	-7.2431 \pm 6.5577i
-5.4949 \pm 15.2798i	-4.8065 \pm 4.2632i	-5.6562 \pm 3.8744i
-1.2166 \pm 3.6599i	-3.4536	-4.1559
-3.8965	-0.1997	-1.3388
-2.0854	-1.5577	-1.0043 \pm 0.0257i
-0.1994	-1.2195	-1.0941
-1.2298		-0.1997
		-0.2000

5.1.2 Heavy Loading Condition (P=1.2, Q=0.4 & V=1.0.5)

The convergence rate of the objective function J for C-based, Φ -based and C& Φ -coordinated based at a heavy loading condition are shown in Fig. 5-2. It can be seen that the damping characteristics of the coordinated design approach is better than those of the individual design one. The final settings of the optimized parameters for the proposed stabilizers and the System's eigenvalues of nominal loading condition, for C -based and Φ -based stabilizers, individual and coordinated design are given in Table 4 and Table 5 respectively.

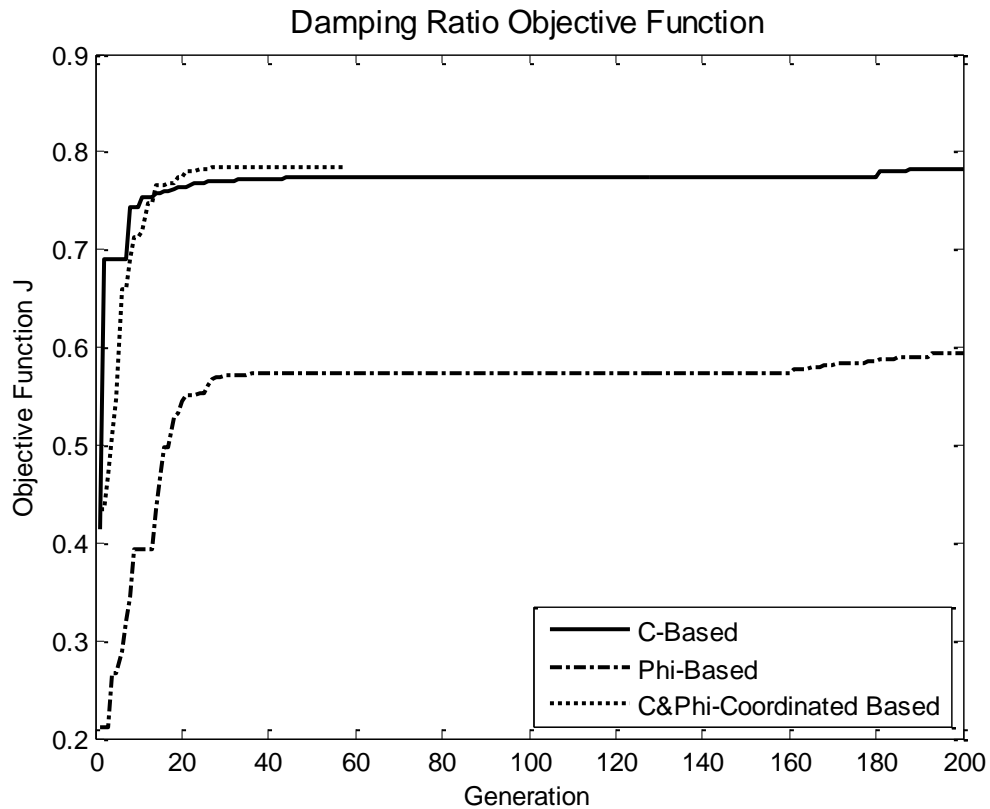


Fig. 5-2 Convergence of objective function in heavy loading condition for different controllers approaches.

Table 4 Optimal Parameter Settings of C-Based & Φ -Based for Individual and Coordinated Design at Heavy Loading.

	Individual		Coordinated	
	C-based Controller	Φ -based Controller	C-based Controller	Φ -based Controller
Controller gain- K	100	83.3722	98.8228	1.5806
T₁	0.9991	0.7935	0.7774	0.9109
T₂	0.8771	0.5892	0.5399	0.9552
T₃	0.7110	0.1000	0.9968	0.1000
T₄	0.4837	0.5850	0.8356	0.8872
KDCP	4.6442	2.0252		4.3950
KDCI	2.8844	0.1265		2.5610

Table 5 System eigenvalues of heavy loading condition, for C -based and Φ -based stabilizers, individual and coordinated design.

C-based controller	Φ -based controller	Coordinated [C & Φ]-based Controllers
-98.9732	-99.0323	-99.0332
-31.9343	-15.5160 \pm 12.3508i	-15.6088 \pm 12.3051i
-6.1218 \pm 7.9256i	-5.9120 \pm 4.6577i	-5.7201 \pm 4.1109i
-3.7538 \pm 5.1509i	-5.1442 \pm 4.0595i	-5.1919 \pm 4.0699i
-0.9896 \pm 1.3578i	-0.2011	-0.5899
-0.1999	-0.6147	-1.4309
-1.5033 \pm 0.3920i	-1.5226	-1.0491
	-1.1304	-1.1859
		-1.1291
		-0.2011
		-0.2000

5.1.3 Light Loading Condition ($P=0.4$, $Q=0.015$ & $V=1.0$)

The convergence rate of the objective function J for C-based, Φ -based and C& Φ -coordinated based at a light loading condition are shown in Fig. 5-3. It can be seen that the damping characteristics of the coordinated design approach is better than those of the individual design one. The final settings of the optimized parameters for the proposed stabilizers and the System's eigenvalues of nominal loading condition, for C -based and Φ -based stabilizers, individual and coordinated design are given in Table 6 and Table 7 respectively.

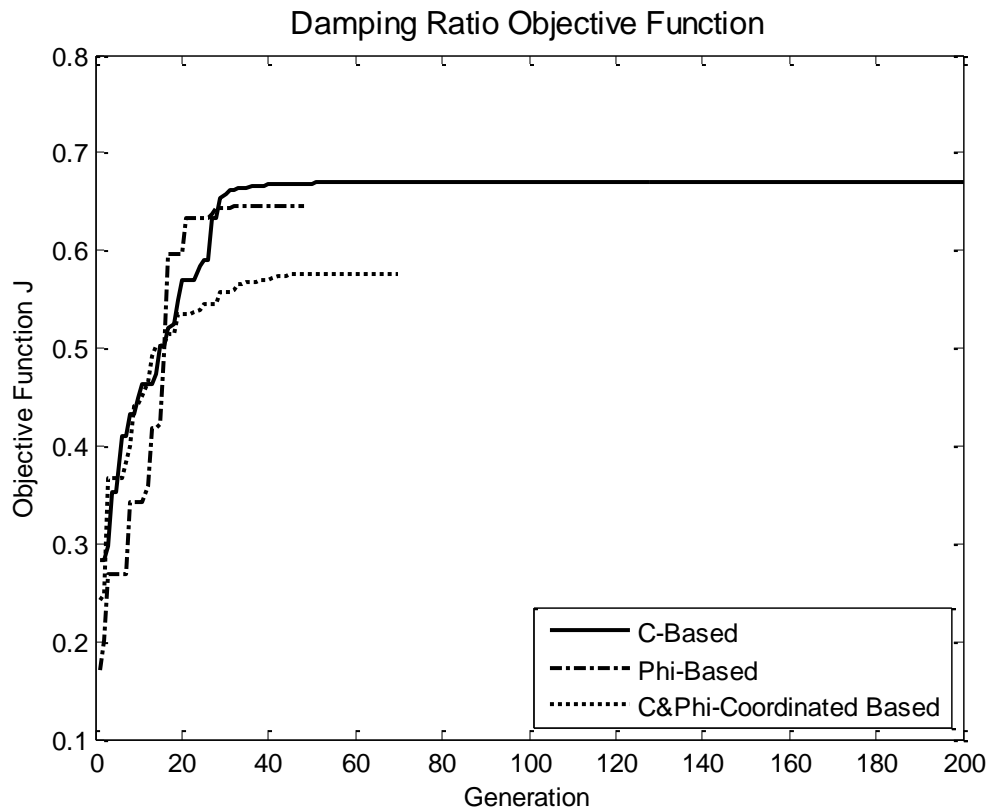


Fig. 5-3 Convergence of objective function in light loading condition for different controllers approaches.

Table 6 Optimal parameter settings of C-based & Φ -based for individual and coordinated design at light loading.

	Individual		Coordinated	
	C-based Controller	Φ-based Controller	C-based Controller	Φ-based Controller
Controller gain- K	100	91.1758	99.8172	75.8782
T₁	0.9710	0.1245	1	0.1000
T₂	0.4195	0.4698	0.6661	0.9578
T₃	0.9689	0.9621	0.6671	0.1000
T₄	0.5138	0.7981	0.2592	0.3438
KDCP	6.2548	1.3571		5.1056
KDCI	28.1797	0.1000		20.8230

Table 7 System eigenvalues of light loading condition, for C -based and Φ -based stabilizers, individual and coordinated design.

C-based controller	Φ-based controller	Coordinated [C & Φ]- based Controllers
-98.8594	-98.9305	-98.9230
-31.6016	-18.1708	-21.1216
-6.3921	-7.9454 \pm 8.8237i	-5.8665 \pm 8.3214i
-3.9554 \pm 4.2222i	-6.0583 \pm 6.7281i	-4.8252 \pm 6.8436i
-3.6598 \pm 3.9067i	-4.1089 \pm 4.5630i	-6.5302 \pm 2.5127i
-0.2002	-0.1999	-2.7994
-0.9157 \pm 0.4815i	-1.4796 \pm 0.1620i	-1.2397 \pm 0.2023i
-1.4226		-1.5008
		-0.1992
		-0.2000

5.2 Simulation Results

5.2.1 Nominal Loading

The single machine infinite bus system shown in Fig. 3-1 is considered for nonlinear simulation studies.

A 6-cycle 3- Φ fault on the STATCOM bus was created, at all loading conditions, to study the performance of the proposed controllers.

Figures (Fig. 5-4 - Fig. 5-11) show the angle deviation, speed deviation, DC voltage, VSC angle, VSC magnitude, electrical power, generator terminal voltage and STATCOM DC voltage responses at nominal operating condition where the coordinated design of STATCOM C & Φ controllers is compared to individual design. It can be seen that, at this loading condition, both individually design STATCOM controllers are performed well in stabilizing the system which confirm the eigenvalue analysis. While there is a excellent improvement in the system response when coordinated design is considered.

The simulation results obtained obviously show that the proposed coordinated design overtake both the individual designs in terms of first swing stability, overshoot, and settling time. On the other hand, the damping effort provided by the UPSS and C-based are not sufficient to keep the system stable at this loading condition. These results confirm the conclusion drawn for eigenvalues analysis.

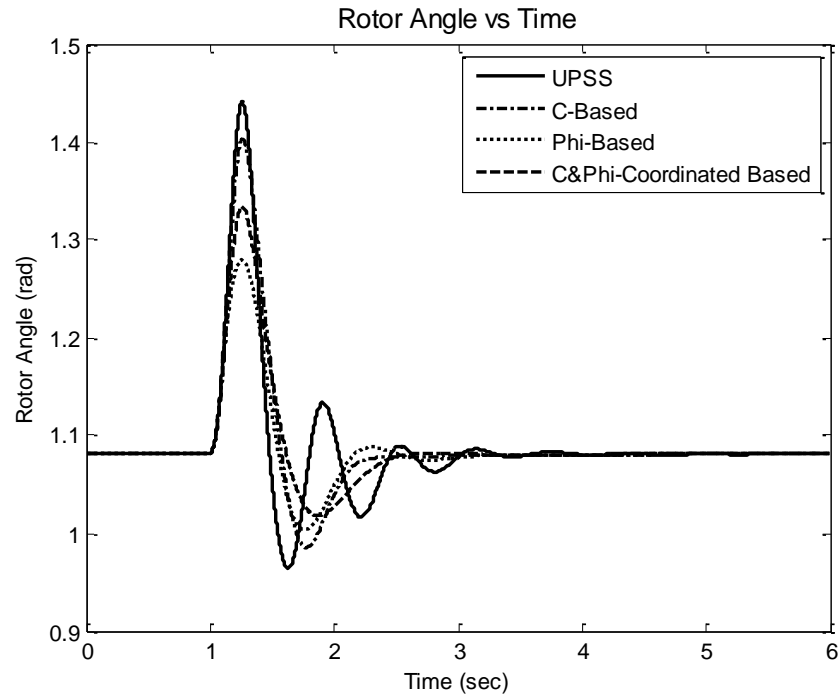


Fig. 5-4 Rotor angle response for 6-cycle fault with nominal loading C & Φ , individual and coordinated design.

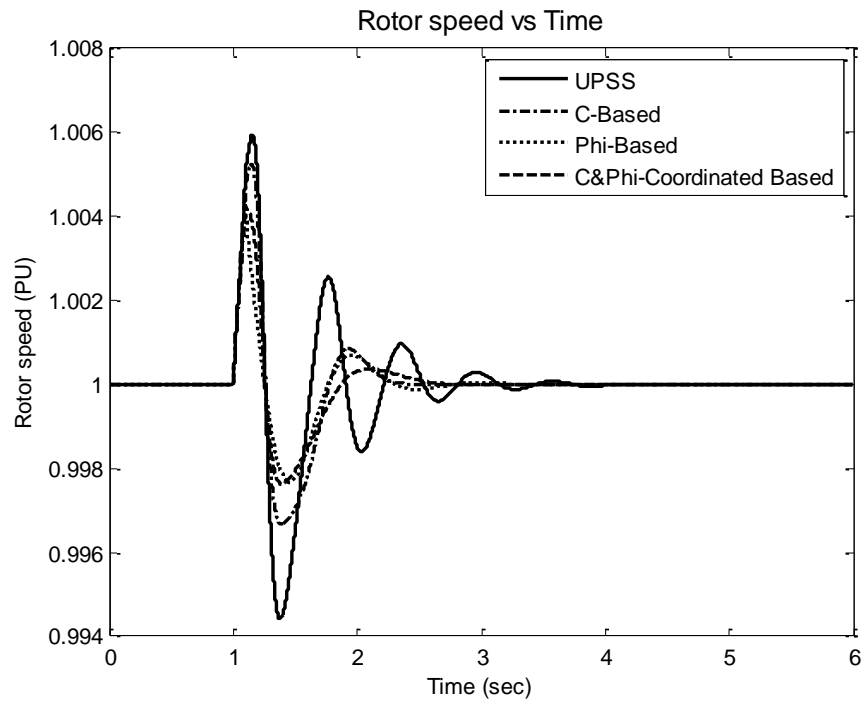


Fig. 5-5 Rotor speed response for 6-cycle fault with nominal loading C & Φ , individual and coordinated design.

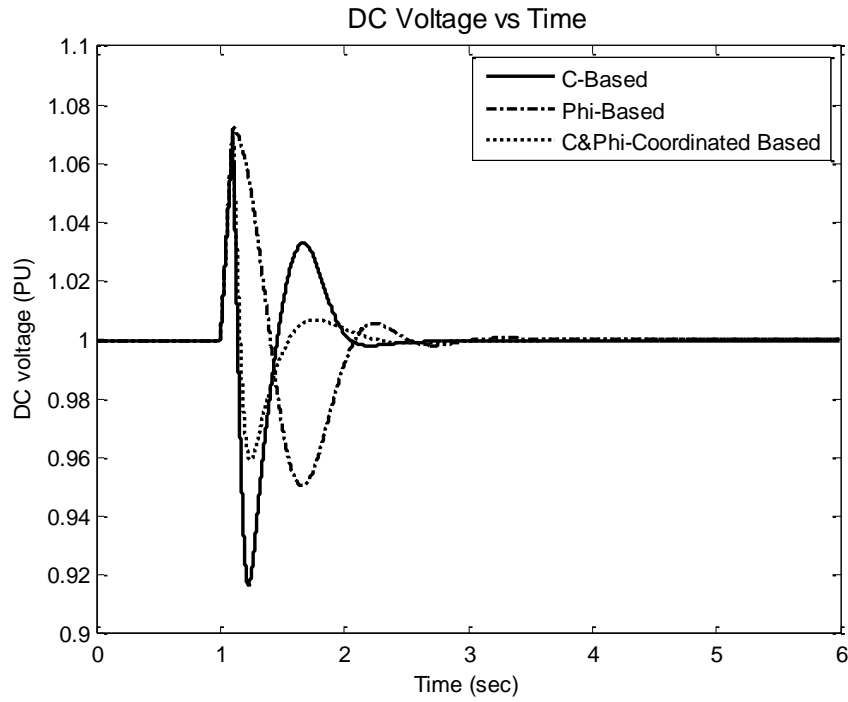


Fig. 5-6 DC voltage response for 6-cycle fault with nominal loading C & Φ , individual and coordinated design.

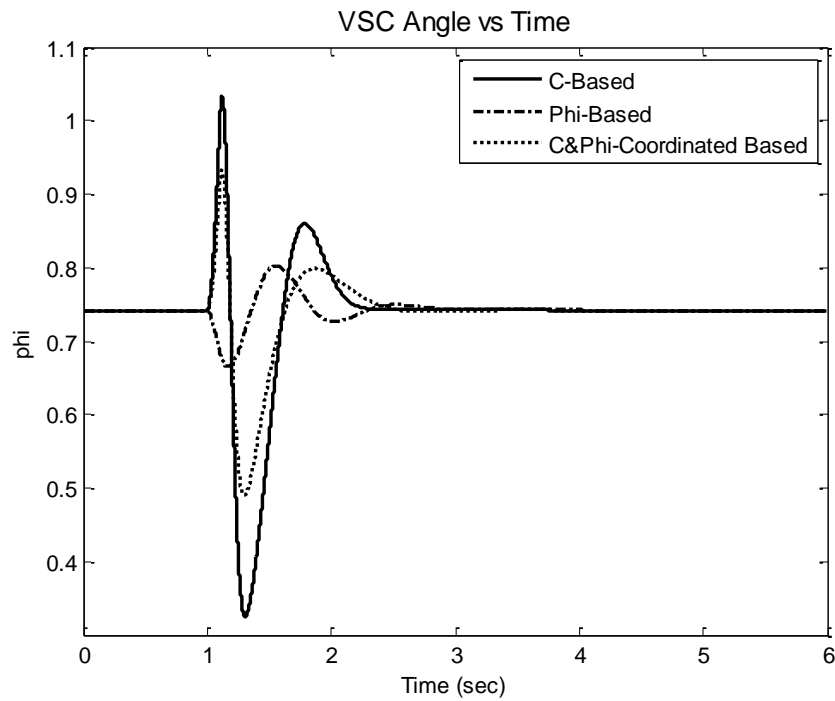


Fig. 5-7 VSC angle response for 6-cycle fault with nominal loading C & Φ , individual and coordinated design.

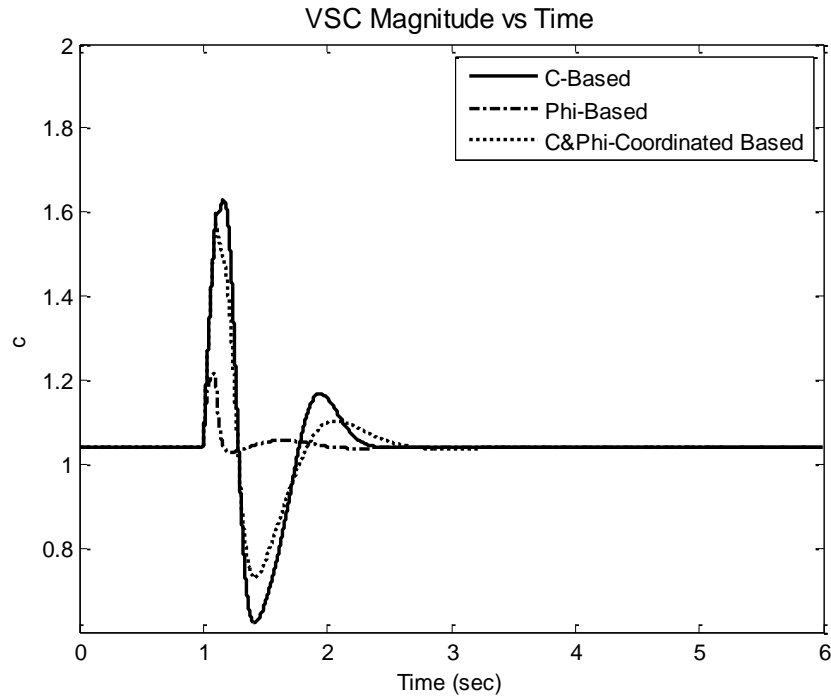


Fig. 5-8 VSC magnitude response for 6-cycle fault with nominal loading C & Φ , individual and coordinated design.

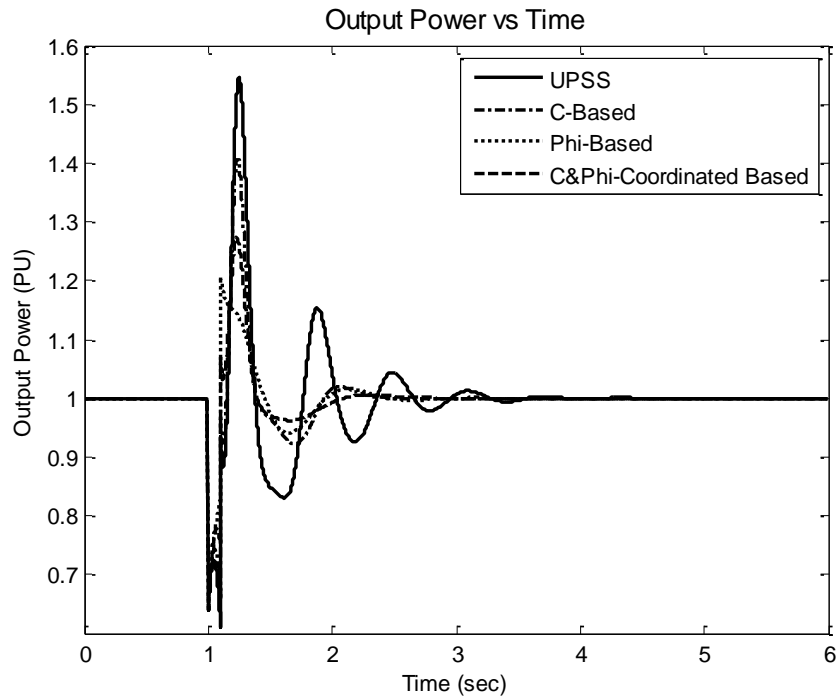


Fig. 5-9 Generator power response for 6-cycle fault with nominal loading C & Φ , individual and coordinated design.

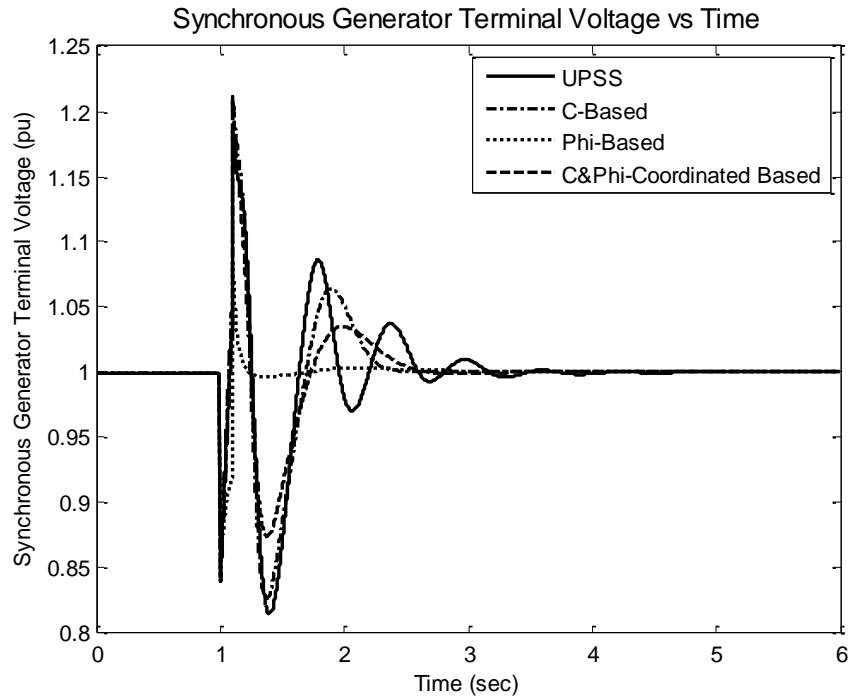


Fig. 5-10 Generator terminal voltage response for 6-cycle fault with nominal loading C & Φ , individual and coordinated design.

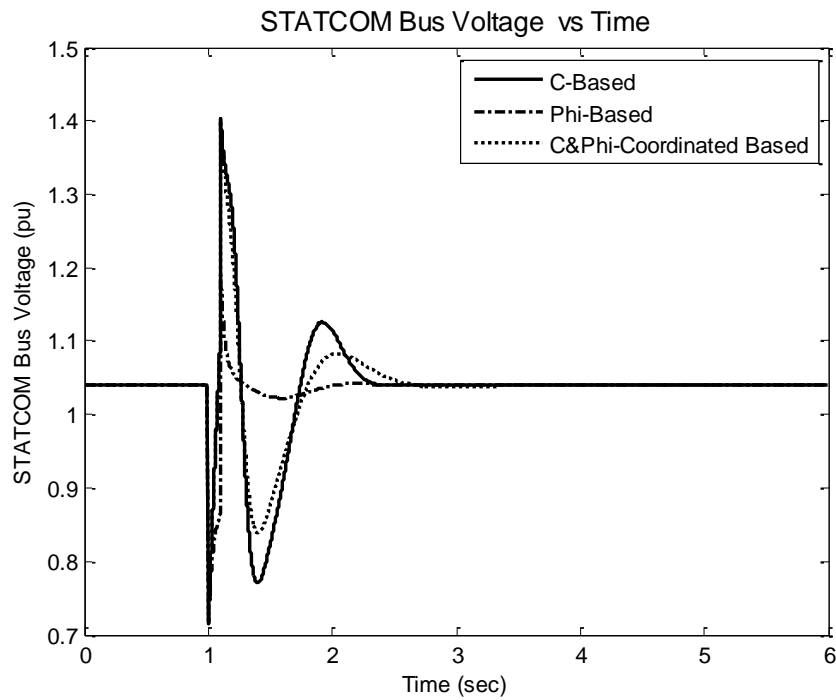


Fig. 5-11 STATCOM bus voltage response for 6-cycle fault with nominal loading C & Φ , individual and coordinated design.

5.2.2 Heavy Loading

Figures (Fig. 5-12 - Fig. 5-19) show the angle deviation, speed deviation, DC voltage, VSC angle, VSC magnitude, electrical power, generator terminal voltage and STATCOM DC voltage responses at heavy operating condition.

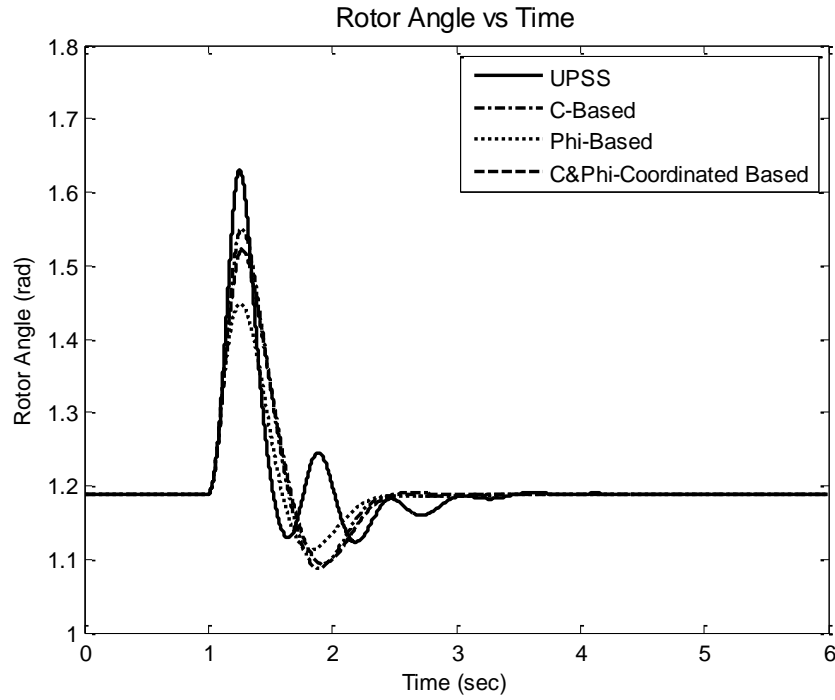


Fig. 5-12 Rotor angle response for 6-cycle fault with heavy loading C & Φ , individual and coordinated design.

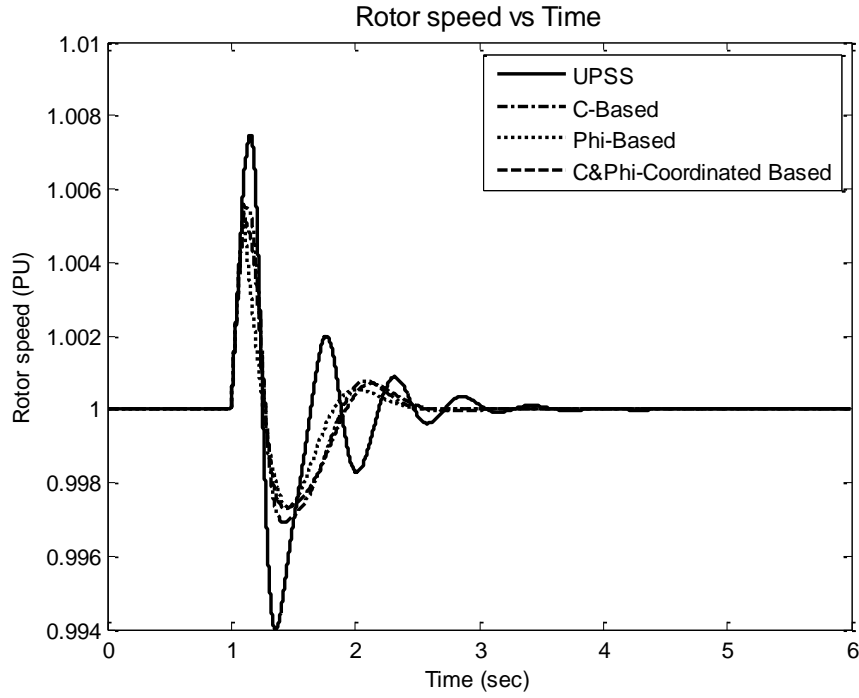


Fig. 5-13 Rotor speed response for 6-cycle fault with heavy loading C & Φ , individual and coordinated design.

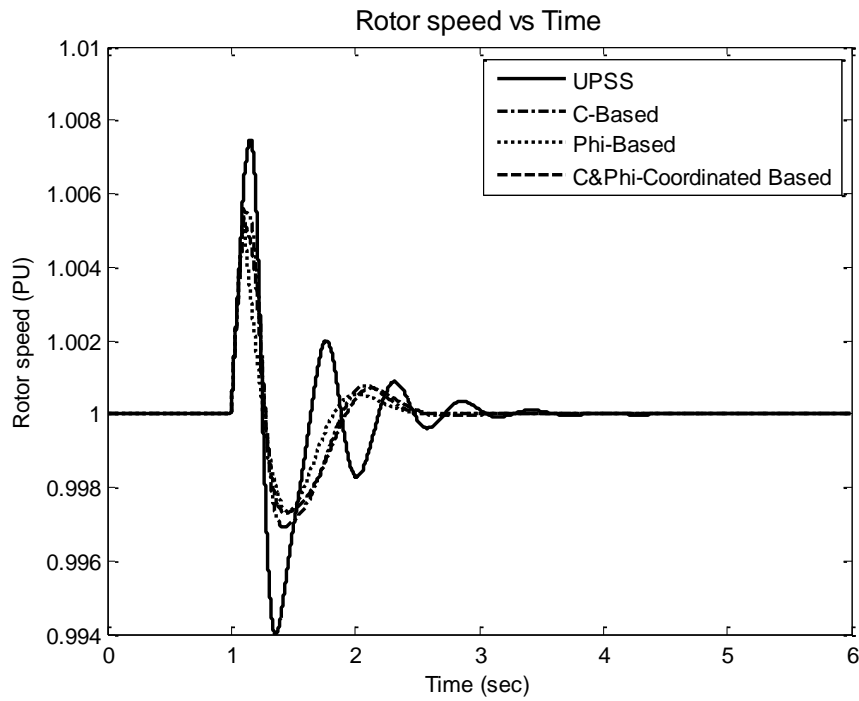


Fig. 5-14 DC voltage response for 6-cycle fault with heavy loading C & Φ , individual and coordinated design.

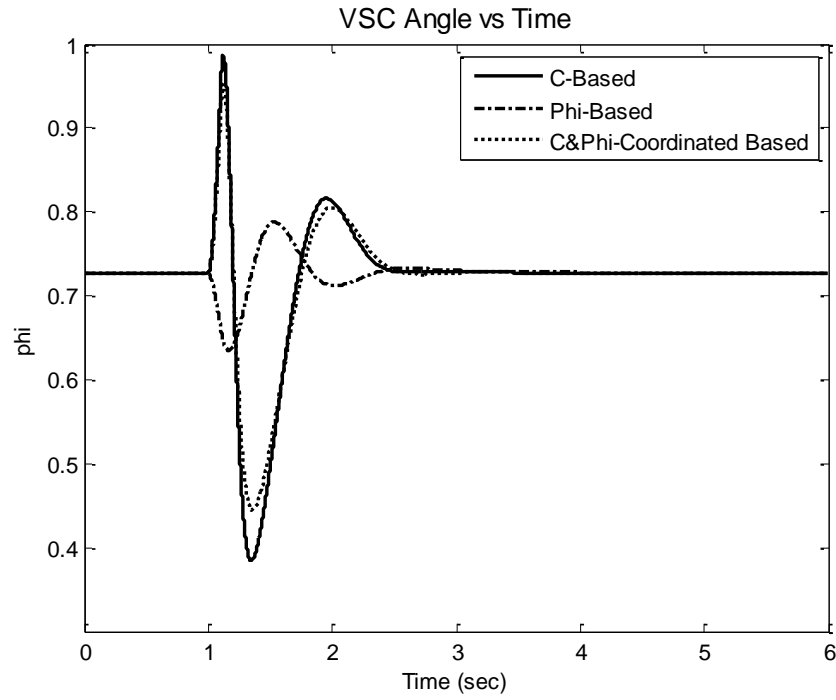


Fig. 5-15 VSC angle response for 6-cycle fault with heavy loading C & Φ , individual and coordinated design.

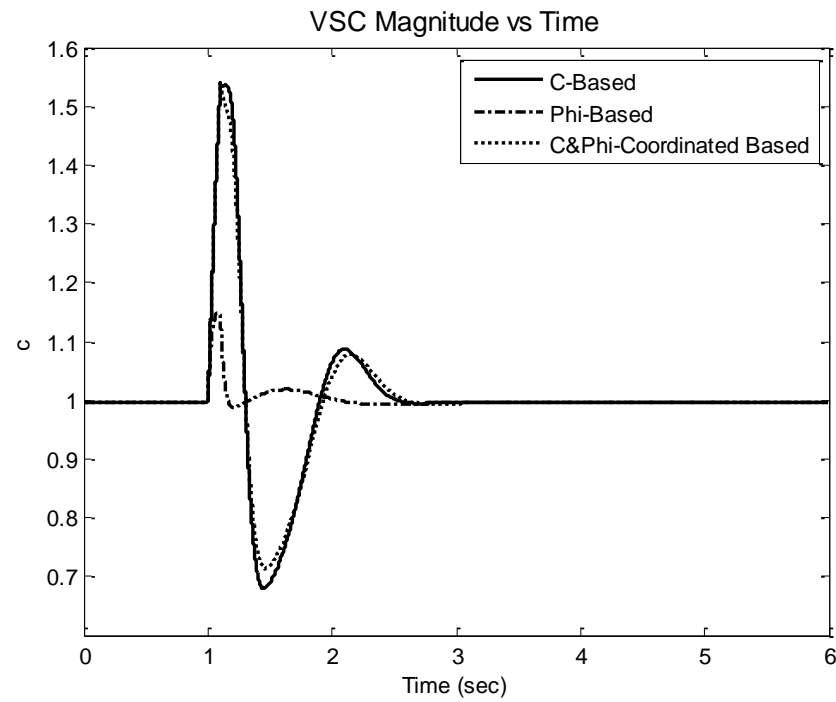


Fig. 5-16 VSC magnitude response for 6-cycle fault with heavy loading C & Φ , individual and coordinated design.

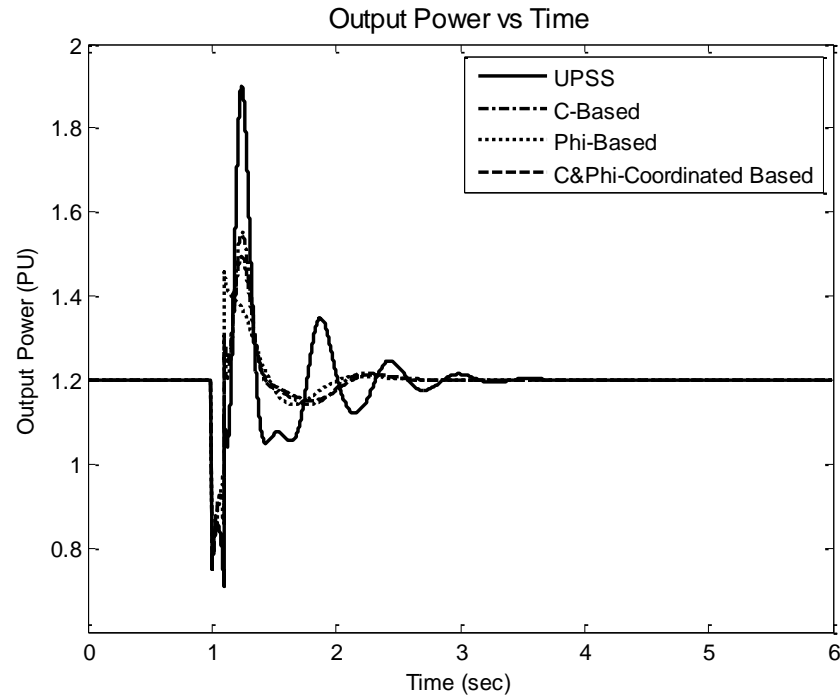


Fig. 5-17 Generator power response for 6-cycle fault with heavy loading C & Φ , individual and coordinated design.

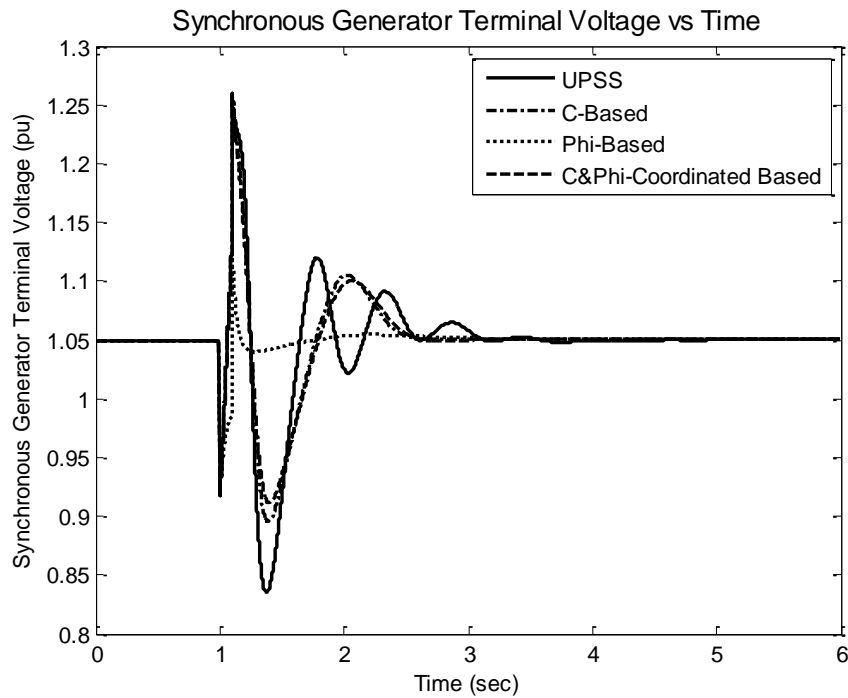


Fig. 5-18 Generator terminal voltage response for 6-cycle fault with heavy loading C & Φ , individual and coordinated design.

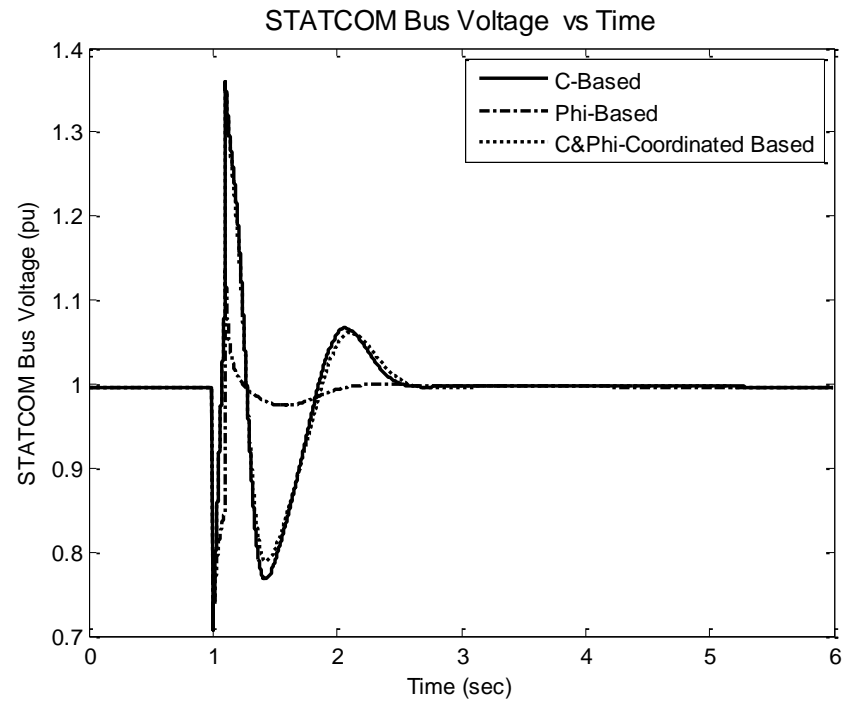


Fig. 5-19 STATCOM bus voltage response for 6-cycle fault with heavy loading C & Φ , individual and coordinated design.

5.2.3 Light Loading

Figures (Fig. 5-20 - Fig. 5-27) show the angle deviation, speed deviation, DC voltage, VSC angle, VSC magnitude, electrical power, generator terminal voltage and STATCOM DC voltage responses at light operating condition.

The coordinated design with Φ solves the problem of very low damping ratio at light loading when C controller is considered.

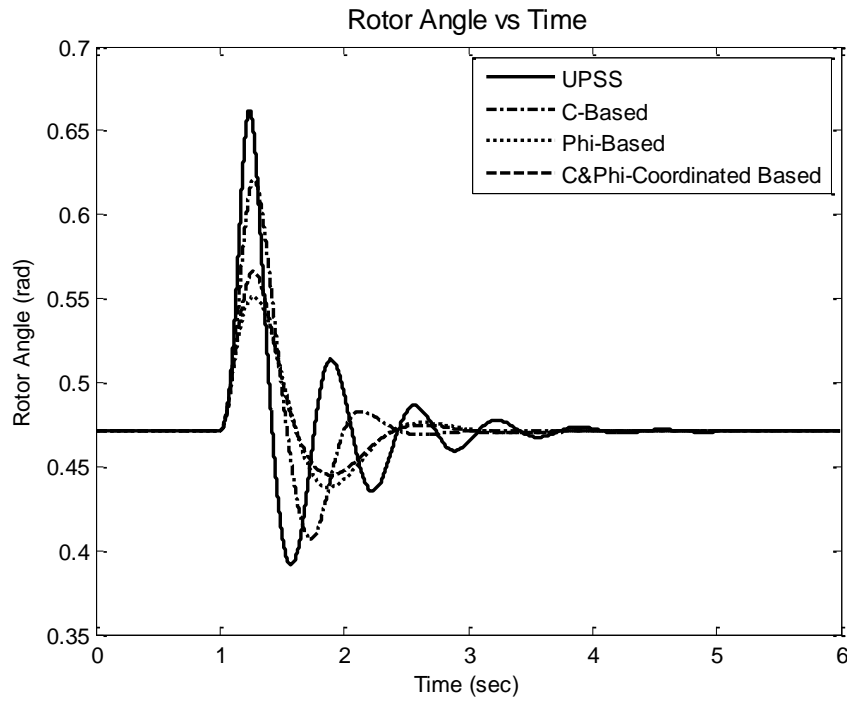


Fig. 5-20 Rotor angle response for 6-cycle fault with light loading C & Φ , individual and coordinated design.

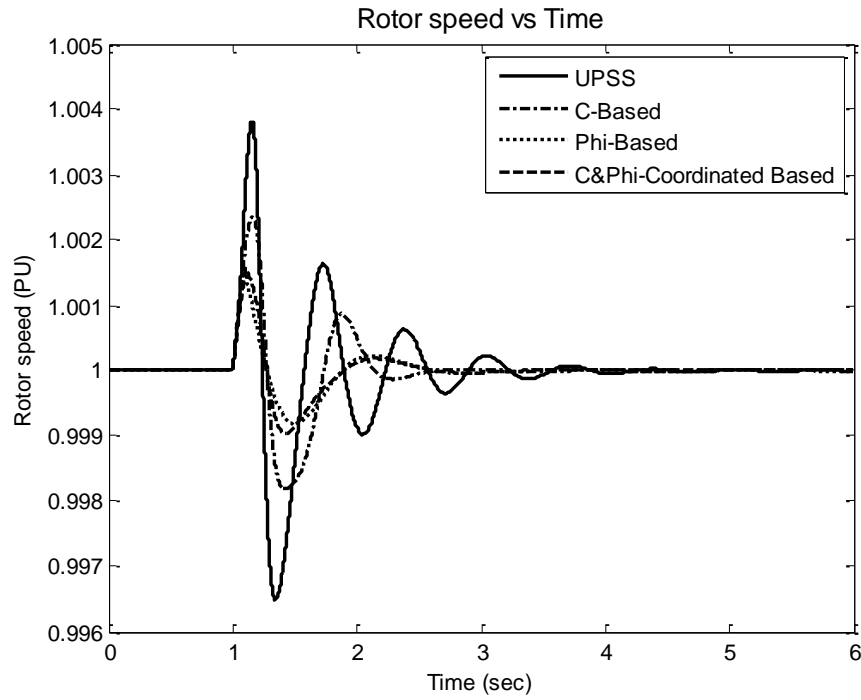


Fig. 5-21 Rotor speed response for 6-cycle fault with light loading C & Φ , individual and coordinated design.

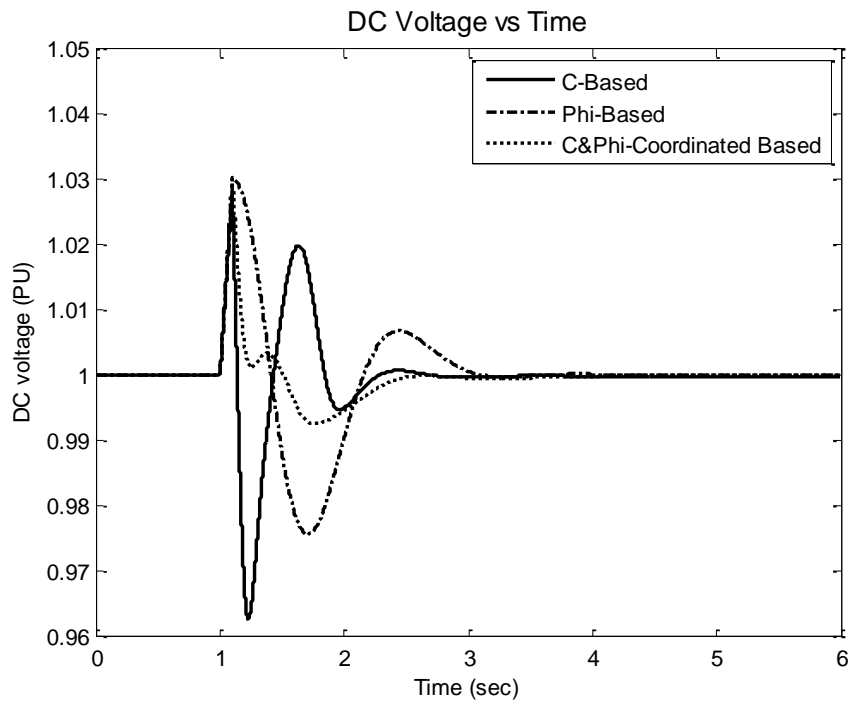


Fig. 5-22 DC voltage response for 6-cycle fault with light loading C & Φ , individual and coordinated design.

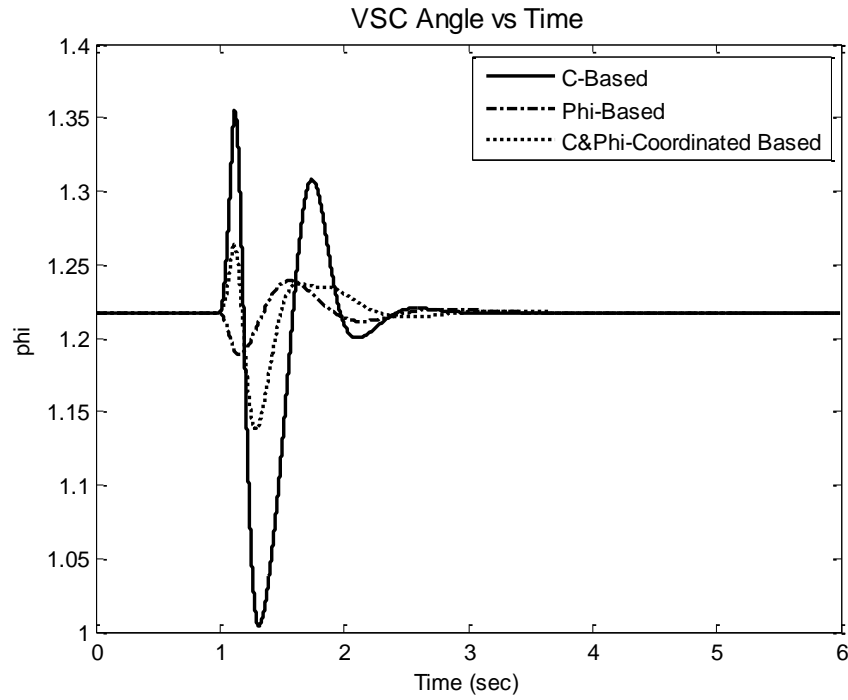


Fig. 5-23 VSC angle response for 6-cycle fault with light loading C & Φ , individual and coordinated design.

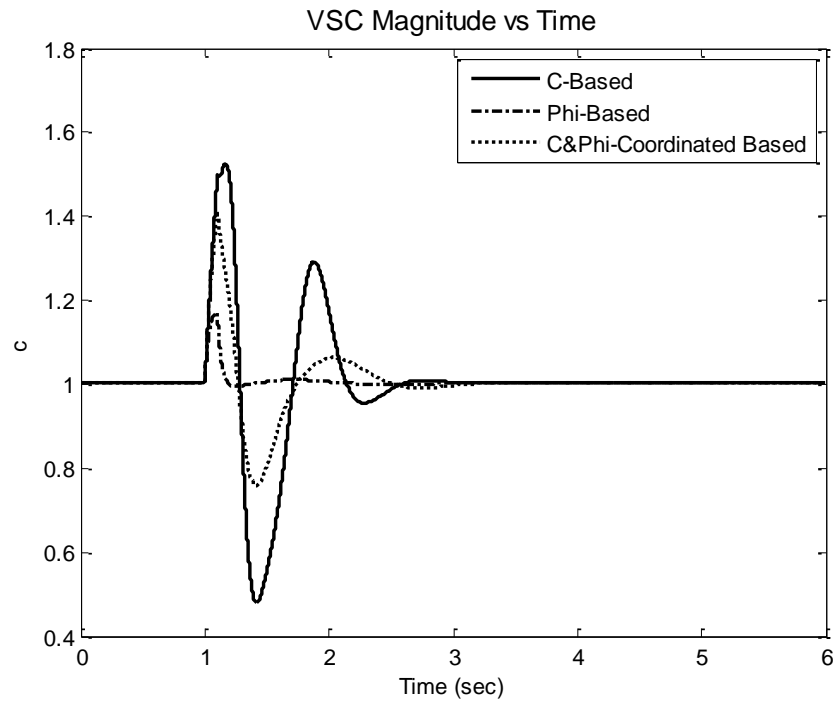


Fig. 5-24 VSC magnitude response for 6-cycle fault with light loading C & Φ , individual and coordinated design.

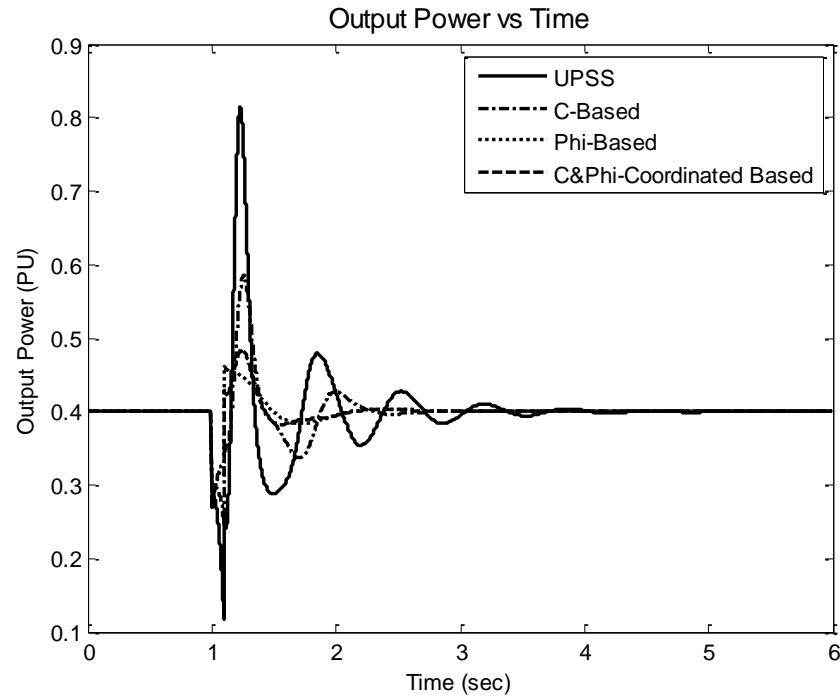


Fig. 5-25 Generator power response for 6-cycle fault with heavy loading C & Φ , individual and coordinated design.

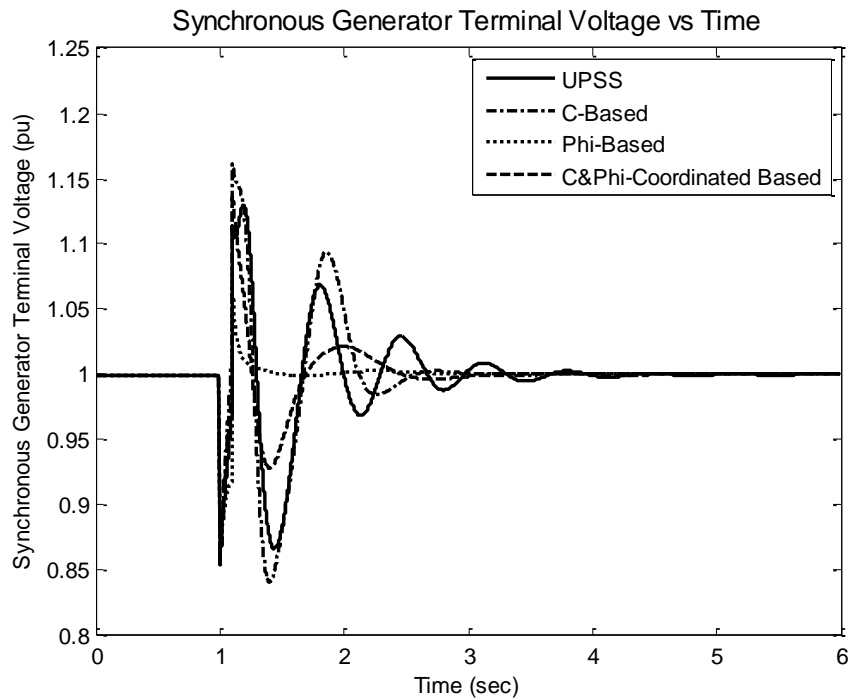


Fig. 5-26 Generator terminal voltage response for 6-cycle fault with light loading C & Φ , individual and coordinated design.

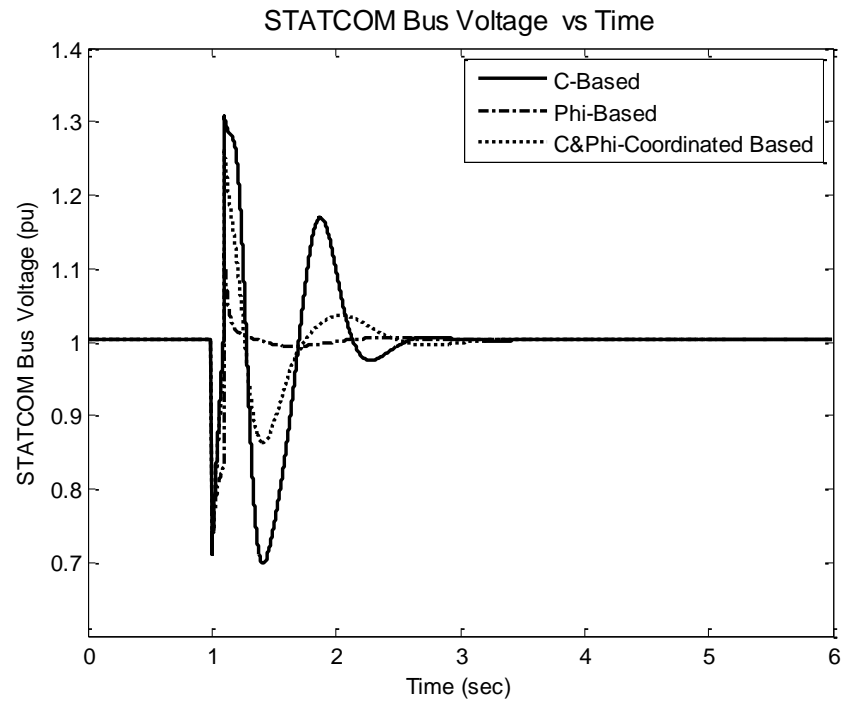


Fig. 5-27 STATCOM bus voltage response for 6-cycle fault with light loading C & Φ , individual and coordinated design.

CHAPTER 6 STATCOM Model in RTDS

and Experimental Setup.

Previously, VSC converters modeled in the RTDS Simulator were restricted to 2-level fixed topology configurations. It was recognized as desirable to allow user configured valve topologies and to be able to accommodate multilevel converters[7].

A technique explored by Hui and Christopoulos, whereby the Dommel network conductance does not need to be decomposed or inverted during the simulation, was implemented [11][12]. The paper describes new developments in the RTDS Simulator with particular focus on the simulation of multilevel VSCs using PWM control. The work conducted clearly shows that the RTDS Simulator can be relied upon to accurately test VSC firing pulse controls using PWM frequencies in the range of 1500 Hz. [7].

When a real time digital simulator, emulating a switched circuit such as a voltage source converter, is interfaced with a digital controller, the controller's firing signals may not be in synchronism with the simulation time step. Several methods to minimize the resulting inaccuracies have been proposed in the past. However, some of these approaches introduce unnecessary delays and/or generate artificial harmonics.

K. L. Lian and P. W. Lehn [13] presented a method based on Time Averaging is presented the Real Time Digital Simulator (RTDS) by RTDS Technologies, Inc [12] are widely used for real time simulations and hardware-in-the-loop experimental applications. The RTDS main network is solved with a typical time-step size of about 50 μ s. Recently, RTDS added the capability of

simulating power electronic switches used in Voltage Source Converters (VSC) on GPC (Gigabyte Processing Card) with significantly smaller time steps from 1.4 to 2.5 μ s.

The basic modeling principle adopted for the switches in the RTDS small timestep environment as described by Maguire et al cause inherent artificial losses. The small time-step switches can be easily interfaced to the main network solution [10]. Actual power electronic switches are not ideal and dissipate power in their applications. Power loss of power electronics switch models in transient simulation programs have been analyzed by some researchers [149][150]. The dependencies of these losses from simulation parameters have already been studied by the authors using a simple DC/DC converter as an example [151]. From a theoretical study it was found that reducing the damping factor and simulation time-step can reduce switching loss. The accompanying sensitivity study verified that inappropriate switch parameters, such as large damping factors, voltages and currents very different from their rated values can contribute to excessive artificial power loss in the switches.

In addition, low switch voltage and high switch current can reduce the Total Harmonic Distortion (THD) in the switch models in the RTDS small time-step environment. With increasing number of switches in power electronic apparatus representation and verification of the model, and the required power loss analysis become more complicated compared to the system studied in [151].

In [9] conclusions from the previous study and extends the previous investigation on validating a five-level STATic synchronous COMpensator (STATCOM) model implemented in the RTDS small time-step environment. STATCOM devices can provide controllable reactive power (VAR) support for dynamic voltage control with their actively controllable VAR injection, especially under voltage depression.

Control-Hardware-In-Loop (CHIL) testing for the STATCOM controller, which is currently carried out at the Center for Advanced Power Systems (CAPS) at Florida State University (FSU), is required by the host utility before the field deployment of the STATCOM. The details of the CHIL testing and the preliminary results are shown in [152]. For the purpose of the CHIL testing, an appropriate five-level voltage source converter (VSC) model is required in RTDS for testing the STATCOM controller with RTDS in a closed loop experiment. Some constraints, such as the number of the D/A output interface channels on the GPC cards, limit the number of switches modeled on each GPC and thus complicate the STATCOM model implementation on the RTDS.

6.1 LABORATORY SETUP FOR RTDS SIMULATION

In this section, the system model shown in Fig. 3-1 is implemented in Real Time Digital Simulator using RSCAD System Modeling. The model in RTDS environment has been developed as single machine infinite bus system which contains synchronous machine, transmission lines, local loads, STATCOM with its VSC and power storage , phasor measurement units and their control schemes. The schematic diagram of the system is shown in Fig. 6-1.

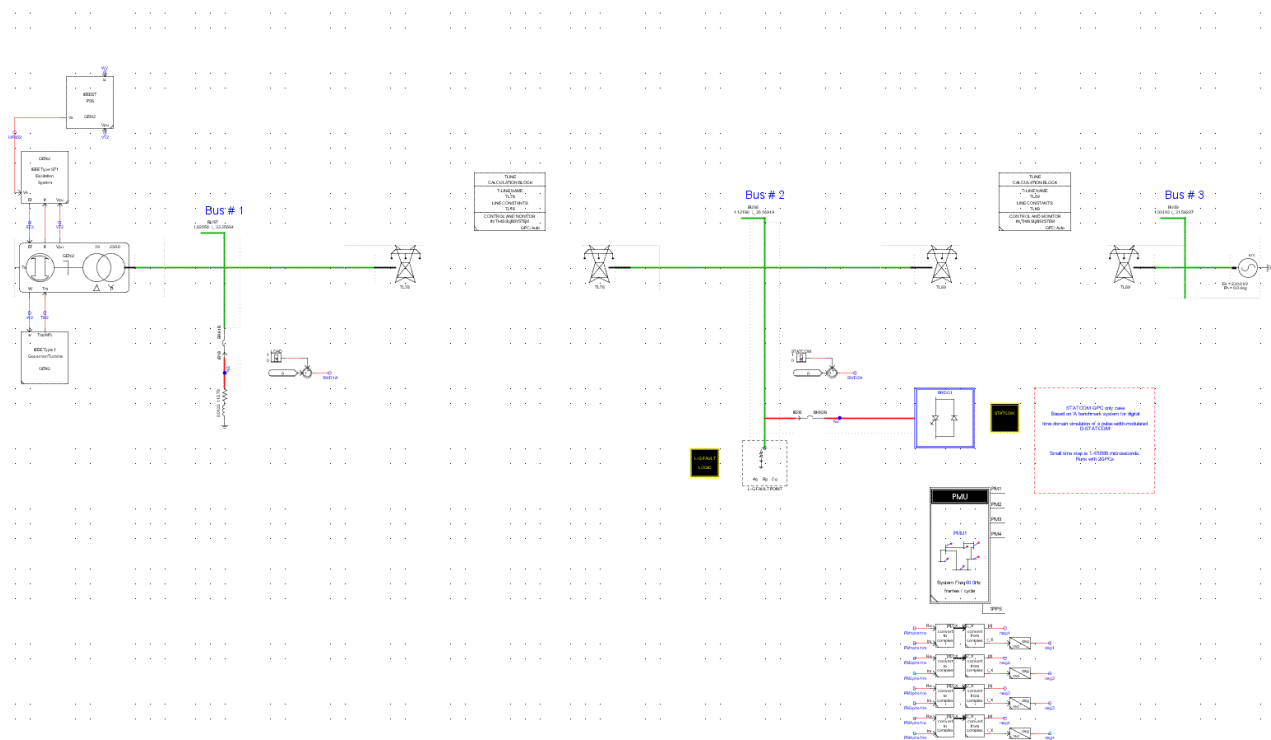


Fig. 6-1 Schematic diagram of single machine infinite bus system with STATCOM.

6.1.1 The Generator Model

The synchronous machine model used in this study as described in Fig. 6-2 allows both the exciter and governor turbine interfaces which used for the machine control system. the machine parameters used in this model are specified in Appendix D - Table 8.

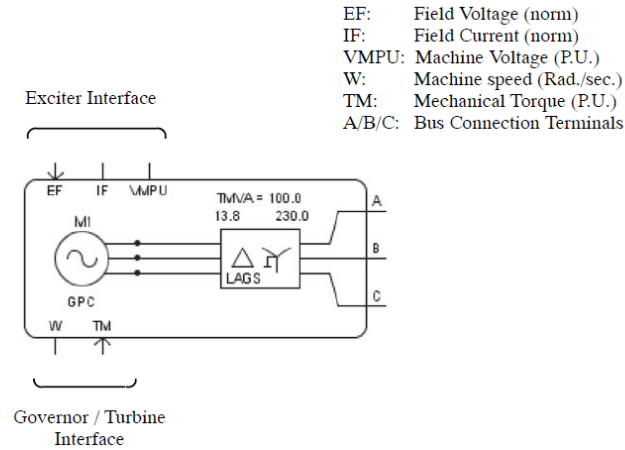


Fig. 6-2 Synchronous machine model with transformer in RSCAD.

6.1.2 Exciter and power system stabilizer (PSS) model.

Exciter model represents a static excitation system whose source voltage is derived from the generator terminals through a transformer. The exciter maximum output voltage is thus limited by the source voltage. The fixed gain K_a assumes that the rectifier controller of the static excitation system being represented includes an inverse cosine function to linearize the exciter gain. Both the block diagram of the PSS is shown in Fig. 6-3 and its controller parameters are listed in Appendix D - Table 9.

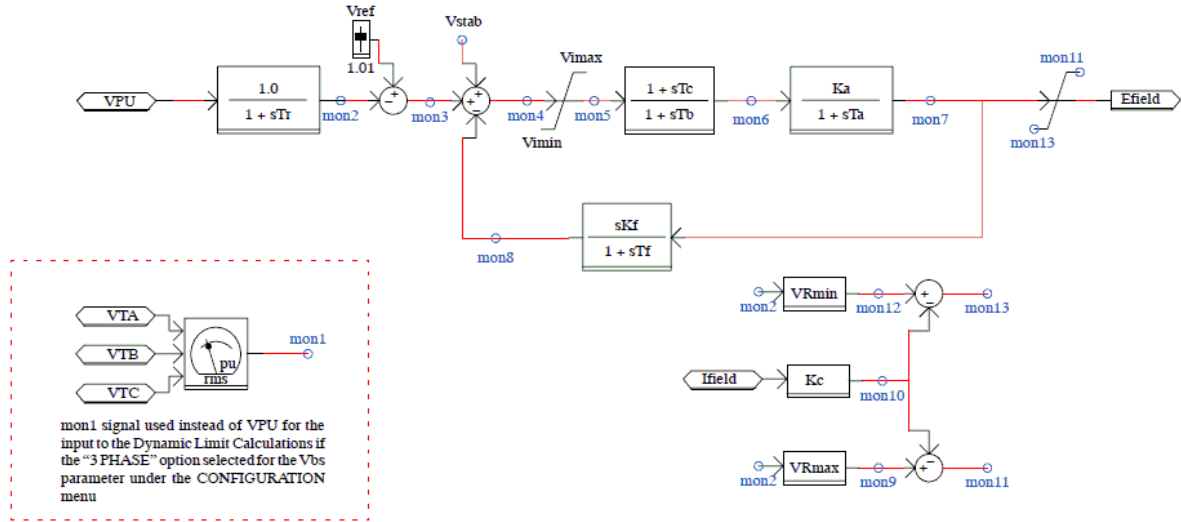


Fig. 6-3 IEEE Type ST1 Excitation System Model.

6.1.3 The Transmission Lines Model.

Travelling wave transmission line model is used to represent transmission lines on the RTDS. However, travelling wave models are generally preferred rather than other models such as PI model unless the line in the system is very short, in which case a PI section model must be used.

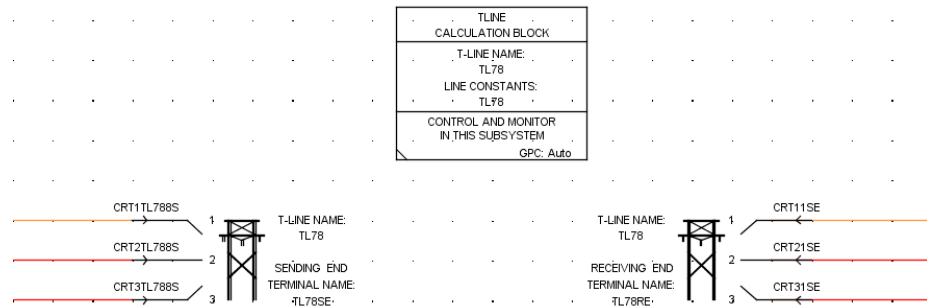


Fig. 6-4 The system's transmission line diagram.

6.1.4 The STATCOM Model and its Controllers.

The RTDS model of STATCOM was designed to meet the required MVA needed at the most dazedness cases, in order to compensate the required real and reactive power desired by the grid network to be sustained during the fault, the STATCOM rating used in the system proposed is listed in Appendix D - Table 11. the STATCOM components such as Voltage storage capacitors, VSC with its controllers, Filters and coupling transformers are shown in Fig. 6-5. The STATCOM voltage and current regulation controller is shown in Fig. 6-6. The rest controlling block diagram like modulating signals generator and the phase locked loop (PLL) used to provide the transformation angle and magnitude for the triangular waves used to generate the firing pulses are explained in Fig. 6-8 and Fig. 6-7 respectively.

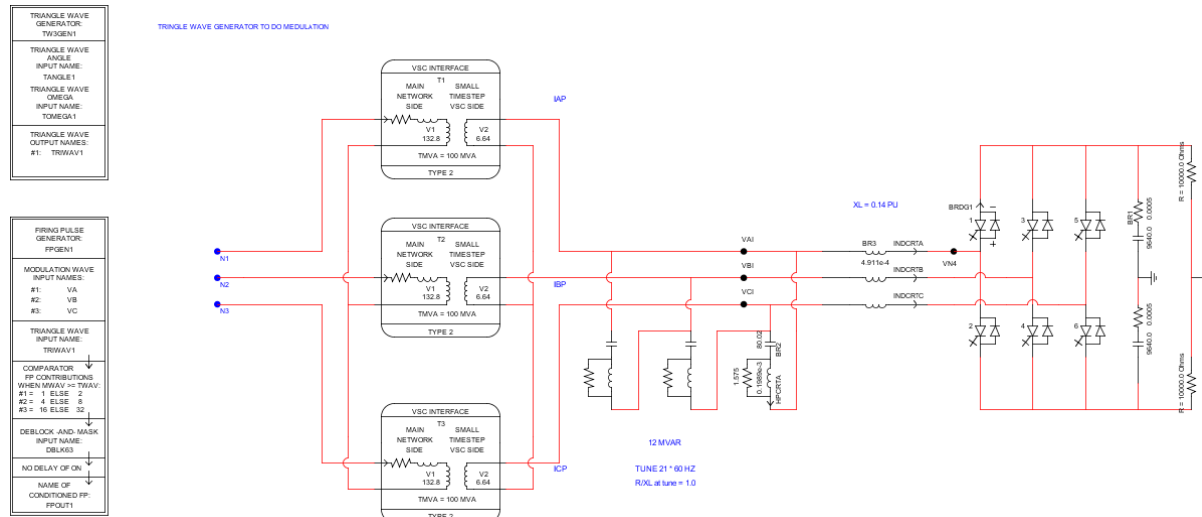


Fig. 6-5 Modeling of STATCOM with its VSC in Small Time Step including pulse and triangle wave generators.

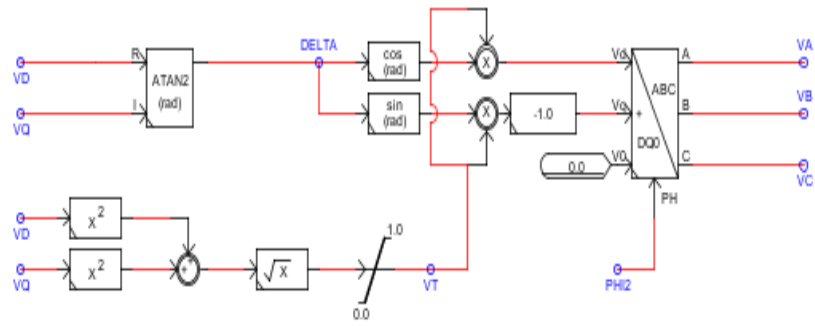


Fig. 6-8 Modulating Signal Generation - DQ to ABC transformation of the STATCOM bus voltage signals in RTDS.

CHAPTER 7 RTDS Experimental Results

In this chapter a comparative study of individual application of the damping stabilizers is investigated and assessed, the RSCAD model shown in Fig. 6-1 is considered for nonlinear simulation studies using RTDS. Different faults scenarios in 10-cycle duration are applied on the STATCOM bus, at a wide loading conditions, to study the performance of the proposed controllers.

Similarly to what have been stated previously in the simulated results about the improvement on the transient stability due to the STATCOM and its proposed novel approached controllers, the C-based shows better performance in terms of overshoot and settling time than UPSS alone. While there is an excellent improvement in the system response when Φ -based and coordinated design is considered.

7.1 Rotor Speed Deviation Response for Different Loading Conditions

under several disturbances.

In this section the simulation results of the rotor speed deviation due to the entire proposed controllers are illustrated all to gather in the same plot for different faults circumstances and in all kind of loading conditions nominal, heavy and light.

7.1.1 Nominal Loading

Figures (Fig. 7-1 - Fig. 7-3) show the speed deviation responses for each proposed controller UPSS, C-based alone, Φ -based alone and C& Φ coordinated-based at a nominal loading condition. it is very clear that Φ -based controller shows better performance since it is controlling the real power injected to the system during the disturbance which would enhance significantly the system damping.

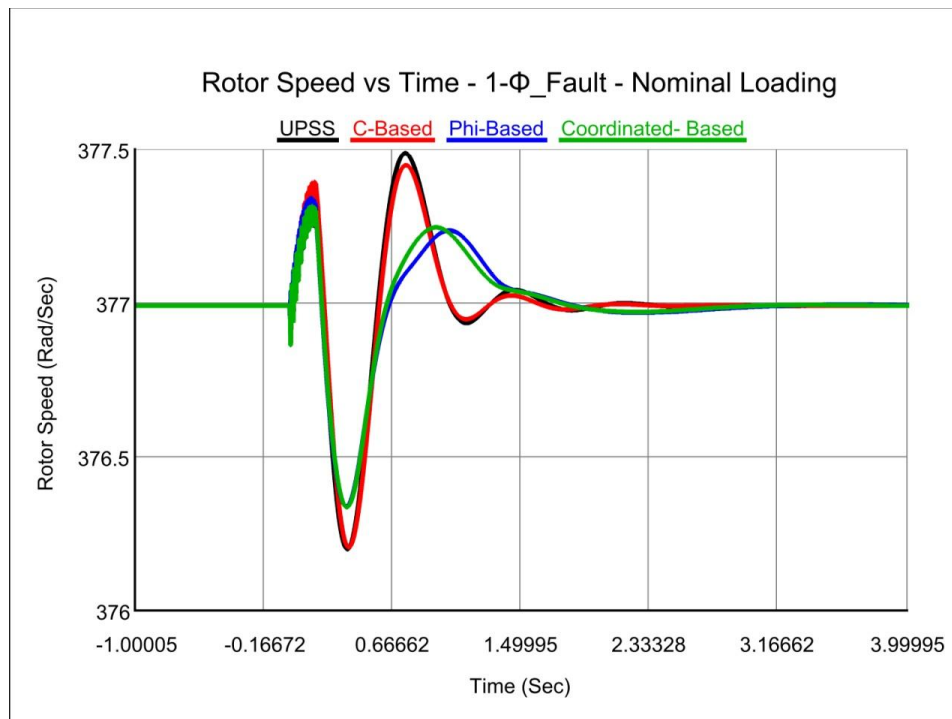


Fig. 7-1 Rotor speed response for 1- Φ fault - nominal loading.

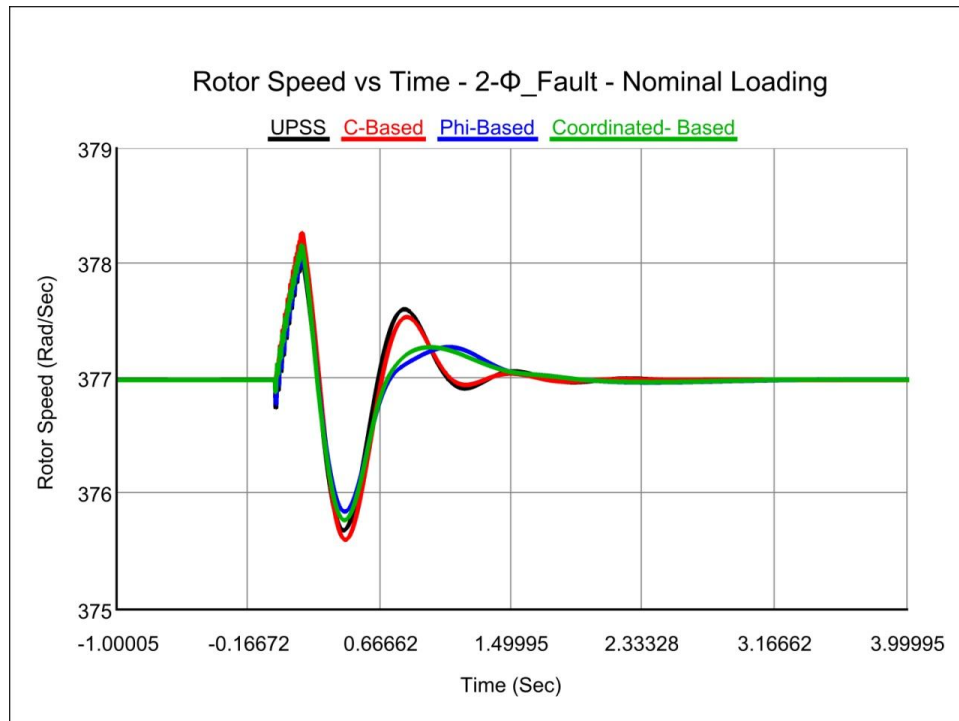


Fig. 7-2 Rotor speed response for 2- Φ fault - nominal loading.

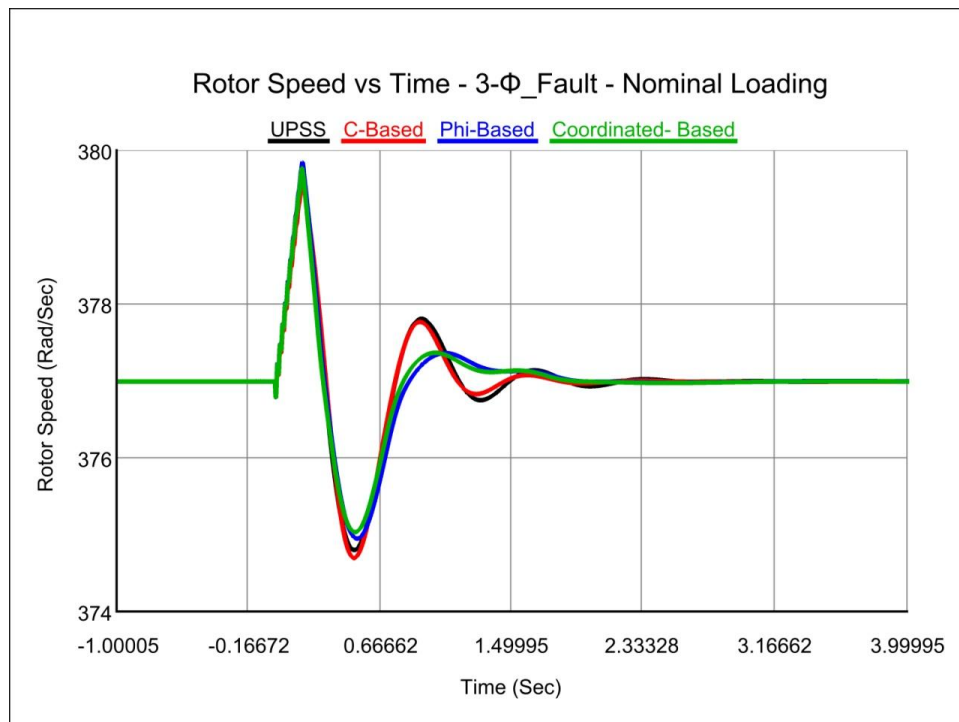


Fig. 7-3 Rotor speed response for 3- Φ fault - nominal loading.

7.1.2 Heavy Loading

Figures (Fig. 7-4 - Fig. 7-6) show the speed deviation responses for each proposed controller UPSS, C-based alone, Φ -based alone and C& Φ coordinated-based at a heavy loading condition.

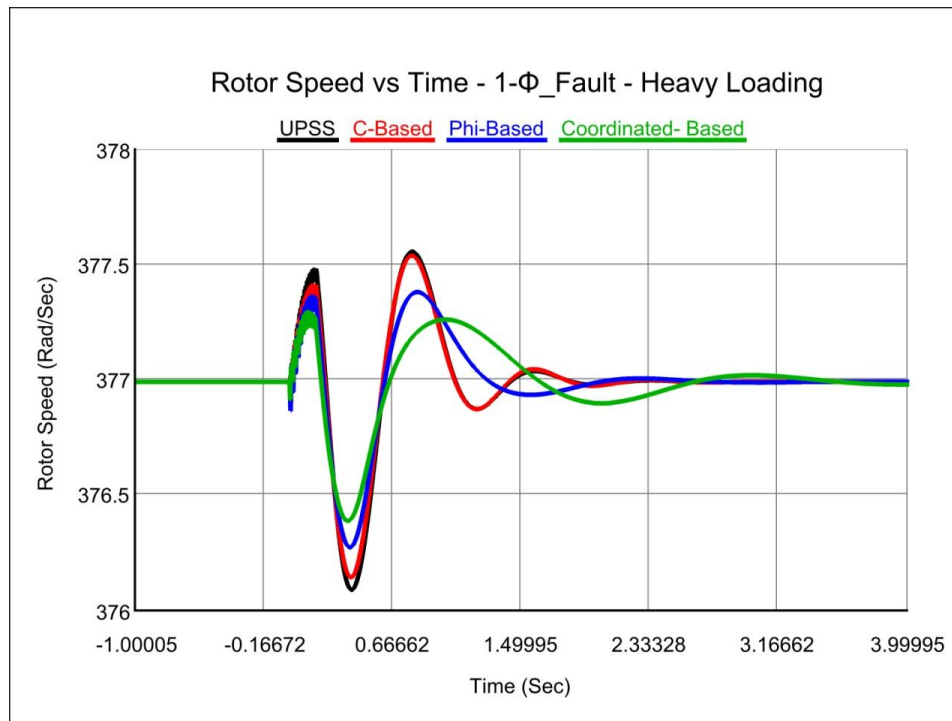


Fig. 7-4 Rotor speed response for 1- Φ fault - heavy loading.

The rotor speed response shown in Fig. 7-4 clearly indicates how the settling time is slightly longer in a heavy loading condition than it is in a nominal loading case, while the overshoot is controlled to be maximum in 377.5 rad/sec in both cases.

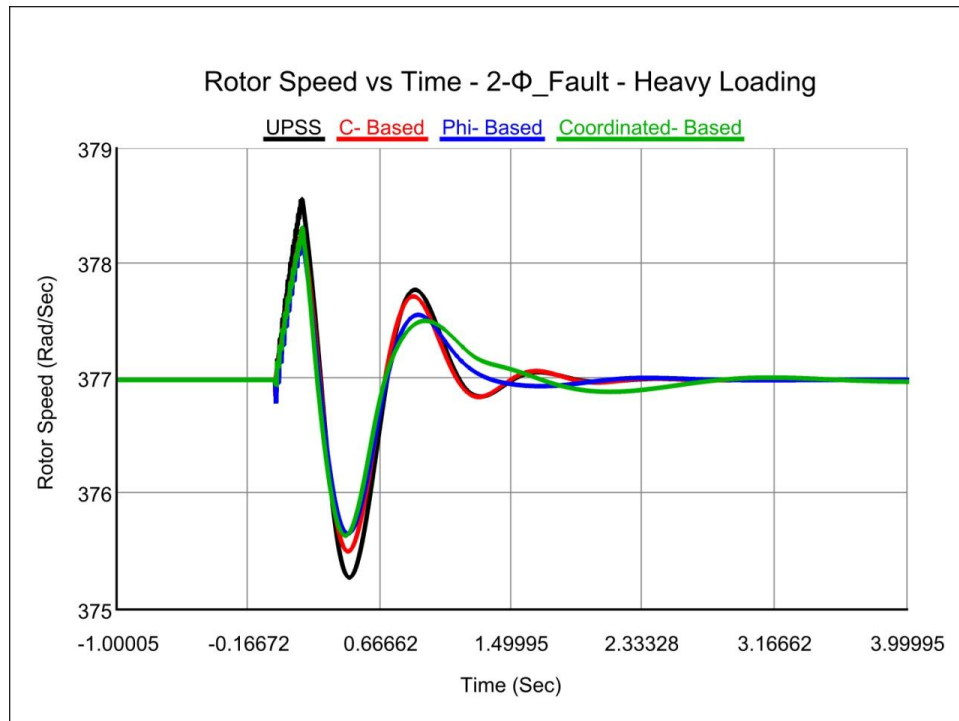


Fig. 7-5 Rotor speed response for 2- Φ fault - heavy loading.

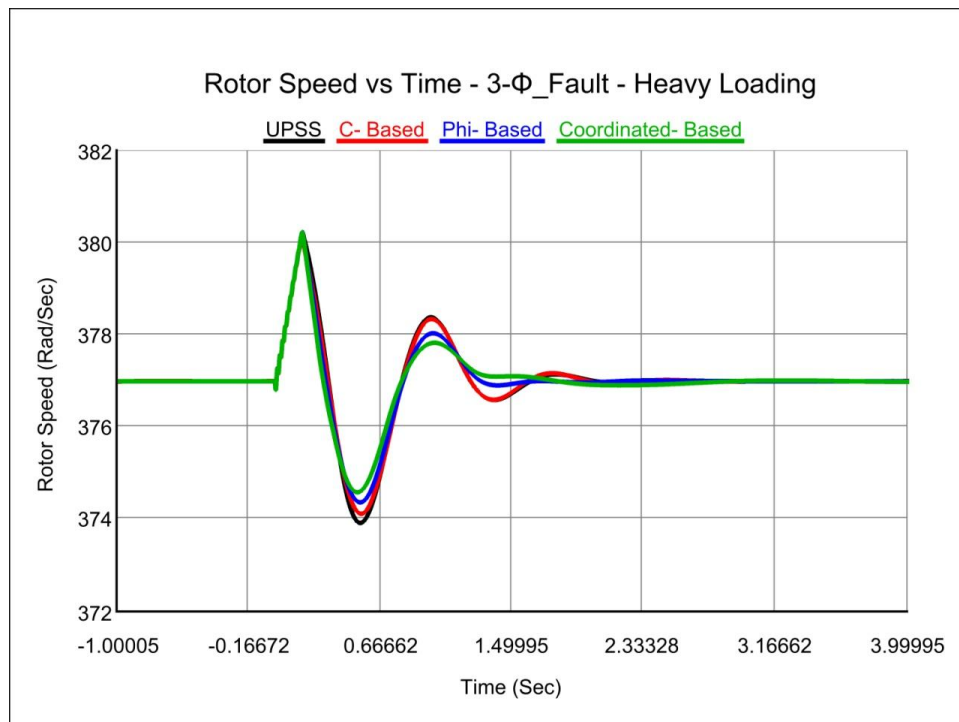


Fig. 7-6 Rotor speed response for 3- Φ fault - heavy loading.

7.1.3 Light Loading

Figures (Fig. 7-7 - Fig. 7-9) show the speed deviation responses for each proposed controller UPSS, C-based alone, Φ -based alone and C& Φ coordinated-based at a light loading condition.

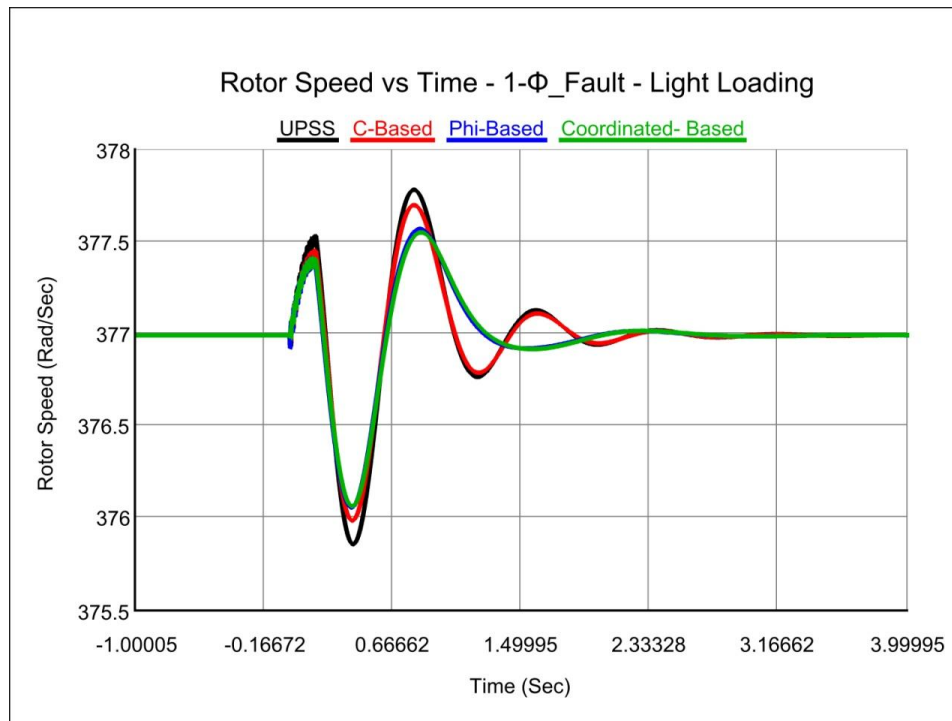


Fig. 7-7 Rotor speed response for 1- Φ fault - light loading.

Throughout the light loading operating condition, the system's controllers are tested to insure its validity to operate in all loading circumstances. The rotor speed response gets better when the phase angle based controller and both phase and magnitude based controller is applied.

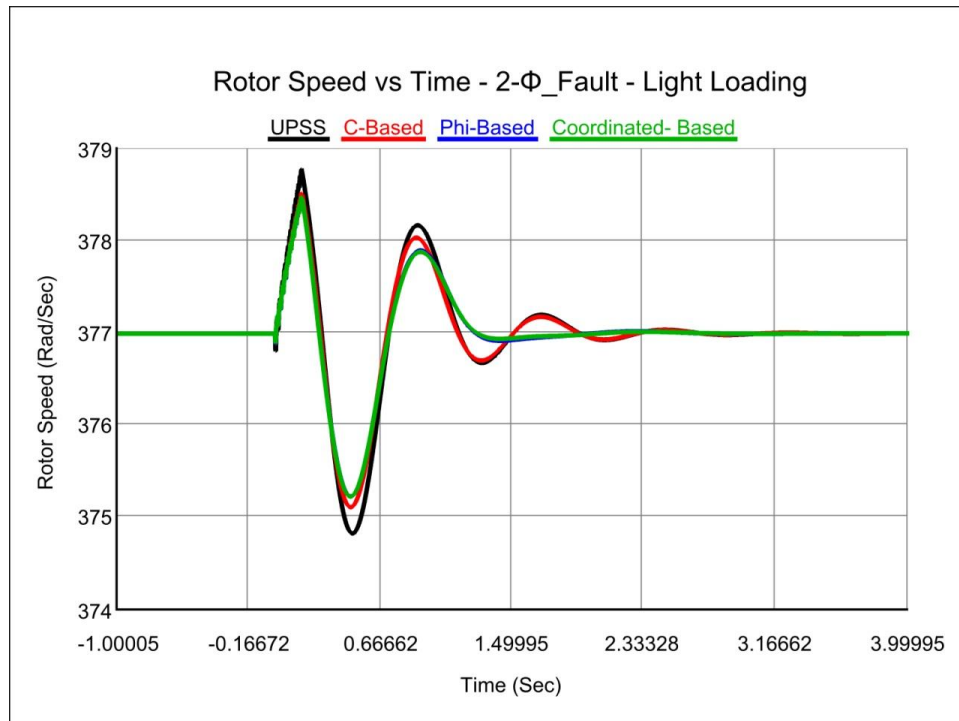


Fig. 7-8 Rotor speed response for 2- Φ fault - light loading.

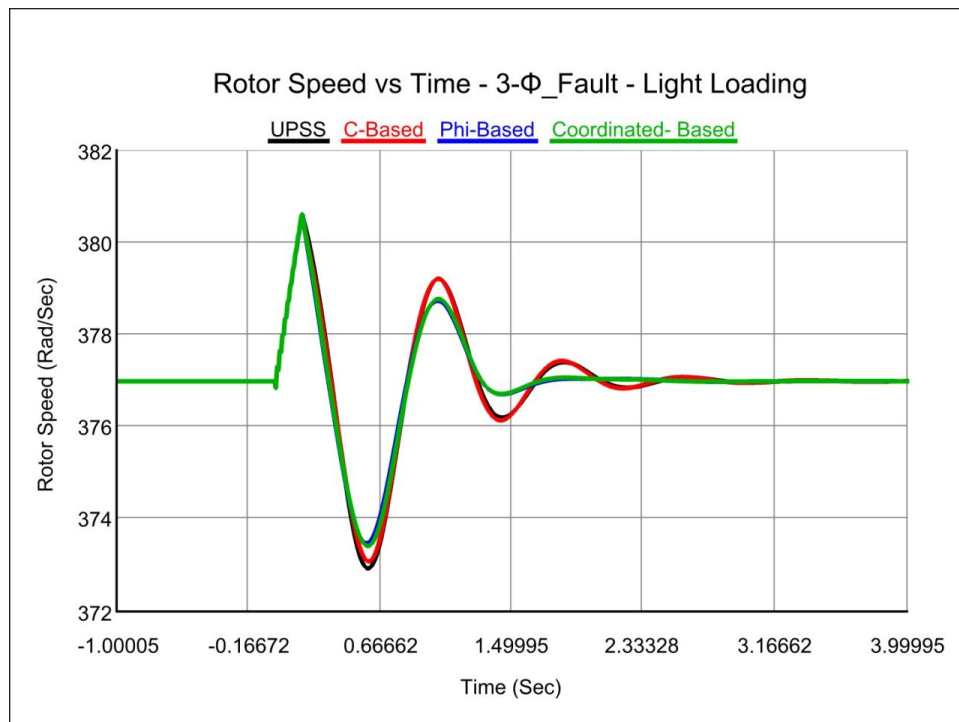


Fig. 7-9 Rotor speed response for 3- Φ fault - light loading.

7.2 Generator Terminal Voltage for Different Loading Conditions under several disturbances

In this section the simulation results of the generator terminal voltage deviation due to the entire proposed controllers are illustrated all to gather in the same plot for different faults circumstances and in all kind of loading conditions nominal, heavy and light.

7.2.1 Nominal Loading

Figures (Fig. 7-10 - Fig. 7-12) show the generator terminal voltage deviation responses for each proposed controller UPSS, C-based alone, Φ -based alone and C& Φ coordinated-based at a nominal loading condition. From these figures it evidently indicate the large voltage drop due to the fault occurred in the STATCOM bus, the system is recovered and reach the study state condition in less than two seconds only.

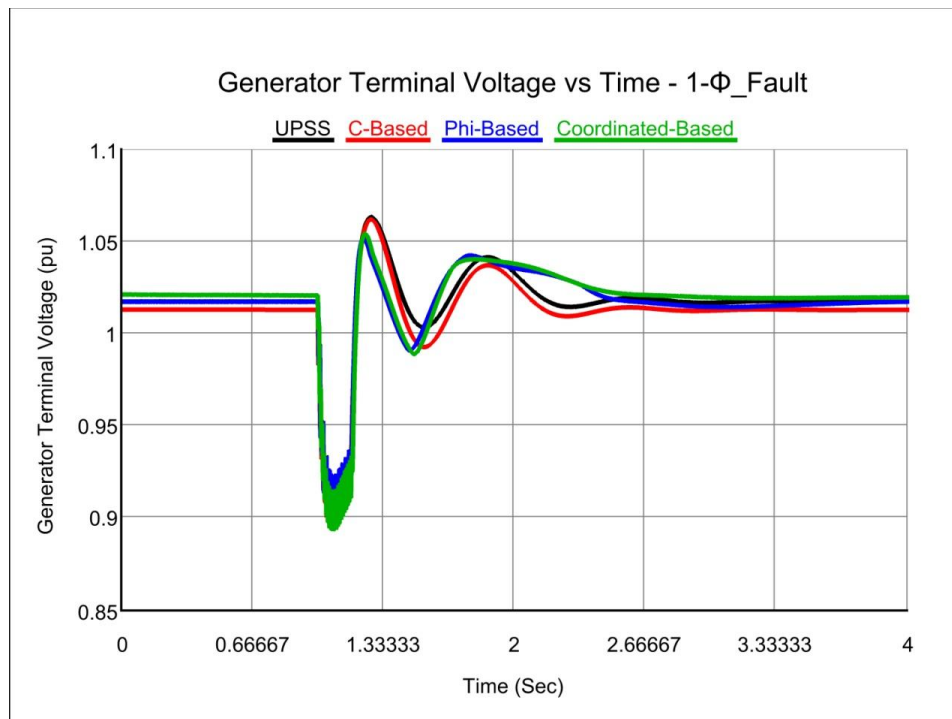


Fig. 7-10 Generator terminal voltage response for 1- Φ fault - nominal loading.

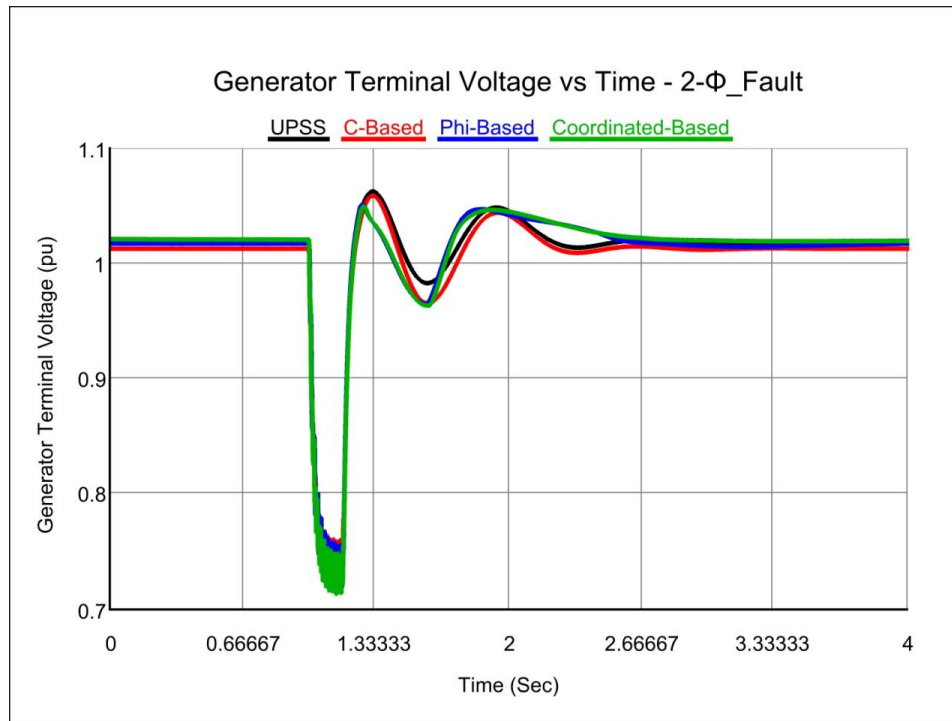


Fig. 7-11 Generator terminal voltage response for 2- Φ fault - nominal loading.

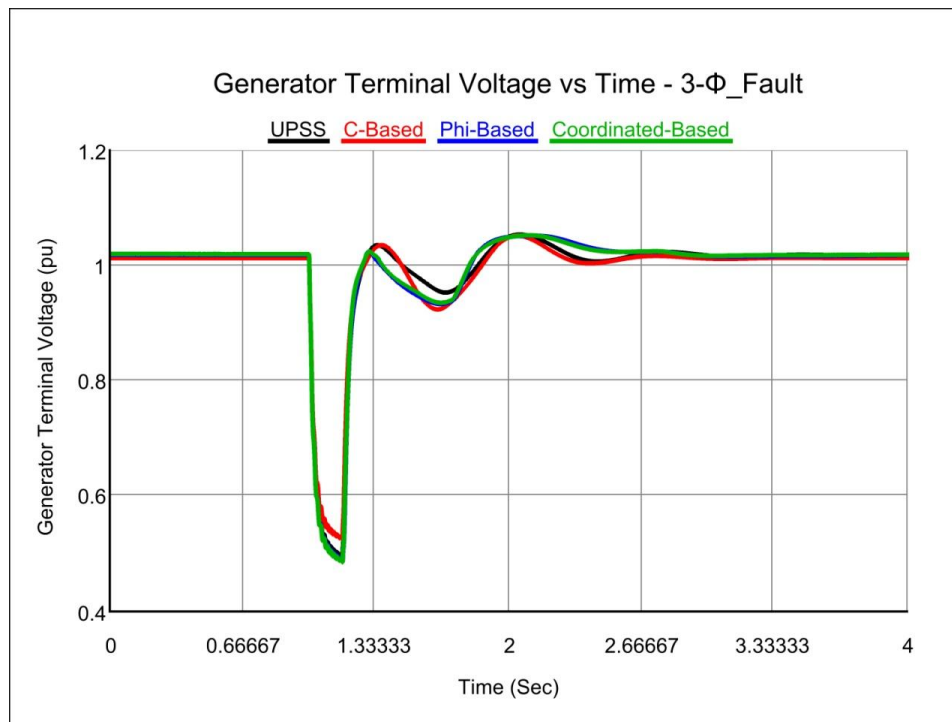


Fig. 7-12 Generator terminal voltage response for 3- Φ fault - nominal loading.

7.2.2 Heavy Loading

Figures (Fig. 7-13 - Fig. 7-15) show the generator terminal voltage deviation responses for each proposed controller UPSS, C-based alone, Φ -based alone and C& Φ coordinated-based at a heavy loading condition.

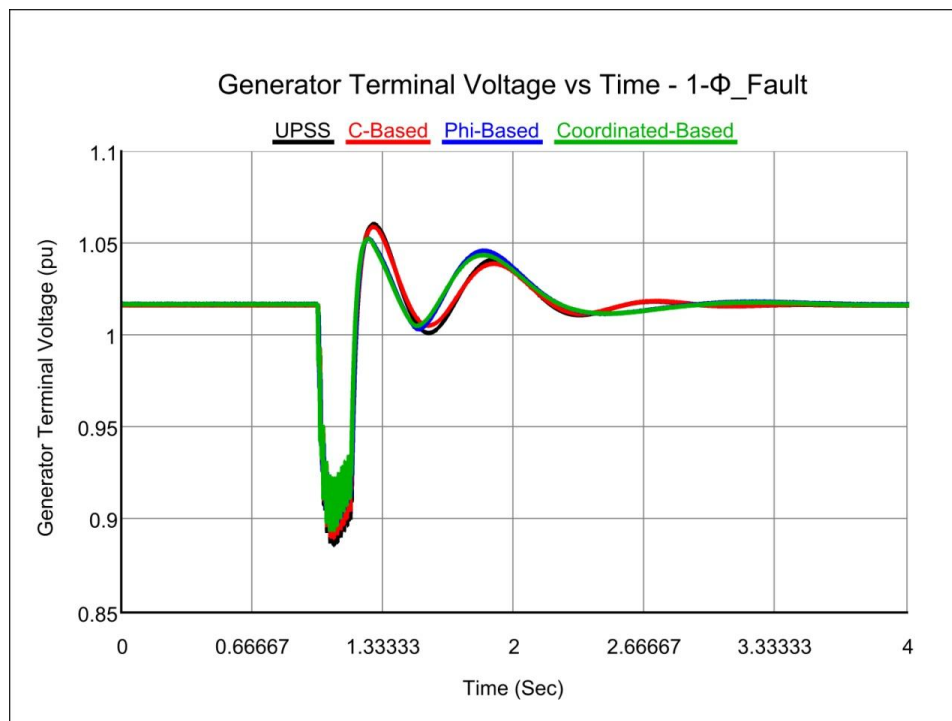


Fig. 7-13 Generator terminal voltage response for 1- Φ fault - heavy loading.

The terminal voltage response due to 3- Φ fault shown in Fig. 7-15 points out an immense enrichment in terms of damping the oscillations as well as reducing the voltage drop in the system controlled by Φ -based controller alone. However, the performance of the other approaches doesn't really show any significant difference on their ability to damp the oscillations and improve the system's stability.

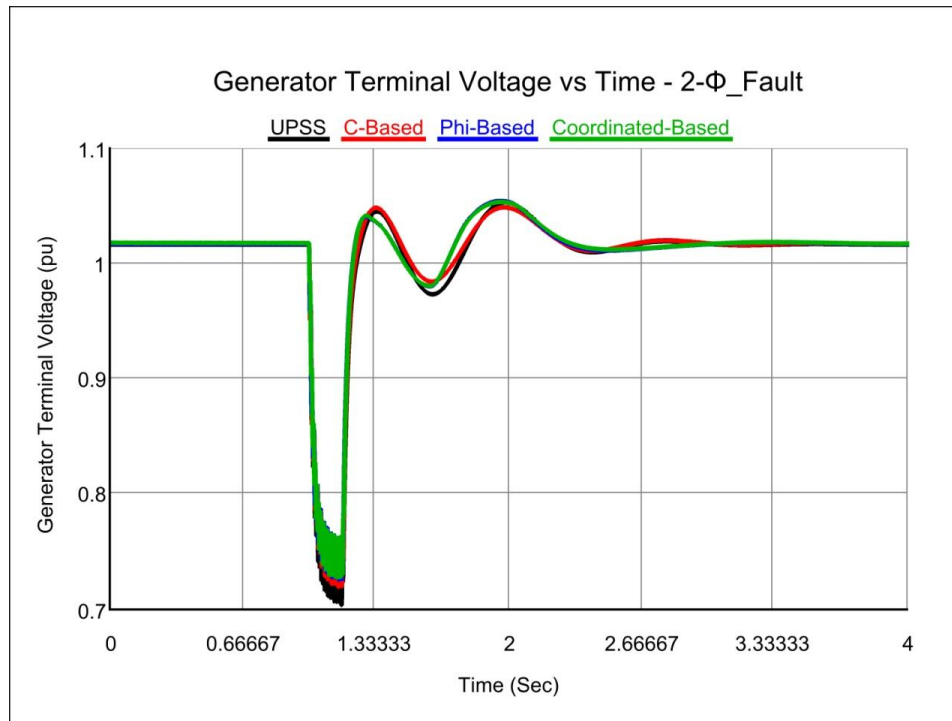


Fig. 7-14 Generator terminal voltage response for 2- Φ fault - heavy loading.

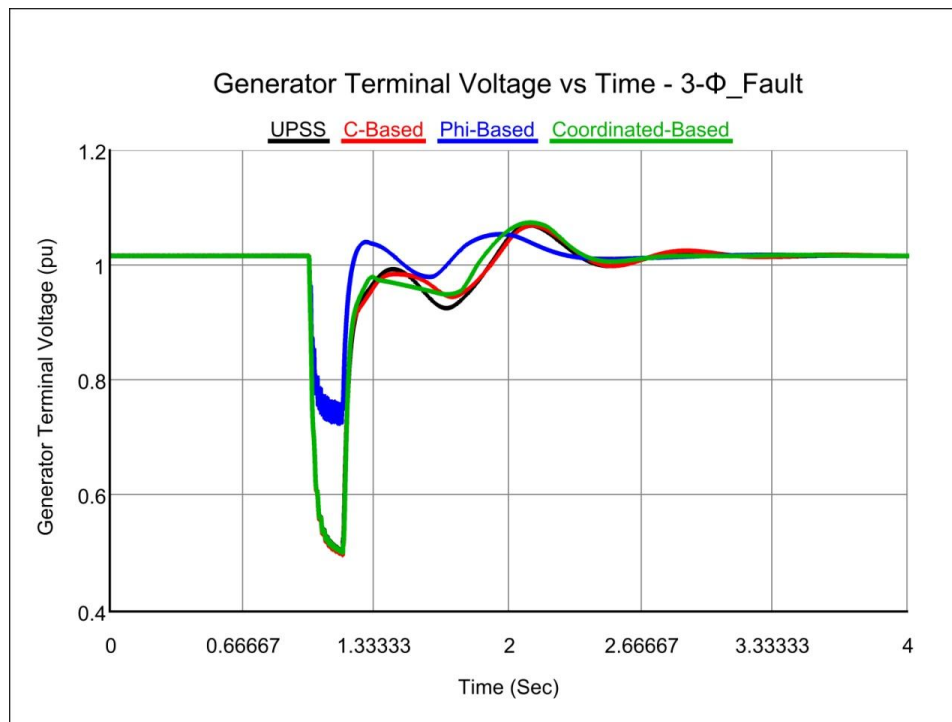


Fig. 7-15 Generator terminal voltage response for 3- Φ fault - heavy loading.

7.2.3 Light Loading

Figures (Fig. 7-16 - Fig. 7-18) show the generator terminal voltage deviation responses for each proposed controller UPSS, C-based alone, Φ -based alone and C& Φ coordinated-based at a light loading condition.

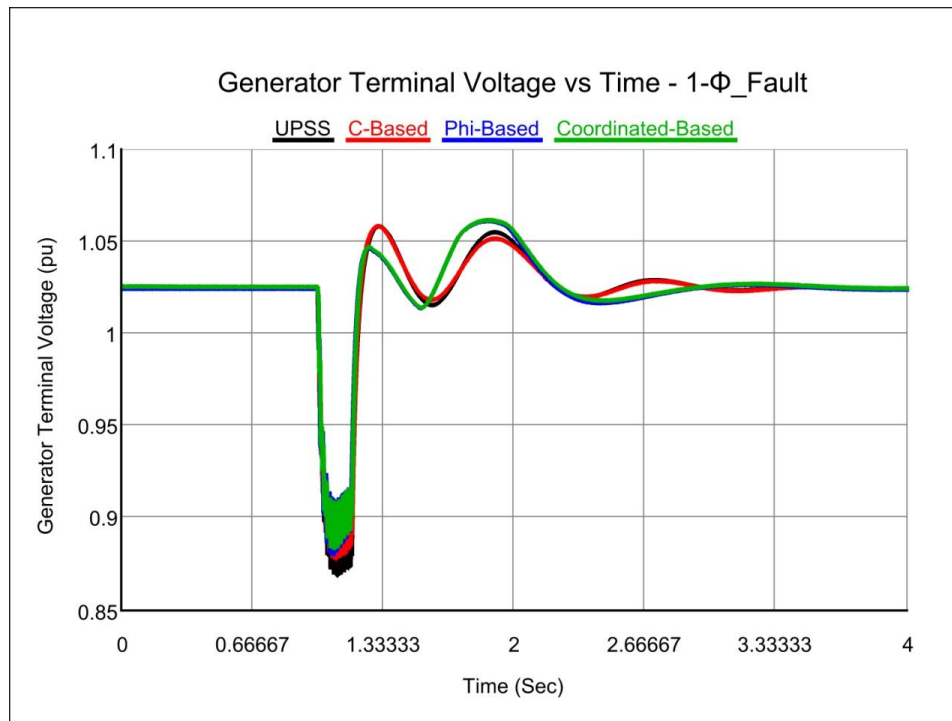


Fig. 7-16 Generator terminal voltage response for 1- Φ fault - light loading.

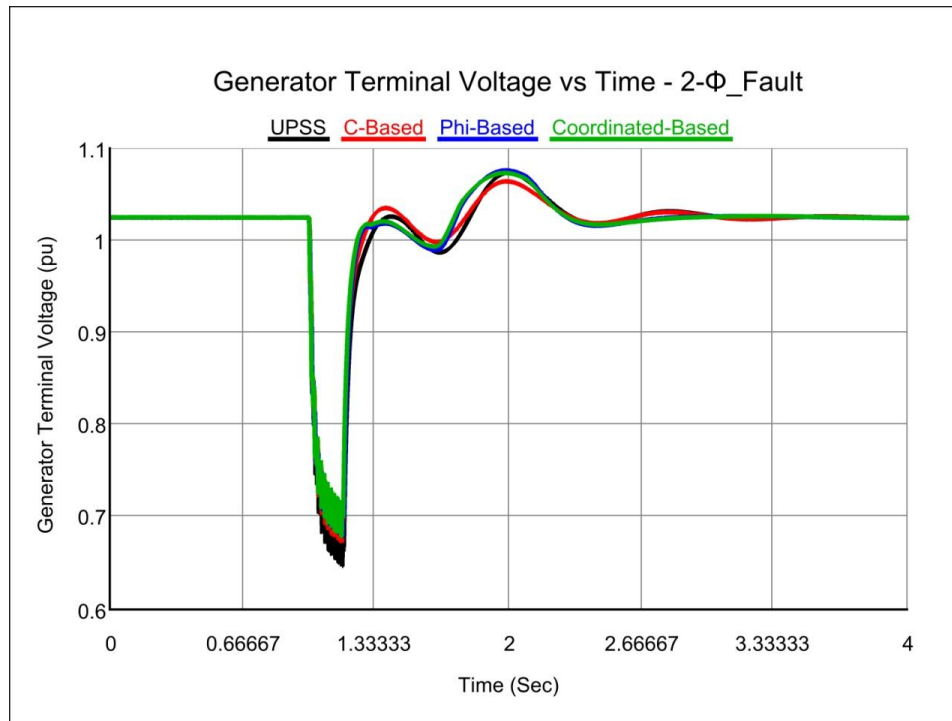


Fig. 7-17 Generator terminal voltage response for 2- Φ fault - light loading.

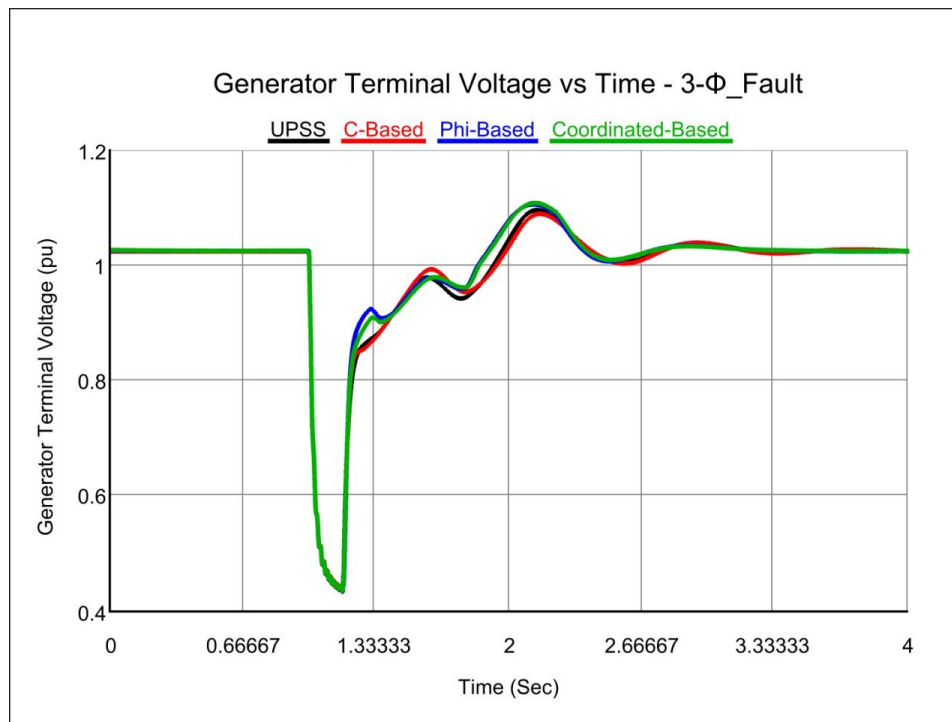


Fig. 7-18 Generator terminal voltage response for 3- Φ fault - light loading.

7.3 DC Voltage for Different Loading Conditions under Several Disturbances

In this section the simulation results of the DC voltage deviation due to the entire proposed controllers are illustrated all to gather in the same plot for different faults circumstances and in all kind of loading conditions nominal, heavy and light.

7.3.1 Nominal Loading

Figures (Fig. 7-19 - Fig. 7-21) show the DC voltage deviation responses for each proposed controller C-based alone, Φ -based alone and C& Φ coordinated-based at a nominal loading condition, these figures give an obvious verification about the success of using the coordinated design controller specially in the responses of the DC voltage deviations.

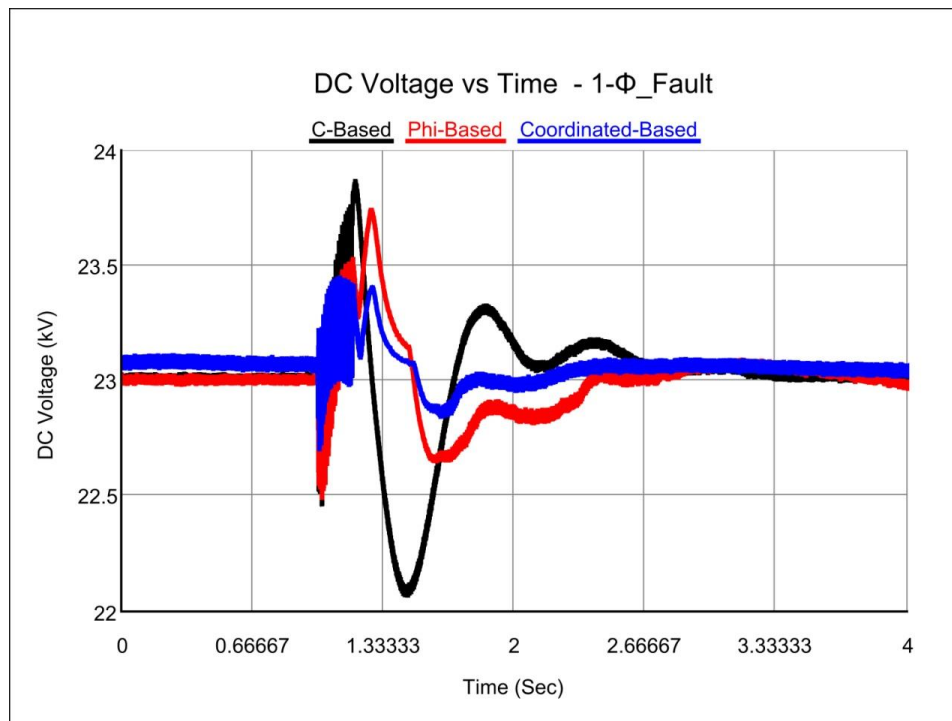


Fig. 7-19 DC voltage response for 1- Φ fault - nominal loading.

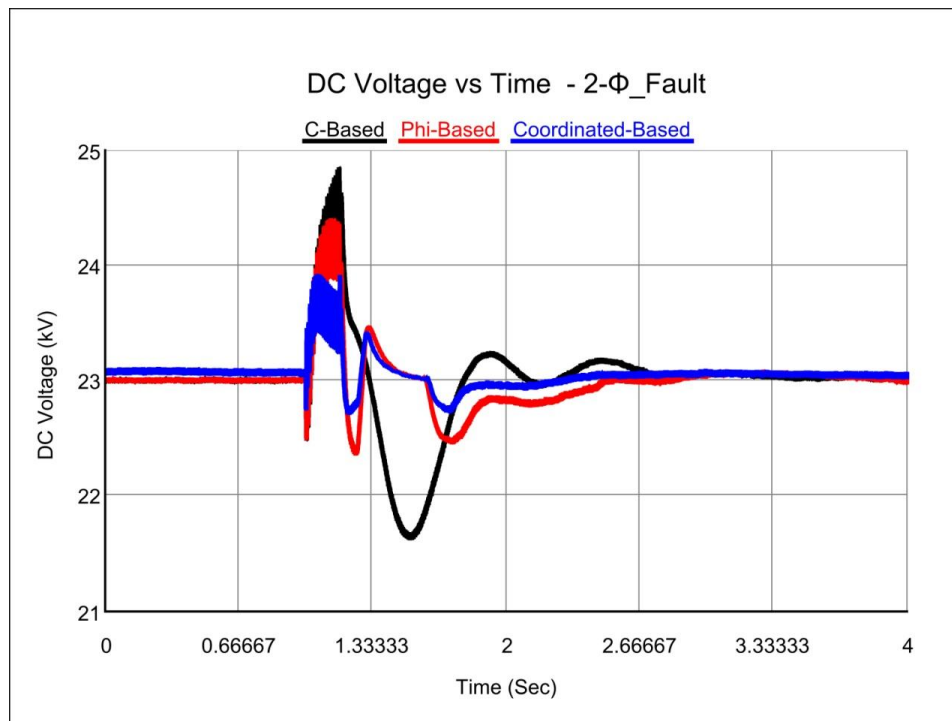


Fig. 7-20 DC voltage response for 2- Φ fault - nominal loading.

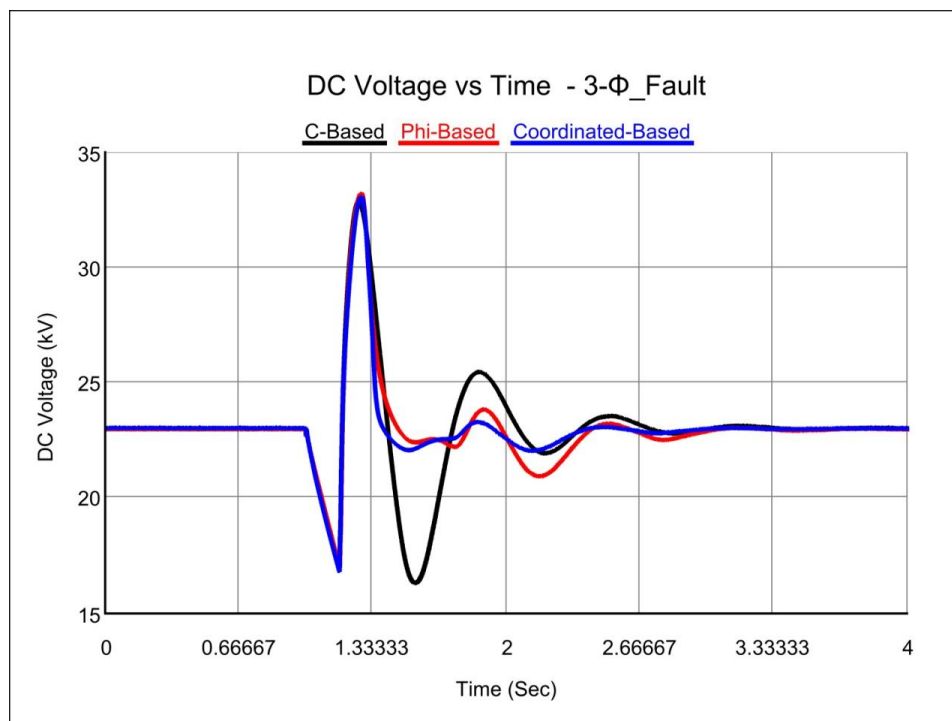


Fig. 7-21 DC voltage response for 3- Φ fault - nominal loading.

7.3.2 Heavy Loading

In this section the DC voltage deviation responses for each proposed controller C-based alone, Φ -based alone and C& Φ coordinated-based at a heavy loading condition. The best controller approach used in this loading condition which would have the best response for the DC voltage deviation is the Φ -based controller alone as explained in Figures (Fig. 7-22 - Fig. 7-24).

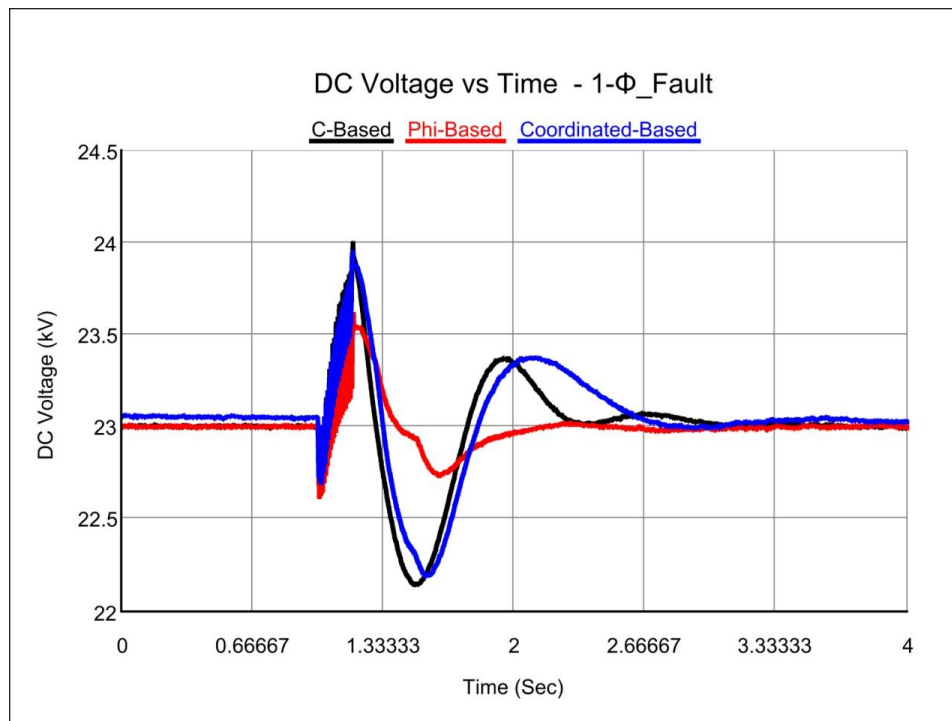


Fig. 7-22 DC voltage response for 1- Φ fault - heavy loading.

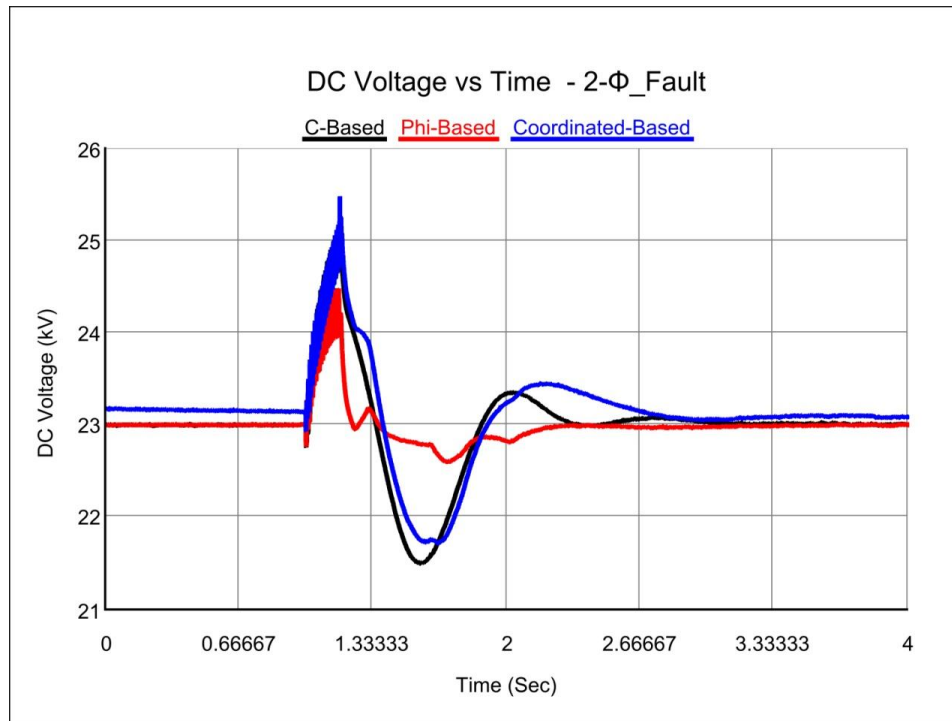


Fig. 7-23 DC voltage response for 2- Φ fault - heavy loading.

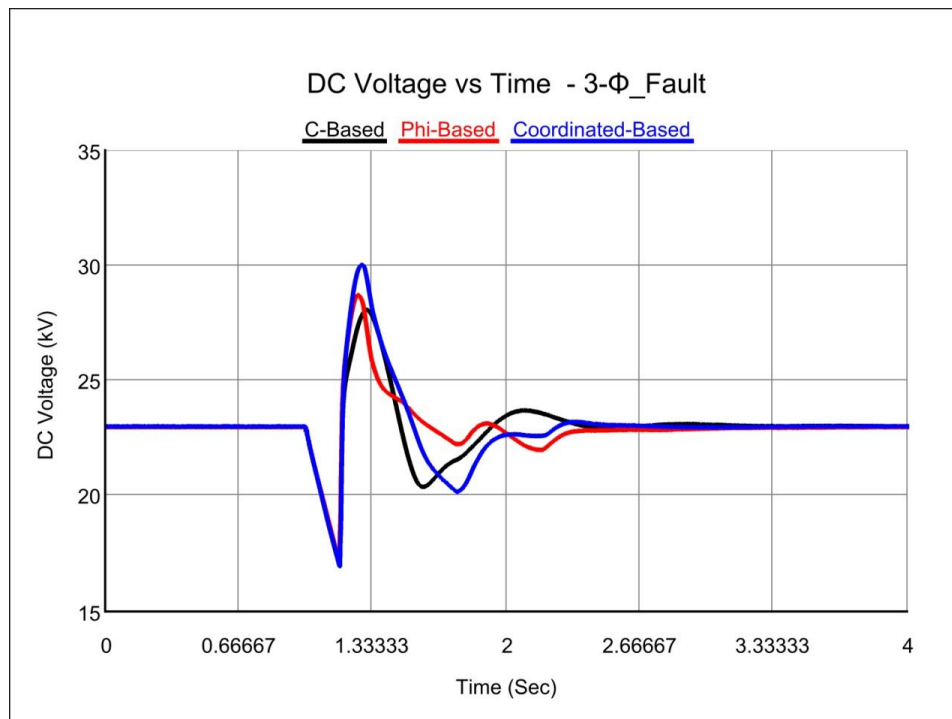


Fig. 7-24 DC voltage response for 3- Φ fault - heavy loading.

7.3.3 Light Loading

Figures (Fig. 7-25 - Fig. 7-27) show the DC voltage deviation responses for each proposed controller C-based alone, Φ -based alone and C& Φ coordinated-based at a light loading condition. The responses in this operating condition show a similar behavior comparing to the results in heavy loading condition where the Φ -based controller is recommended to be used.

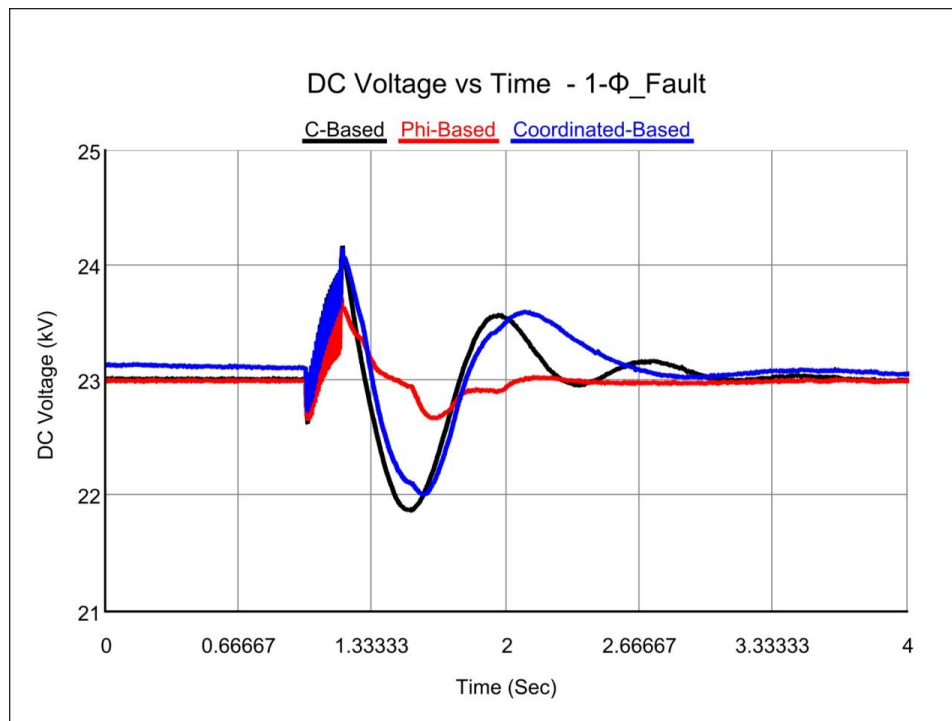


Fig. 7-25 DC voltage response for 1- Φ fault - light loading.

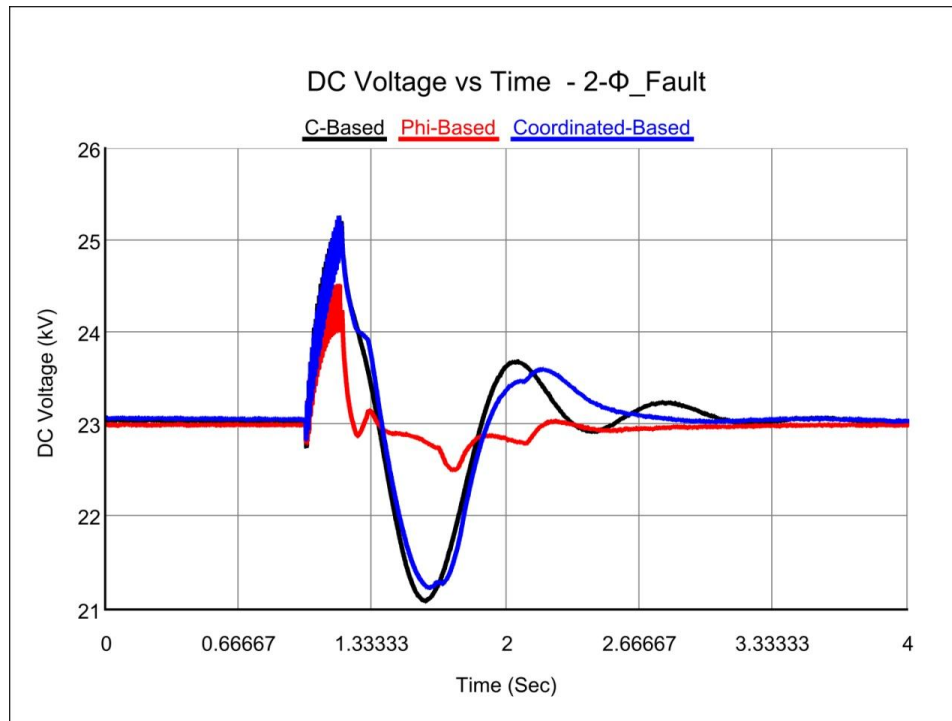


Fig. 7-26 DC voltage response for 2- Φ fault - light loading.

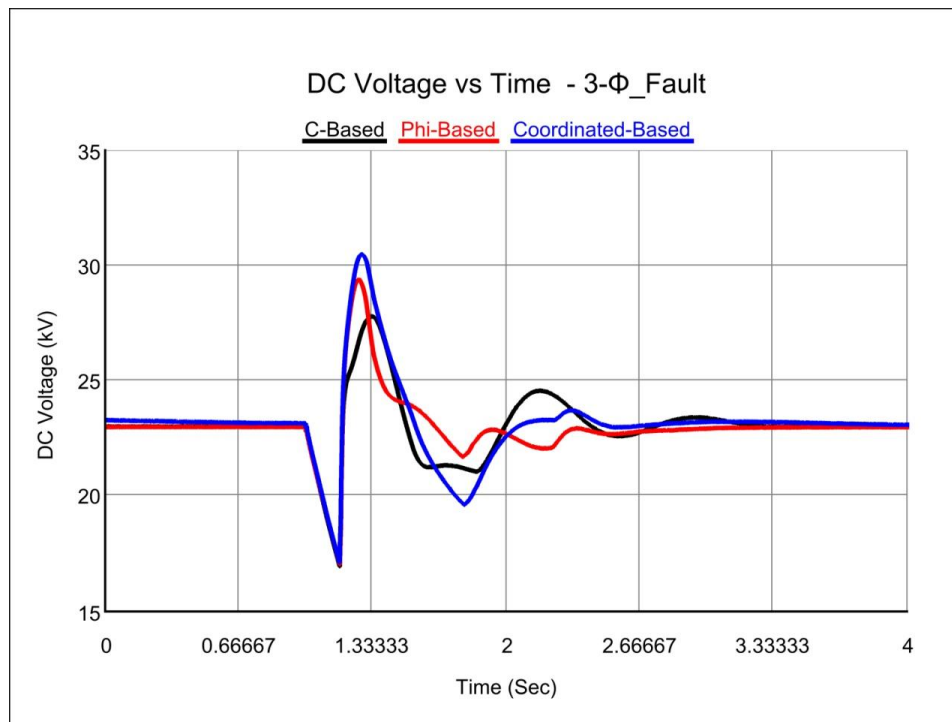


Fig. 7-27 DC voltage response for 3- Φ fault - light loading.

7.4 Generator Power for Different Loading Conditions Under several Disturbances

In this section the simulation results of the generator output power deviation due to the entire proposed controllers are illustrated all to gather in the same plot for different faults circumstances and in all kind of loading conditions nominal, heavy and light.

7.4.1 Nominal Loading

Figures (Fig. 7-28 - Fig. 7-30) show the generator output power deviation responses for each proposed controller UPSS, C-based alone, Φ -based alone and C& Φ coordinated-based at a nominal loading condition.

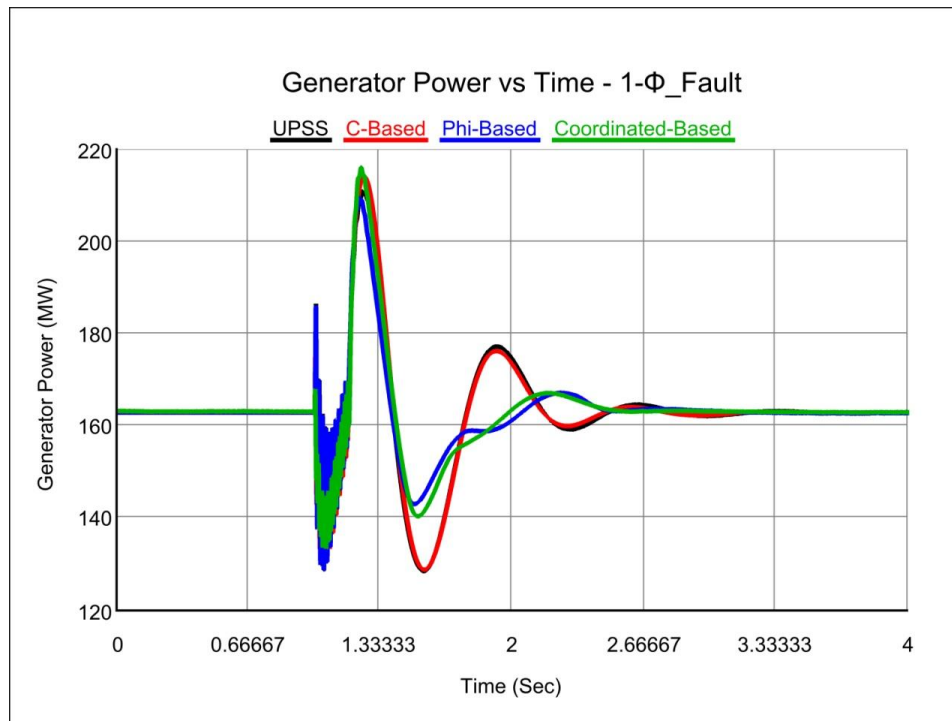


Fig. 7-28 Generator power response for 1- Φ fault - nominal loading.

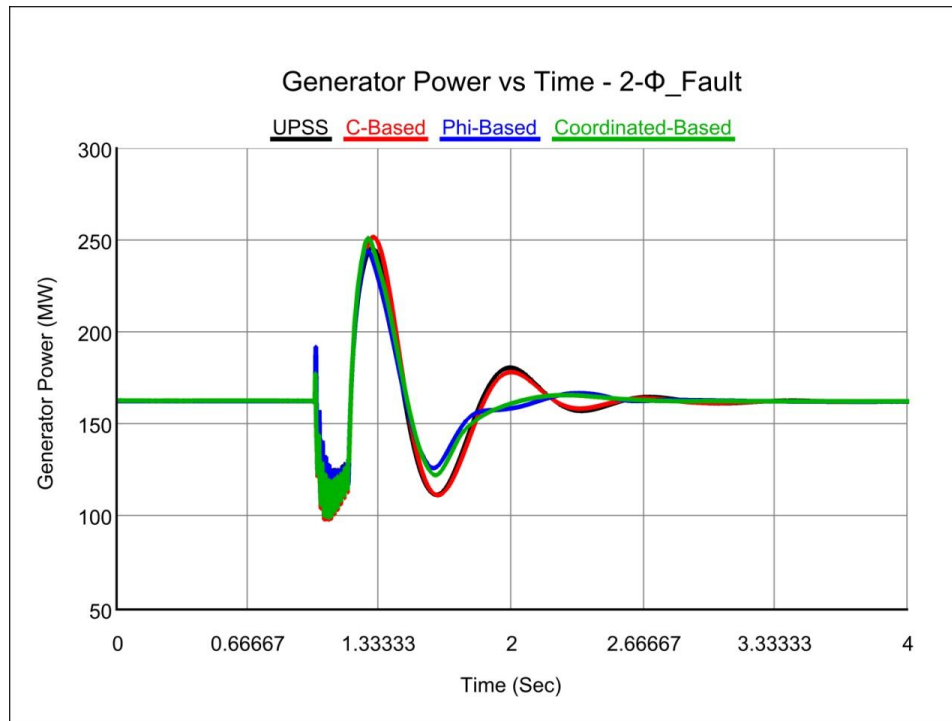


Fig. 7-29 Generator power response for 2- Φ fault - nominal loading.

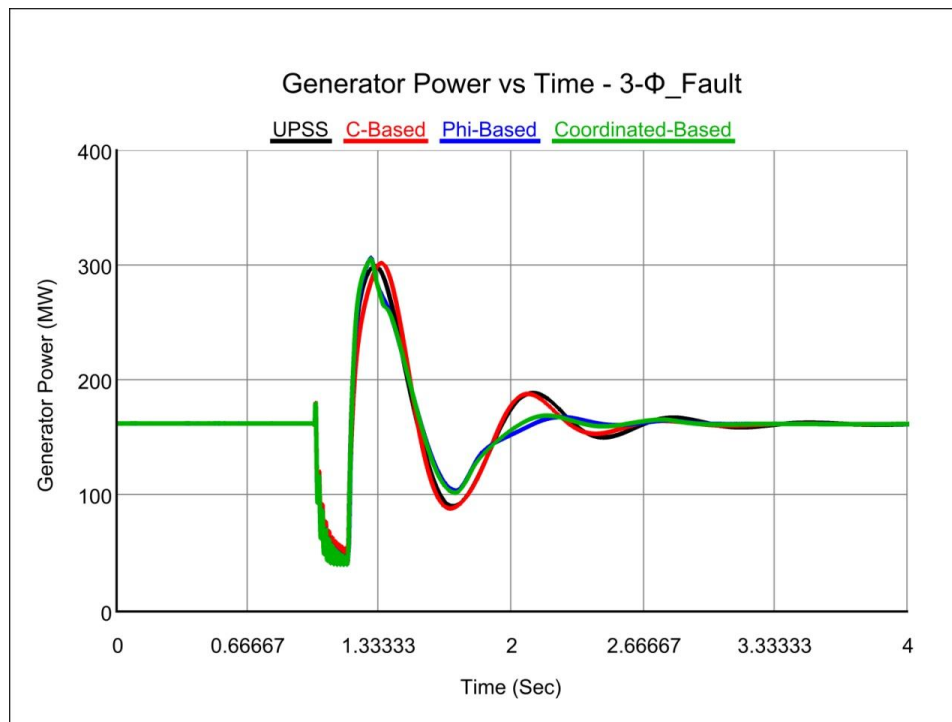


Fig. 7-30 Generator power response for 3- Φ fault - nominal loading.

7.4.2 Heavy Loading

Figures (Fig. 7-31 - Fig. 7-33) show the generator output power deviation responses for each proposed controller UPSS, C-based alone, Φ -based alone and C& Φ coordinated-based at a heavy loading condition.

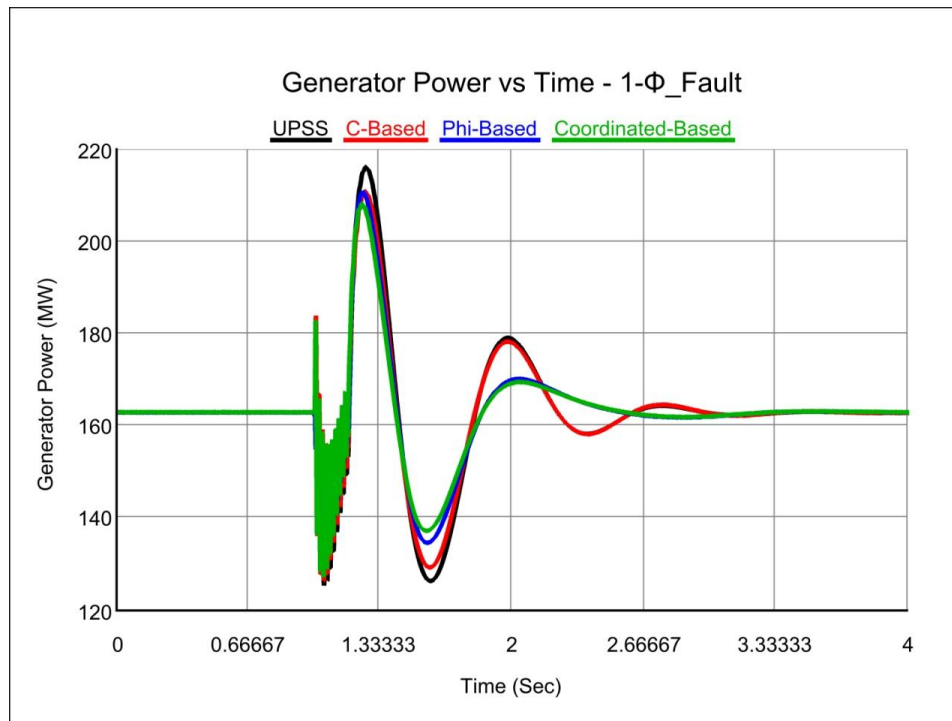


Fig. 7-31 Generator power response for 1- Φ fault - heavy loading.



Fig. 7-32 Generator power response for 2- Φ fault - heavy loading.

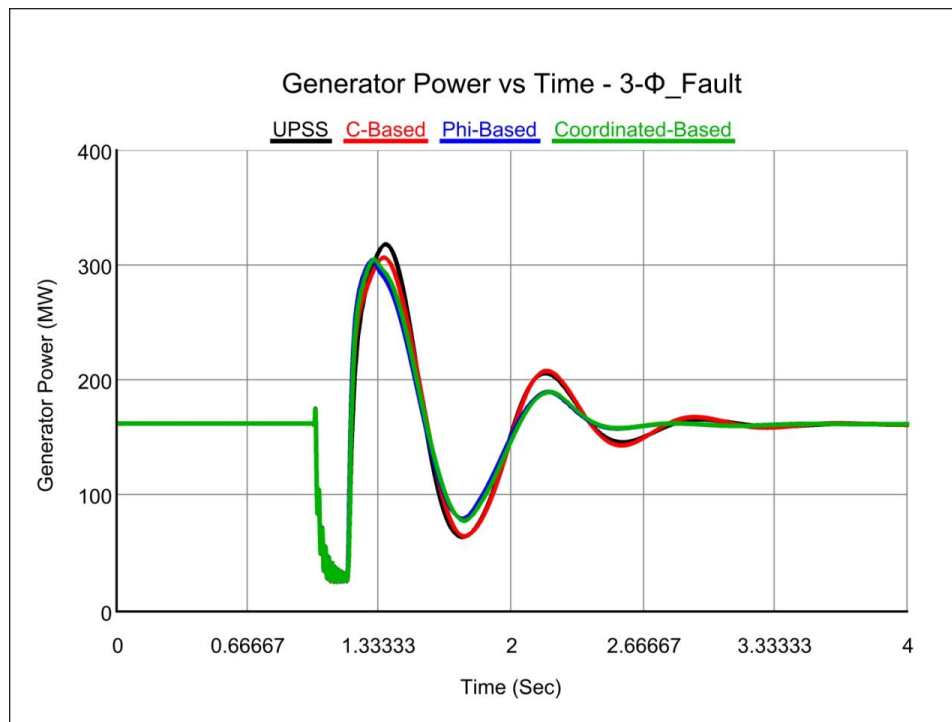


Fig. 7-33 Generator power response for 3- Φ fault - heavy loading.

7.4.3 Light Loading

Figures (Fig. 7-34 - Fig. 7-36) show the generator output power deviation responses for each proposed controller UPSS, C-based alone, Φ -based alone and C& Φ coordinated-based at a light loading condition.

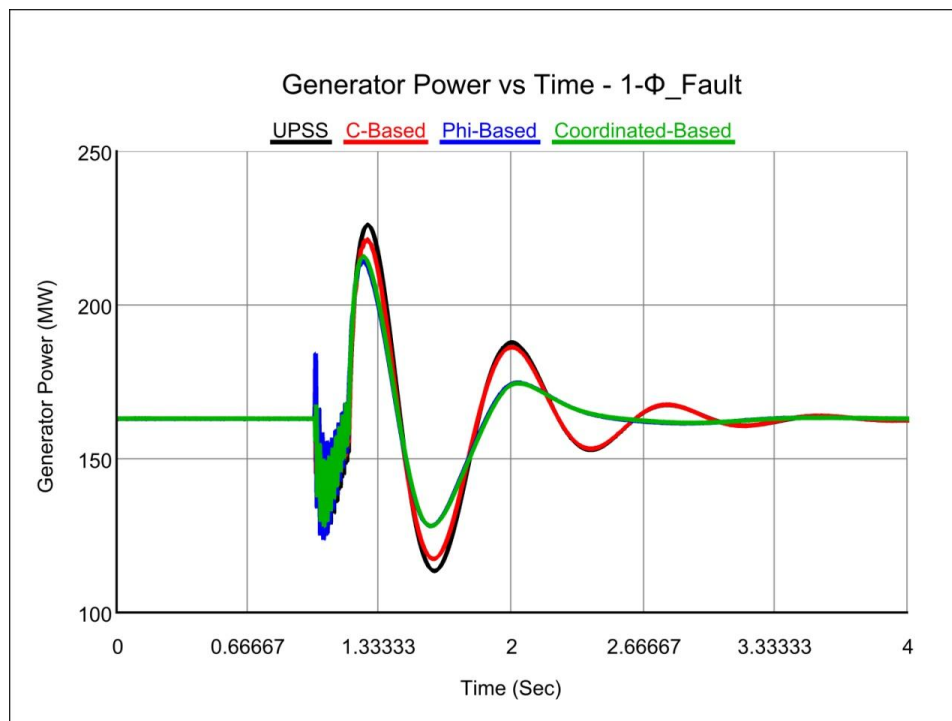


Fig. 7-34 Generator power response for 1- Φ fault - light loading.

For two stabilizers designed in coordinated manner controller, it is clear that the coordinated-based and Φ -based stabilizers provide the best damping characteristics and improve greatly the first swing stability. It can be seen that STATCOM-based stabilizers are more effective in oscillation damping compared to PSS.

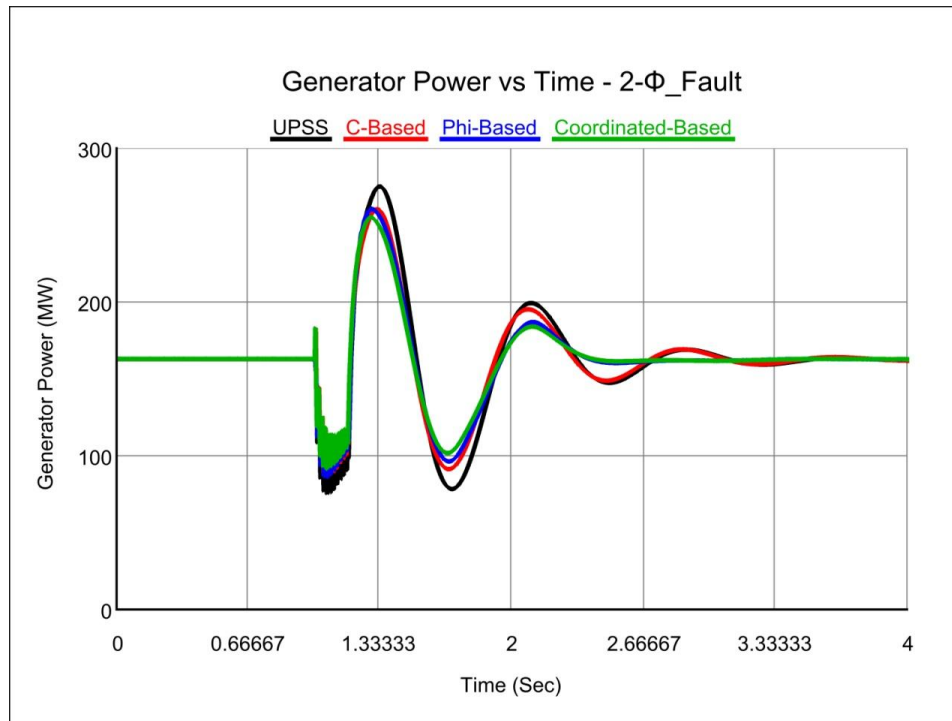


Fig. 7-35 Generator power response for 2- Φ fault - light loading.

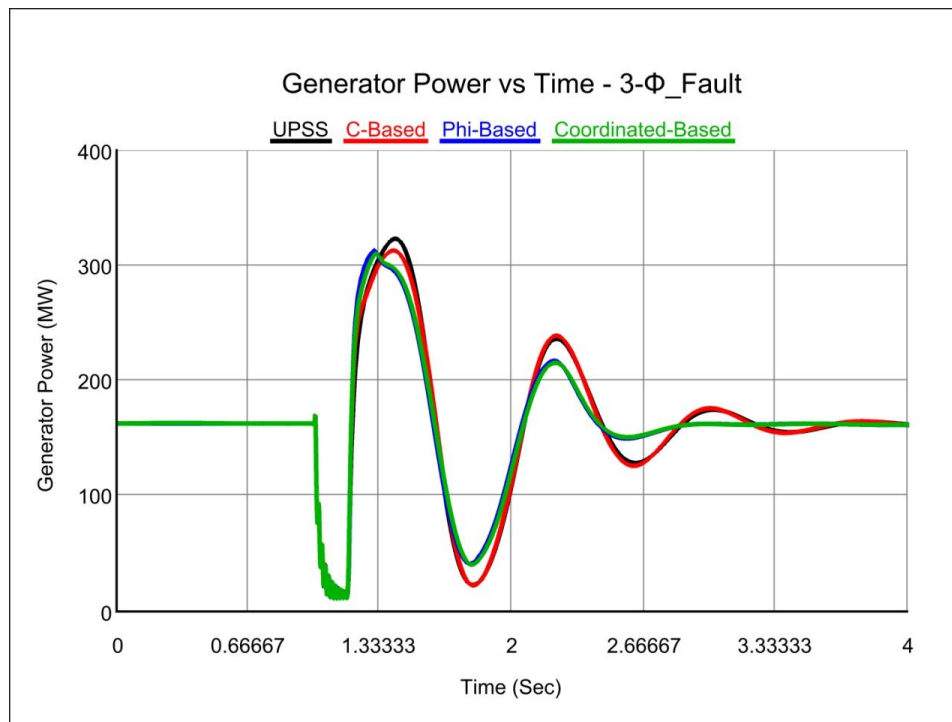


Fig. 7-36 Generator power response for 3- Φ fault - light loading.

7.5 Comparison Between Simulated and RTDS Implemented Results

The simulated results are compared with RTDS results to explore the validity of the proposed controller. Usually in the simulation process, it is necessary to simplify the model firstly according to simulation requirements in order to improve simulation speed. While implementing simulation in RTDS, the calculation is carried out firstly, then the simulation results is processed according to analysis requirements[153].

The system is tested under a 6-cycle 3- Φ fault which is applied on the STATCOM for the three controllers strategies. The rotor angle responses due to such disturbances are shown in figures (Fig. 7-37- Fig. 7-45). The implemented results in addition to the simulated results have confirmed the effectiveness and the accuracy of such proposed controllers.

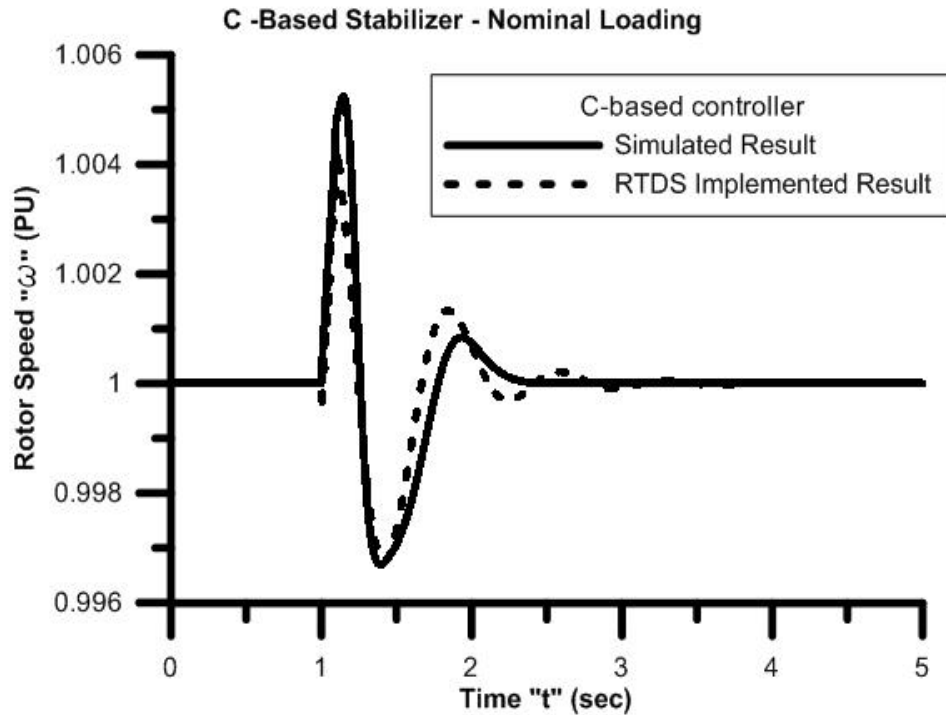


Fig. 7-37 Comparison between simulated and RTDS implemented results due to 6-cycle fault in a c-based controller designed system - Nominal Loading.

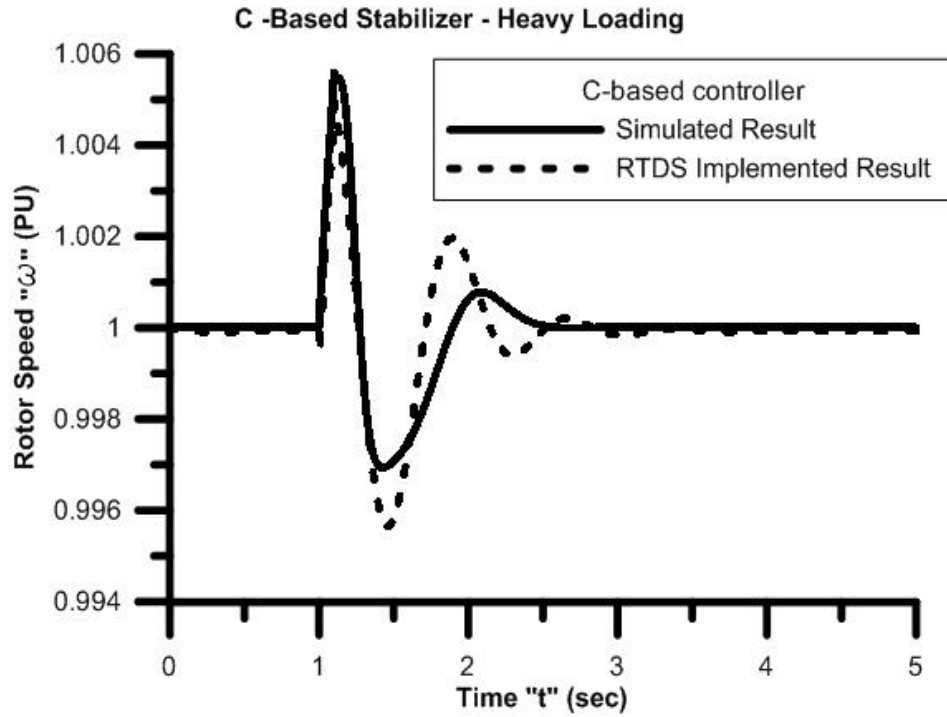


Fig. 7-38 Comparison between simulated and RTDS implemented results due to 6-cycle fault in a C-based controller designed system - Heavy Loading.

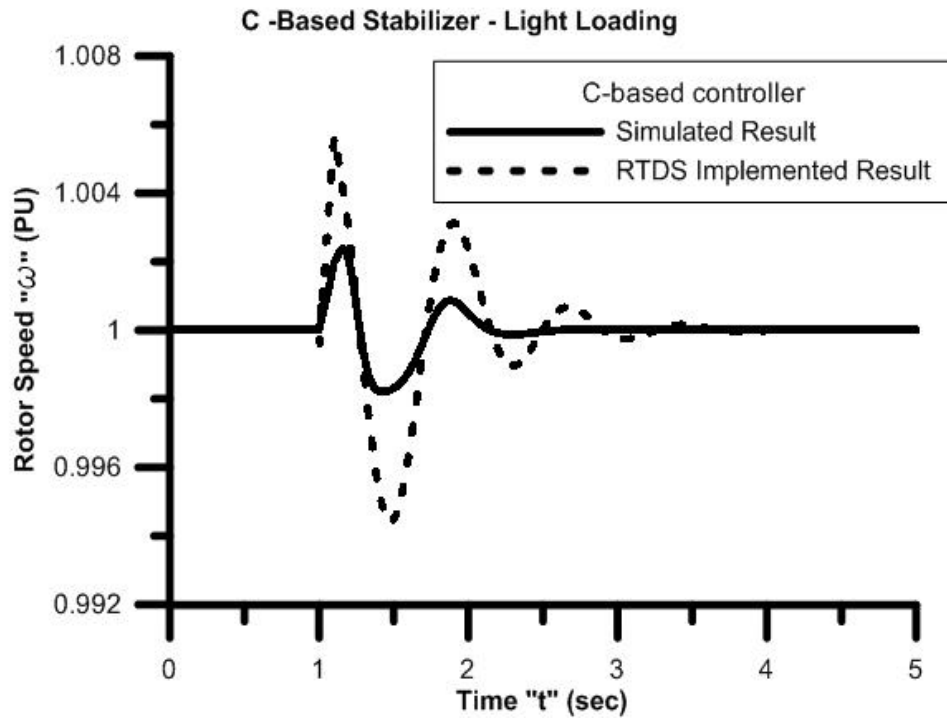


Fig. 7-39 Comparison between simulated and RTDS implemented results due to 6-cycle fault in a C-based controller designed system - Light Loading.

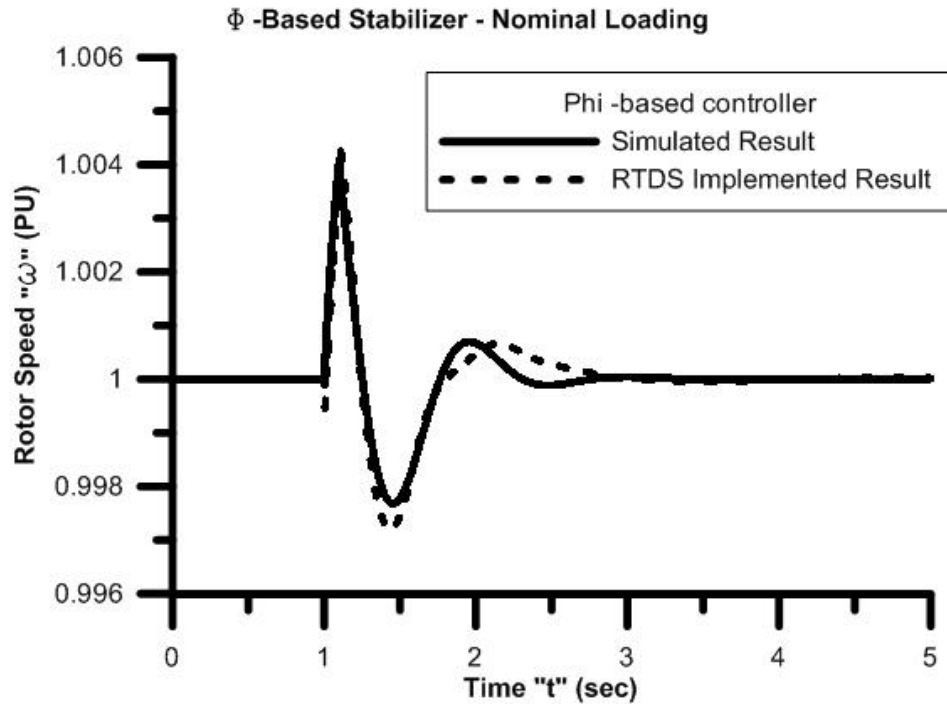


Fig. 7-40 Comparison between simulated and RTDS implemented results due to 6-cycle fault in a Φ -based controller designed system - Nominal Loading.

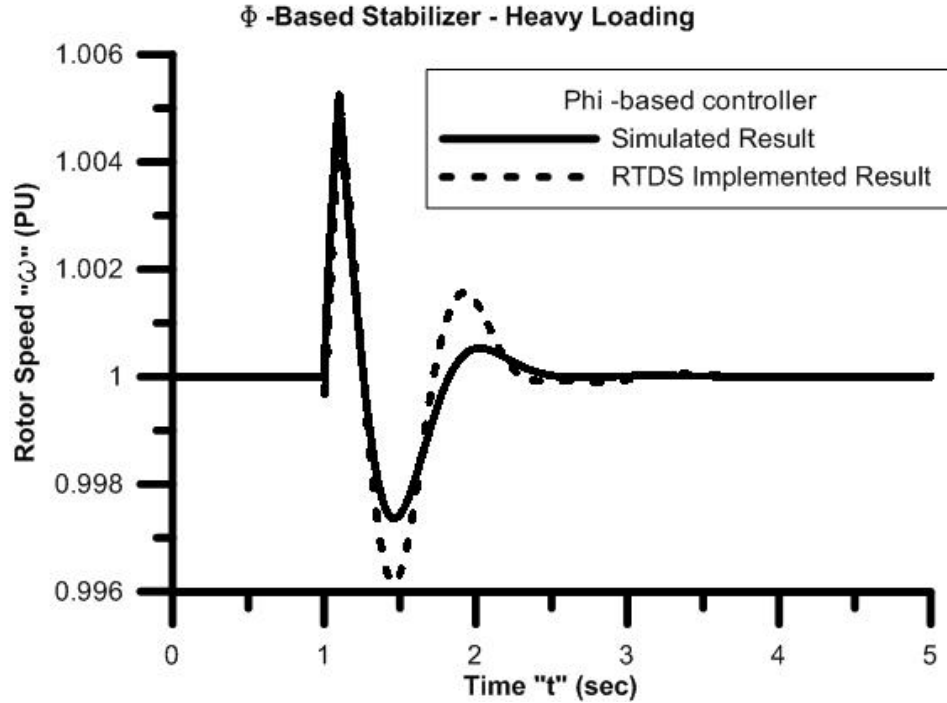


Fig. 7-41 Comparison between simulated and RTDS implemented results due to 6-cycle fault in a Φ -based controller designed system - Heavy Loading.

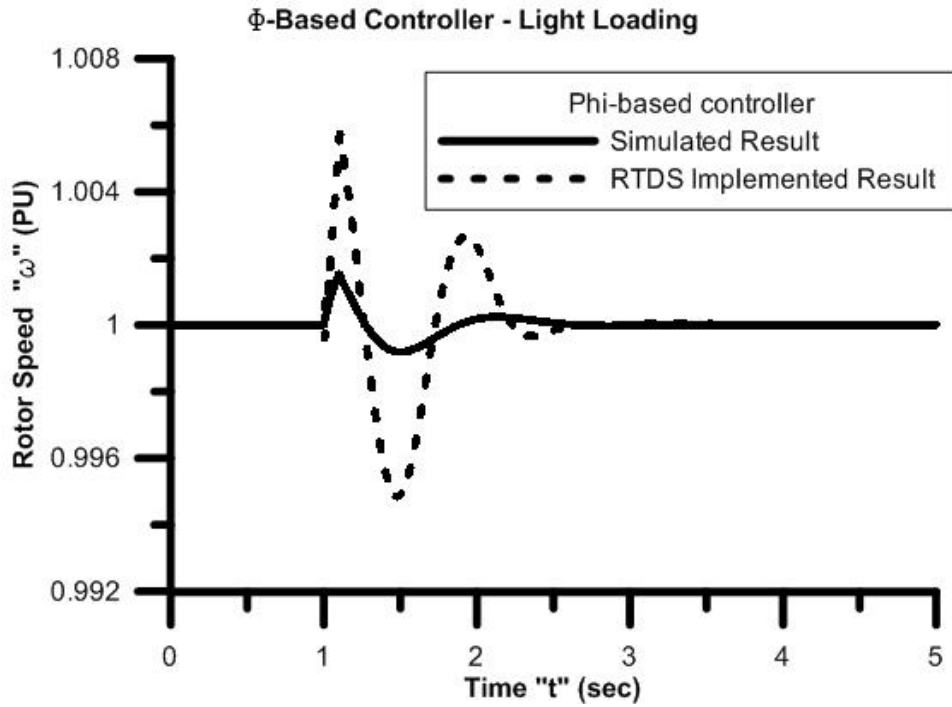


Fig. 7-42 Comparison between simulated and RTDS implemented results due to 6-cycle fault in a Φ -based controller designed system - Light Loading.

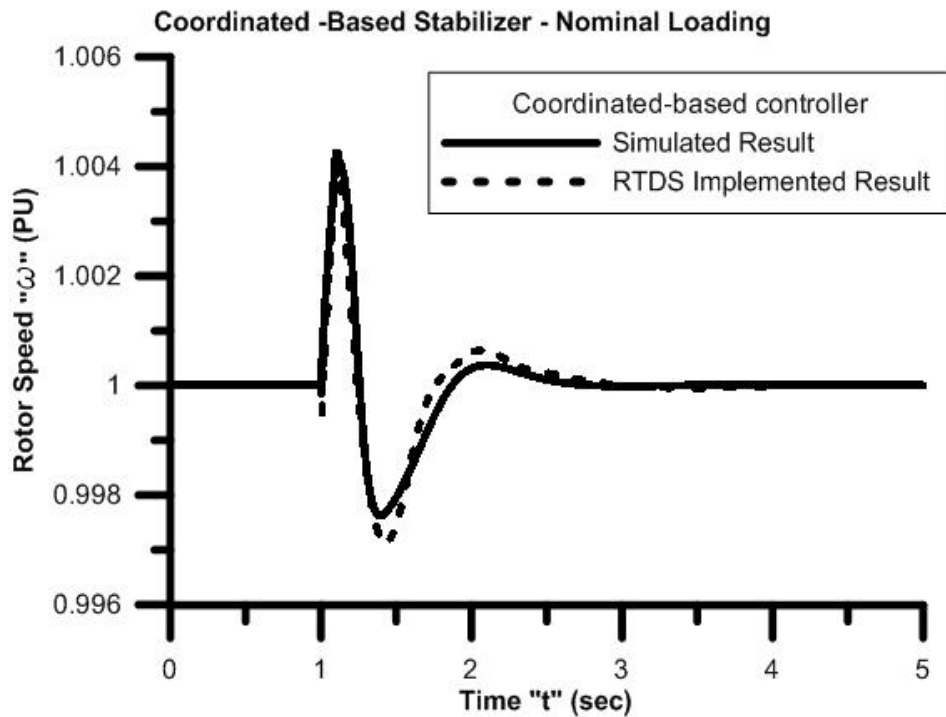


Fig. 7-43 Comparison between simulated and RTDS implemented results due to 6-cycle fault in a Φ &C Coordinated-based controller designed system - Nominal Loading.

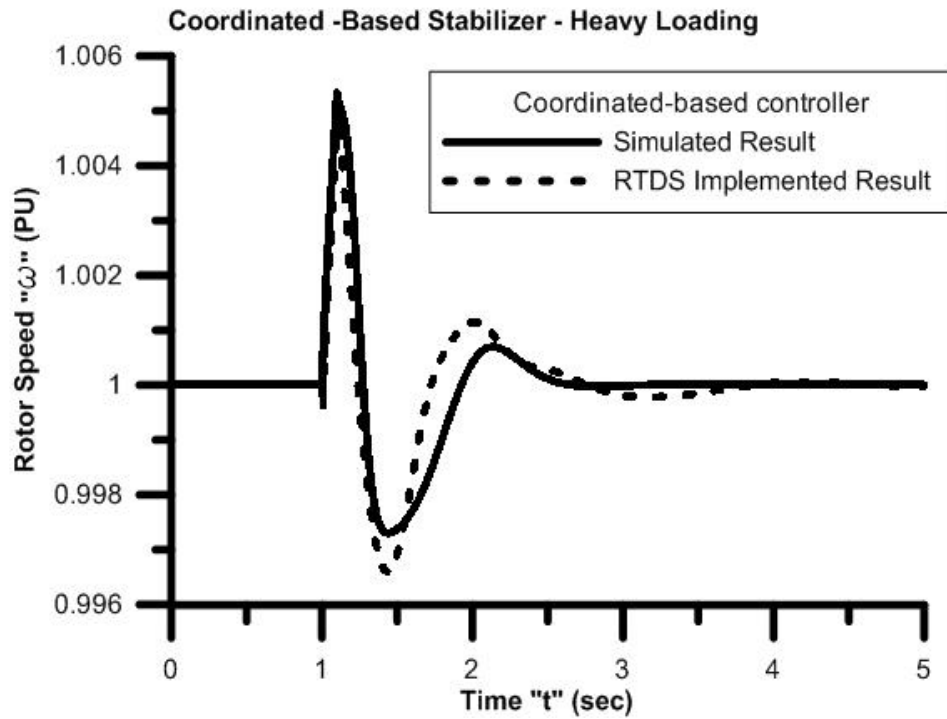


Fig. 7-44 Comparison between simulated and RTDS implemented results due to 6-cycle fault in a Φ &C Coordinated-based controller designed system - Heavy Loading.

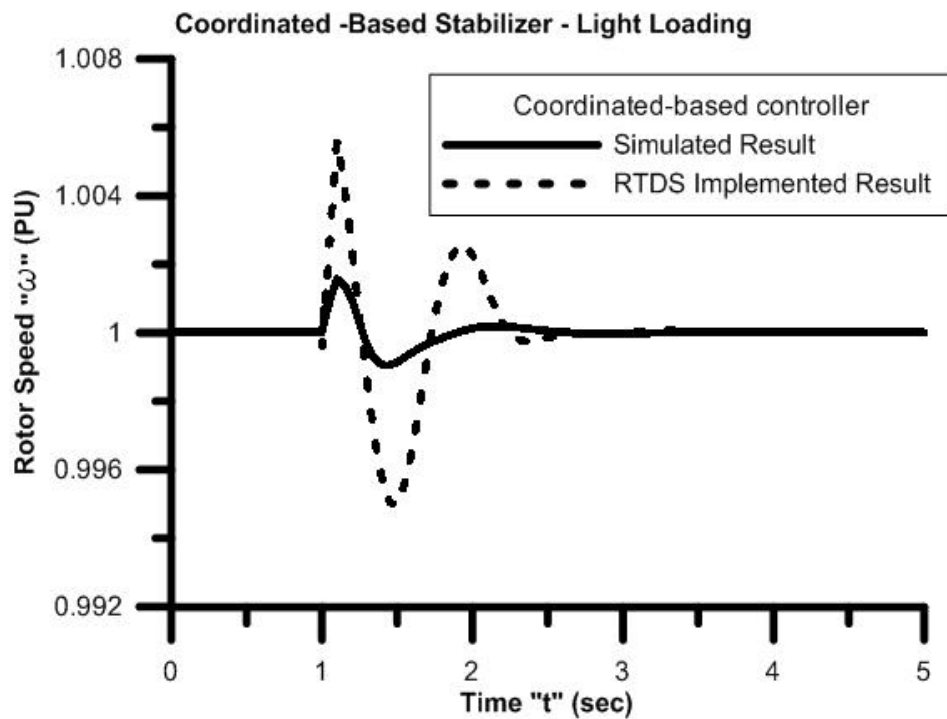


Fig. 7-45 Comparison between simulated and RTDS implemented results due to 6-cycle fault in a Φ &C Coordinated-based controller designed system - Light Loading.

CHAPTER 8 CONCLUSION

8.1 Conclusion

In this thesis the problem of enhancing the power system dynamic stability through individual and coordinated design of power system stabilizers and STATCOM-based stabilizers. The coordination between the various damping stabilizers and the STATCOM internal voltage PI controllers is taken into consideration to improve the system dynamic stability as well as the system voltage regulation. The controllability of the electromechanical mode over a wide range of operating conditions by a given control input has been measured using a Singular Value Decomposition-based approach. Such a study is very important as it laid the foundations of the requirements of the coordinated design problem. The stabilizer design problem has been formulated as an optimization problem, which was then solved by real-coded Differential Evolution . In this regard, the proposed objective function ensures the improvement in the system damping as well as the AC and DC voltage regulations. It is also aimed to improve the system response in terms of the settling time and overshoots..

Individual design as well as coordinated design of the proposed stabilizers have been investigated and discussed. In all cases, the damping characteristics of the proposed control schemes to low frequency oscillations over a wide range of operating conditions has been evaluated using the damping torque coefficient.

The effectiveness of the proposed control schemes in enhancing the power system dynamic stability has been verified through a comprehensive nonlinear time-domain simulations for a variety of loading conditions. It was clearly shown that the coordinated design of PSS and

different STATCOM-based stabilizers outperforms the individual design of these stabilizers. In addition, the STATCOM-based damping stabilizers outperform the PSS and provide better damping characteristics. It can be concluded that the Φ -based stabilizer enhances greatly the system transient stability more than other approaches.

The system is implemented experimentally in the Real Time Digital Simulator where the machine model and the STATCOM along with its control scheme are presented. The model of STATCOM is built in small time step. The dynamic behavior of the system was obtained for fault disturbance. It is also reported that RTDS is an effective tool to conduct transient and dynamic analysis of power system due to fast computation in real time and external hardware interfacing capability.

8.2 Future Work

There are several ideas that could be addressed in the area of power system stability enhancement using STATCOM based stabilizer to damp the low frequency oscillations:

- The phasor measurement unit (PMU) could be used to send the required measurements as an input signals to the STATCOM controllers specially if the STATCOMS is located far away from the signal source, so this application could be implemented to test the STATCOM enhancements in damping the inter area oscillations, furthermore, if the PMU technology is utilize the application of STATCOM into the a multi machine system stability studies would be more realistic.
- The STATCOMs which have been used so far are limited in their ability to deliver a significant amount of real power due to their relatively small energy storage. However, with the recent developments of the super capacitors technology which can store

significant amounts of energy, and are able to quickly release it would tremendously improve the capability of STATCOM and its performance to improve the transient stability of the system.

APPENDICES

Appendix A The System's Data

The system data are as follows:

$$\begin{array}{llll} M = 6.0\text{s}; & T'_{do} = 5.044; & D = 4.0; & x_d = 1.0; \\ x'_d = 0.3; & x_q = 0.6; & R_1 = R_2 = 0.0; & X_1 = X_2 = 0.3; \\ g = 0.0; & b = 0.0; & K_A = 10; & T_A = 0.01; \\ K_s = 1.0; & T_s = 0.05; & |u_{PSS}| \leq 0.2 \text{ pu}; & v = 1.0 \text{ pu.} \\ x_t = 0.15; & C_{DC} = 1.0; & V_{DC} = 1.0; & \end{array}$$

All resistances and reactances are in pu and time constants are in seconds.

Appendix B The System Linearization Model

Referring to Fig. 3-1, the d and q components of the machine current i and terminal voltage v can be written as:

$$i = i_d + ji_q \quad (1)$$

$$v = v_d + jv_q \quad (2)$$

The load current

$$i_L = vY_L, \quad (3)$$

where the load admittance Y_L is given as:

$$Y_L = g + jb \quad (4)$$

The d and q components of i_L can be written as:

$$i_{Ld} = gv_d - bv_q \quad (5)$$

$$i_{Lq} = gv_q + bv_d \quad (6)$$

Then, the line current through the first section

$$i_1 = i - i_L \quad (7)$$

The d and q components of i_1 can be written as:

$$i_{1d} = i_d - i_{Ld} \quad (8)$$

$$i_{1q} = i_q - i_{Lq} \quad (9)$$

The STATCOM-bus voltage

$$v_m = v - i_1(R_1 + jX_1) \quad (10)$$

Hence, the d and q components of v_m can be written as:

$$v_{md} = c_1 v_d - c_2 v_q - R_1 i_d + X_1 i_q \quad (11)$$

$$v_{mq} = c_2 v_d + c_1 v_q - X_1 i_d - R_1 i_q \quad (12)$$

where

$$c_1 = 1 + R_1 g - X_1 b \quad (13)$$

$$c_2 = R_1 b + X_1 g \quad (14)$$

Substituting of v_d and v_q , v_m can be rewritten as:

$$v_{md} = c_3 i_d + c_4 i_q - c_2 E'_q \quad (15)$$

$$v_{mq} = c_5 i_d + c_6 i_q + c_1 E'_q \quad (16)$$

The d and q components of v_s can be written as:

$$v_{sd} = CV_{DC} \cos \phi \quad (17)$$

$$v_{sq} = CV_{DC} \sin \phi \quad (18)$$

The STATCOM AC current is can be given as:

$$i_s = \frac{v_m - v_s}{jx_t} \quad (19)$$

Then the current in the second section of the line i_2 is given as:

$$i_2 = i_1 - i_s \quad (20)$$

The d and q components of i_2 can be written as:

$$i_{2d} = c_7 i_d + c_8 i_q + c_9 E'_q + CV_{DC} \sin \phi / x_t \quad (21)$$

$$i_{2q} = c_{10}i_d + c_{11}i_q + c_{12}E_q' - CV_{DC} \cos \phi / x_t \quad (22)$$

The infinite bus voltage

$$v_b = v_m - i_2(R_2 + jX_2) \quad (23)$$

The components of v_b can be written as:

$$v_{bd} = v_b \sin \delta = v_{md} - R_2 i_{2d} + X_2 i_{2q} \quad (24)$$

$$v_{bq} = v_b \cos \delta = v_{mq} - X_2 i_{2d} - R_2 i_{2q} \quad (25)$$

Substituting, the following two equations can be obtained

$$c_{13}i_d + c_{14}i_q = v_b \sin \delta - c_{15}E_q' + CV_{DC} (R_2 \sin \phi + X_2 \cos \phi) / x_t \quad (26)$$

$$c_{16}i_d + c_{17}i_q = v_b \cos \delta - c_{18}E_q' + CV_{DC} (X_2 \sin \phi - R_2 \cos \phi) / x_t \quad (27)$$

Solving (26) and (27) simultaneously, i_d and i_q expressions can be obtained in the design of electromechanical mode damping controllers, the linearized incremental model around a nominal operating point is usually employed.

Linearizing (26) and (27) at the nominal loading condition, Δi_d and Δi_q can be expressed in terms of $\Delta \delta$, $\Delta E_q'$, ΔV_{DC} , ΔC , and $\Delta \phi$ as follows.

$$\Delta i_d = c_{19}\Delta \delta + c_{20}\Delta E_q' + c_{21}\Delta V_{DC} + c_{22}\Delta C + c_{23}\Delta \phi \quad (28)$$

$$\Delta i_q = c_{24}\Delta \delta + c_{25}\Delta E_q' + c_{26}\Delta V_{DC} + c_{27}\Delta C + c_{28}\Delta \phi \quad (29)$$

The constants c_1 - c_{28} are expressions of $R_1, X_1, R_2, X_2, Y_L, x_d', x_q, i_{d0}, i_{q0}, E_{q0}', V_{DC0}, C_0$, and ϕ_0

The linearized form of v_d and v_q can be written as

$$\Delta v_d = x_q \Delta \dot{i}_q \quad (30)$$

$$\Delta v_q = \Delta E'_q - x'_d \Delta \dot{i}_d \quad (31)$$

Using Equations (38-28-40-30), the following expressions can be easily obtained

$$\Delta P_e = K_1 \Delta \delta + K_2 \Delta E'_q + K_{pDC} \Delta V_{DC} + K_{pC} \Delta C + K_{p\phi} \Delta \phi \quad (32)$$

$$(K_3 + sT'_{do}) \Delta E'_q = \Delta E_{fd} - K_4 \Delta \delta - K_{qDC} \Delta V_{DC} - K_{qC} \Delta C - K_{q\phi} \Delta \phi \quad (33)$$

$$\Delta v = K_5 \Delta \delta + K_6 \Delta E'_q + K_{vDC} \Delta V_{DC} + K_{vC} \Delta C + K_{v\phi} \Delta \phi \quad (34)$$

$$\Delta \dot{V}_{DC} = K_7 \Delta \delta + K_8 \Delta E'_q + K_{DC} \Delta V_{DC} + K_{\Delta C} \Delta C + K_{\Delta \phi} \Delta \phi \quad (35)$$

where the constants K_1 - K_8 , K_{pDC} , K_{pC} , $K_{p\phi}$, K_{qDC} , K_{qC} , $K_{q\phi}$, K_{vDC} , K_{vC} , $K_{v\phi}$, K_{DC} , $K_{\Delta C}$, and $K_{\Delta \phi}$ are expressions of C_1 - C_{28} .

The linearizing procedure yields the following linearized power system model

$$\begin{bmatrix} \dot{\Delta \delta} \\ \dot{\Delta \omega} \\ \dot{\Delta E'_q} \\ \dot{\Delta E_{fd}} \\ \dot{\Delta V_{DC}} \end{bmatrix} = \begin{bmatrix} 0 & 377 & 0 & 0 & 0 \\ -\frac{K_1}{M} & -\frac{D}{M} & -\frac{K_2}{M} & 0 & -\frac{K_{pDC}}{M} \\ -\frac{K_4}{T'_{do}} & 0 & -\frac{K_3}{T'_{do}} & \frac{1}{T'_{do}} & -\frac{K_{qDC}}{T'_{do}} \\ -\frac{K_A K_5}{T_A} & 0 & -\frac{K_A K_6}{T_A} & -\frac{1}{T_A} & -\frac{K_A K_{vDC}}{T_A} \\ K_7 & 0 & K_8 & 0 & K_{DC} \end{bmatrix} \begin{bmatrix} \Delta \delta \\ \Delta \omega \\ \Delta E'_q \\ \Delta E_{fd} \\ \Delta V_{DC} \end{bmatrix} + \begin{bmatrix} 0 & 0 & 0 \\ 0 & -\frac{K_{pDC}}{M} & -\frac{K_{p\phi}}{M} \\ 0 & -\frac{K_{qDC}}{T'_{do}} & -\frac{K_{q\phi}}{T'_{do}} \\ \frac{K_A}{T_A} & -\frac{K_A K_{vDC}}{T_A} & \frac{K_A K_{v\phi}}{T_A} \\ 0 & K_{\Delta C} & K_{\Delta \phi} \end{bmatrix} \begin{bmatrix} u_{PSS} \\ \Delta C \\ \Delta \phi \end{bmatrix} \quad (36)$$

Appendix C RTDS Overview

Digital technique is believed to be the one of the most important techniques which stimulates the development of modern power systems since later 1960s, especially for power system simulation [154], protection [155] and power electronics [156]. In the past, modern technology has gone through tremendous development in the area of power system and digital simulation. The microprocessor progresses, communication and transducer technologies have provided new means for the development in power system protection and relay testing.



Fig. C. 1. RTDS applications.

The Real Time Digital Simulator which developed at the Manitoba HVDC Research Centre in the late 1980's is a fully digital electromagnetic transient power system simulator. The RTDS Simulator responsibility was transferred to RTDS Technologies in 1994 where it has since undergone numerous hardware and software developments. It can be used to conduct close-loop testing of physical devices such as protection equipment and control equipment; to perform analytical system studies and to educate operators, engineers and students [156]. It is a cost-

effective replacement for transient network analyzers and analogue/hybrid simulators. RTDS allows the user to investigate the effects of disturbances on power system equipment and networks to prevent outages or complete failure. Moreover, RTDS added the capability to improve the simulation accuracy and better capture the switching events [157]. The simulator is now widely used in the electric power industry by utilities, equipment manufacturers and research organizations.

C.1 RTDS Capability

RTDS shown in Fig. C. 2 is generally designed to simulate power systems in real time with time step-sizes on the order of $50\mu\text{s}$. The system uses a number of digital signal processors (DSPs) which operated in parallel. It provides a number of digital and analog I/O ports for interfacing hardware to the simulation. It features a more powerful processor combined with FPGAs which allow the simulation of a limited number of power electronics devices with time step as small as $1.4\text{-}2.5\ \mu\text{s}$ embedded in the $50\mu\text{s}$ time-step environment. Therefore, it allows the simulation of power electronics converter operating at higher switching frequency with sufficient accuracy. In addition, its real time capability allows the user to incorporate real devices into the simulation in a closed loop environment .



Fig. C. 2. RTDS Simulator components.

C.2 Simulator Design

The beauty of the RTDS is that it works in continuous, sustained real time. This means that it can solve the power system equations fast enough to continuously produce output conditions that realistically represent conditions in the real network. Because the solution is real time, the simulator can be connected directly to power system control and protective relay equipment and adjust its calculations based on their operation [38]. RTDS is a combination of advanced computer hardware and comprehensive software. Real-time implementation setup using RTDS is shown in Fig. C. 3.

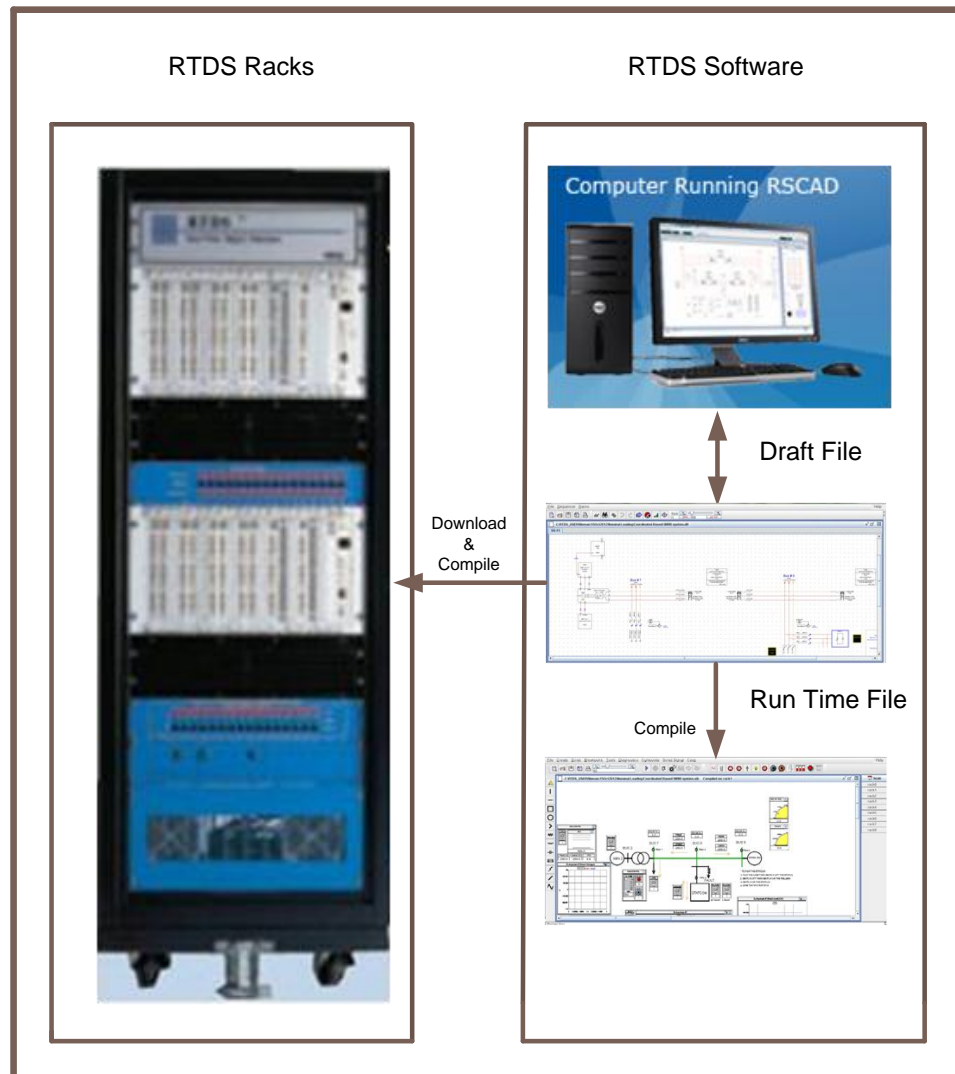


Fig. C. 3. Real-time implementation setup using RTDS.

C.3 Hardware

The RTDS Simulator hardware is based on a customized parallel processing architecture. It is designed specifically to solve the electromagnetic transient simulation algorithm developed by Dr. Hermann Dommel [154]. The design is modular so that different size power systems can be accommodated by adding units to the simulator. These units are called racks. Each rack of hardware includes both communication and processor cards linked through a common backplane. A large network is divided into separate subsystems. Each subsystem is solved by one rack. Each rack has an InterRack Communication (IRC) card to share the information between the subsystems and contains a Workstation InterFace (WIF) card to synchronize the simulation calculations and to coordinate the communication between processor cards as well as the communication between racks. Additionally the WIF provides Ethernet communication to and from the graphical user interface during real times simulations. The processor cards are responsible for calculating the overall network behavior. Different components are assigned to different processors so that their contribution to the subsystem response can be calculated in parallel. The current RTDS Simulator uses two different processor cards; the Triple Processor Card (3PC) and the Giga Processor Card (GPC). Each 3PC card contains three floating point Digital Signal Processors (DSP) running at 40 MHz, a significant increase over the original Tandem Processor Card (TPC) which had only two DSP's running at 11 MHz. The processors can communicate directly to another one at any time via shared memory, without having to access the backplane, and can therefore be used independently or together to solve more complex component models. The GPC is the most recently developed processor card which contains two RISC processors running at 1 GHz. Due to their computational power, the GPC processors are often used to calculate more than one component model at the same time. Starting at the concept stage, the RTDS Simulator was intended for testing of physical protection and control

equipment, thus making input/output (I/O) a primary design consideration. In some instances, hundreds of signals are passed to and from the simulator to external equipment. Great care was given to ensure that large amounts of I/O could be provided without significantly affecting the simulation timestep. Instead of providing a central communication link, the processor cards and I/O were designed to communicate directly with another one to minimize the communication time. The Giga-Transceiver Input/Output (GT-I/O) cards are a family of I/O developed for the GPC card shown in Fig. C. 4. The GT-I/O cards connect to the GPC via 2 GHz fiber optic links and provide complete optical isolation from the simulator. The GT-I/O cards include analogue input and output with 16-bit data converters as well as digital input and output.

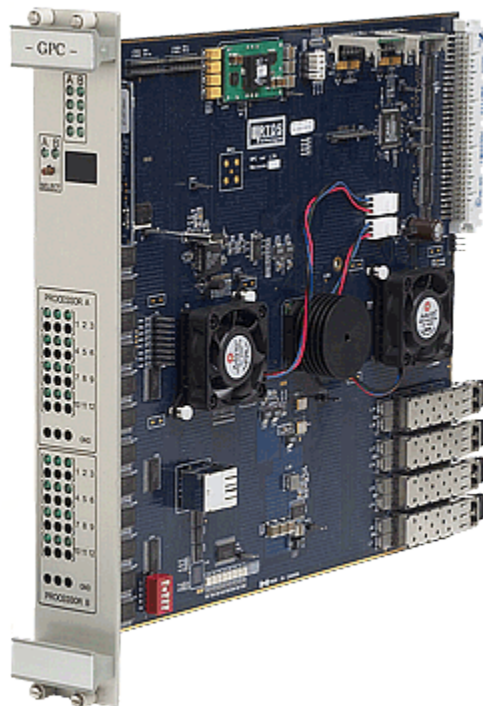


Fig. C. 4. GPC card.

Typically the simulation timestep for real time operation of the RTDS Simulator is in the order of 50 μ s. Hard real time is ensured by the WIF card. If any processor cannot complete the calculations and I/O required within the given timestep, the simulation is stopped and an error

message issued. The largest simulation ever run in real time provided a full electromagnetic transient representation for a network with over 500 three-phase buses and 90 generators. Special hardware, algorithms and technique have been developed to provide a high degree of accuracy in representing high speed power electronics that typically require a response in the order of 1 μ s.

C.4 Software

There are several levels of software involved with the RTDS Simulator. At the lower level are the component models (i.e. lines, transformers, generators, etc.) which have been optimized for real time operation. Over the years a comprehensive library of both power system and control components has been developed and refined. The highest level of software is the graphical user interface known as RSCAD. RSCAD allows simulation circuits to be constructed, run, operated and results to be recorded and documented. The RSCAD Draft module shown in Fig. C. 5 allows simulations to be constructed graphically by copying and connecting generic components from the library. The parameters of a particular component can be entered through a data menu. After the network has been constructed, it is compiled to create the simulation code required by the simulator. Once the compile process has been executed, the simulation can be run using RSCAD RunTime shown in Fig. C. 6.

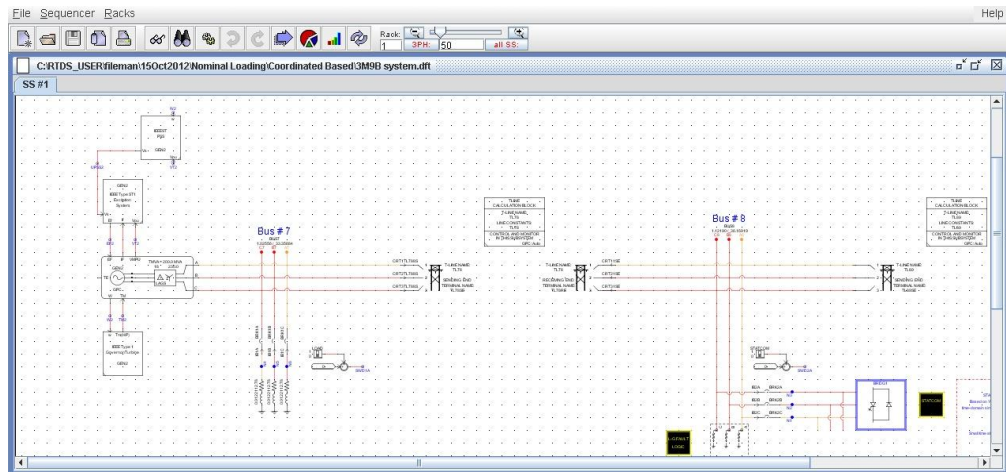


Fig. C. 5. RSCAD Draft.

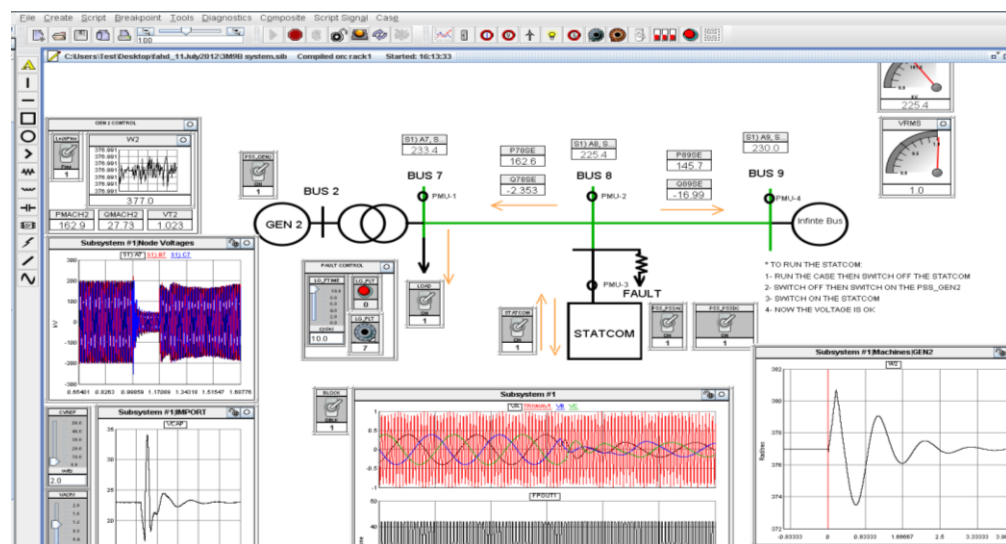


Fig. C. 6. RSCAD Run Time.

RunTime, which operates on a PC or workstation, communicates back and forth with the simulator WIF cards via Ethernet. The bidirectional communication allows simulations to be downloaded and run as well as for simulation results to be transferred to the RunTime screen. The network can be operated from RunTime by changing switching states or set points. Slow moving signals such as power, RMS bus voltage, machine speed, etc. can be monitored on a continuous basis to allow transient behavior and state of the network to be observed. Detailed

plots of transient events, with a resolution as high as every timestep, can also be recorded by the simulator WIF cards and displayed in RunTime plots.

Appendix D RTDS Model Parameters

Table 8 The Generator General Model Configuration

Generator		
General Model Configuration	Value	Unite
Rated MVA of the machine	192	MVA
Rated RMS Line-to-Line Voltage	18	KV
Base Angular Frequency	60	Hertz
Mechanical Data and Configuration	Value	Unite
Inertia Constant (H)	6.4	MWs/MVA
Synchronous Machine Damping (D)	2	p.u./p.u.
Machine Electrical Data	Value	Unite
Stator Leakage Reactance (X_a)	0.1	p.u.
D-axis: Unsaturated Reactance(X_d)	1.73	p.u.
D-axis: Unsaturated Transient Reactance(X_d')	0.23	p.u.
D-axis: Unsaturated Sub-Transient Reactance(X_d'')	0.22	p.u.
Q-axis: Unsaturated Reactance(X_q)	1.66	p.u.
Q-axis: Unsaturated Transient Reactance(X_q')	0.378	p.u.
Q-axis: Unsaturated Sub-Transient Reactance(X_q'')	0.377	p.u.
Stator Resistance (R_a)	0.002	p.u.
D-axis: Unsaturated Transient Open T Constant (T_{do}')	6	sec
D-axis: Unsaturated Sub-Transient Open T Constant (T_{do}'')	0.001	sec
Q-axis: Unsaturated Transient Open T Constant (T_{qo}')	0.535	sec
Q-axis: Unsaturated Sub-Transient Open T Constant (T_{qo}'')	0.001	sec

Table 9 IEEE Type st1 Excitation System Model Data.

IEEE Type st1 Excitation System Model		
Description	Value	Unite
Rated RMS Phase Voltage (V_b)	10.393	KV
Time Constant (T_r)	0.00	sec
Upper Limit Vimax ($V_{i \max}$)	1.00	p.u.
Lower Limit Vimin ($V_{i \min}$)	-1.00	p.u.
Time Constant (T_c)	1.00	sec
Time Constant (T_b)	0.00	sec
Gain (K_a)	50	
Time Constant (T_a)	0.05	sec
Upper Limit VRmax ($V_{r \max}$)	7.30	p.u.
Lower Limit VRmin ($V_{r \min}$)	-7.30	p.u.
Constant (K_c)	0.175	
Feedback Gain (K_f)	0.00	
Feedback Time Constant (T_f)	1.00	sec

Table 10 Transmission Line Parameters Data.

Transmission line Parameters		
Description	Value	Unite
MVA Base	100.0	MVA
Rated Voltage	230.0	KV
Number of Phases	3	p.u.
Positive Sequence Series Resistance	0.0085	p.u.
Positive Sequence Series Ind. Reactance	0.072	p.u.
Positive Sequence Shunt Cap. Reactance	6.7114	p.u.
Zero Sequence Series Resistance	0.0085	p.u.
Zero Sequence Series Ind. Reactance	0.21	p.u.
Zero Sequence Shunt Cap. Reactance	20.0	p.u.

Table 11 The STATCOM Rating.

STATCOM Rating Information		
Description	Value	Unite
Rated MVA of the STATCOM	60	MVA
Rated RMS Line-to-Line Voltage at STATCOM Bus	230	KV
Base Angular Frequency	60	Hertz

BIBLIOGRAPHY

- [1] R.Srinivas Rao, P.Lakshmi Narayana, "A Five Level DSTATCOM for Compensation of Reactive Power and Harmonics," *International Journal of Engineering Research and Development*, vol. 1, no. 11, pp. 23-29, 2012.
- [2] P. Asare, T. Diez, A. Galli, E. O'Neill-Carillo, J. Robertson, and R. Zhao, "An Overview of Flexible AC Transmission Systems," *ECE Technical Reports, Purdue University*, 1994.
- [3] Y.H.Song, A.T.John, "Flexible A.C. Transmission Systems," *IEEE Power Energy*, vol. 30, 1999.
- [4] D.Shen, XU Liang, Y.Hani, "A Modified per unit STATCOM Model and Analysis of Open Loop Response Time," *IEEE Proceedings*, pp. 2624-2629, 2000.
- [5] C.A.Canizares, M.Pozzi, S.Corz, "STATCOM Modelling for Voltage and Angle Stability Studies," *Electric Power and Energy Systems*, 2003.
- [6] K.R.Padiyar, A.M. Kulkarni, "Analysis and Design of Voltage Control of Static Condenser," *IEEE Conference on Power Electronics, Derives and Energy Systems for Industrial Growth*, vol. 1, pp. 393-398, 1996.
- [7] Tomas Larsson, Jean-Philippe Hasler, Paul Forsyth, Trevor Maguire, "Voltage Source Converter Modeled in RTDS Experiences and Comparison with Field Results," *The International Conference on Power Systems Transients (IPST'07) in Lyon Presented at , France, June 4-7, 2007*.
- [8] Y.YU, Chen, H.Yimgoduo, "STATCOM Modelling and Analysis in Damping Power System Oscillations," *Energy Conversion Engineering Conference and Exhibit, (IECEC) 35th intersociety , 24-28 July , vol. 2, pp. 756-762 , 2000*.
- [9] L. Qi, J. Langston, M. Steurer, A. Sundaram, "Implementation and Validation of a Five-Level STATCOM Model in the RTDS Small Time-Step Environment," *Power & Energy Society General Meeting, PES '09. IEEE*, 2009.
- [10] Real Time Digital Simulator , "Power System Users Manual," *RTDS Technologies, November , pp. 1.5-1.7, 2006*.
- [11] S. Hui, C. Christopoulos, "A Discrete Approach to the Modeling of Power Electronic Switching Networks," *IEEE Transaction on Power Electronics*, vol. 5, pp. 398-403, Oct.,

1990.

- [12] T. Maguire and J. Giesbrecht, "Small timestep ($<2 \mu\text{s}$) VSC Model for the Real Time Digital Simulator," in *International Conference on Power System Transients (IPST'05)*, Montreal, Canada, June 19-23, 2005.
- [13] K. L. Lian, P. W. Lehn, "Real-Time Simulation of Voltage Source Converters Based on Time Average Method," *IEEE Transactions on Power Systems*, vol. 20, no. 1, pp. 110-118, FEB 2005.
- [14] Kazuhiro Kobayashi, Masuo Goto, Kai Wu, Yasunobu Yokomizu, Toshiro Matsumura, "Power System Stability Improvement by Energy Storage Type STATCOM," in *PowerTech Conf.*, Bologna, Italy, JUN 2003.
- [15] Dwivedi, Ashutosh, "Flexible AC Transmission System," *International Journal of Electrical and Electronics Engineering (IJEEE)*, vol. 1, no. 2, pp. 1-10, Nov 2012.
- [16] K. Kobayashi, M. Goto, T. Matsukawa, Y. Yokomizu, and T. Matsumura, "Transient and Dynamic Stability Enhancement by Employing Energy Storage Type STATCOM," in *European Power and Energy Systems*, Marbella, Spain, September 3 – 5, 2003.
- [17] Liu W, Venayagamoorthy GK, Wunsch DC, "A Heuristic Dynamic Programming Based Power System Stabilizer for Turbo Generator in a Single Machine Power System," *IEEE Transactions on Industry Applications*, vol. 41, no. 5, pp. 1377-1385 , Sept.-Oct. 2005.
- [18] M. Osman, "An overview of fuzzy logic based power system stabilizers," in *38th North American Power Symposium*, Sep. 2006.
- [19] G. P. Chen, O. P. Malik, G. S. Hope, Y. H. Qin, and G. Y. Xu, "An adaptive power system stabilizer based on the self-optimizing pole shifting control strategy," *IEEE Transactions on Energy Conversion*, vol. 8, no. 4, pp. 639-645, Dec. 1993.
- [20] B. Pal, B. Chaudhuri, *Robust Control in Power Systems*, New York: Springer Science and Business Media Inc., 2005.
- [21] S. Cui, Y. Takagi, H. Ukai, H. Kando, K. Nakamura, and H. Fujita, "Design of Power System Stabilizer Based on Robust Gain Scheduling Control Theory," in *International Conference on Power System Technology*, Perth, WA, Australia, APR 2000.
- [22] Y. L. Abdel-Magid, M. A. Abido, "Optimal Multiobjective Design of Robust Power System Stabilizers using Genetic Algorithms," *IEEE Transactions on Power Systems*, vol. 18, no. 3, pp. 1125-1132, AUG 2003.

- [23] M. A. Abido, Y. L. Abdel-Magid, "Optimal Design of Power System Stabilizers using Evolutionary Programming," *IEEE Transactions on Energy Conversion*, vol. 17, no. 4, pp. 429-436, DEC 2002.
- [24] M. A. Abido, "Robust Design of Multi-Machine Power System Stabilizers using Simulated Annealing," *IEEE Transaction on Energy Conversion*, vol. 15, no. 3, pp. 297-304, 2000.
- [25] M. A. Abido, "Optimal Design of Power-System Stabilizers using ParticleSwarm Optimization," *IEEE Transaction on Energy Conversion*, vol. 17, no. 3, pp. 406-413, SEP 2002.
- [26] Z. Jiang, "Design of Power System Stabilizers using Synergetic Control Theory," in *IEEE Power Engineering Society General Meeting*, Tampa, FL, USA, JUN 2007.
- [27] P. Kundur, M. Klein, G. J. Rogers, and M. S. Zywno, "Application of Power SystemStabilizers for Enhancement of Overall System Stability," *IEEE Trans. PWRs*, vol. 4, no. 2, pp. 614-626, MAY 1989.
- [28] M. J. Gibbard, "Robust Design of Fixed-Parameter Power System Stabilizers over a Wide Range of Operating Conditions," *IEEE Trans. PWRs*, vol. 6, no. 2, pp. 794-800, 1991.
- [29] Y. L. Abdel-Magid, M. A. Abido, S. Al-Baiyat, and A. H. Mantawy, "Simultaneous Stabilization of Multimachine Power Systems Via Genetic Algorithms," *IEEE Trans. PWRs*, vol. 14, no. 4, pp. 1428-1439, 1999.
- [30] deMello, C. Concordia, "Concepts of Synchronous Machine Stability as Affected by Excitation Control," *IEEE Trans. PAS*, vol. 88, pp. 316-329, 1969.
- [31] M. Klein, G. J. Rogers, P. Kundur, "A Fundamental Study of Inter-Area Oscillations in Power Systems," *IEEE Transactions on Power Systems*, vol. 6, no. 3, pp. 914 -921, AUG 1991.
- [32] M. Klein, G.J. Rogers, S. Moorthy, P. Kundur, "Analytical Investigation of Factors Influencing Power System Stabilizers Performance," *IEEE Transactions on Energy Conversion*, vol. 7, no. 3, pp. 382-390, SEP 1992.
- [33] G. T. Tse, S. K. Tso, "Refinement of Conventional PSS Design in Multimachine System by Modal Analysis," *IEEE Trans. PWRs*, vol. 8, no. 2, pp. 598-605, 1993.
- [34] Y.Y. Hsu, C.Y. Hsu, "Design of a Proportional-Integral Power System Stabilizer," *IEEE Trans. PWRs*, vol. 1, no. 2, pp. 46-53, 1986.

- [35] Y.Y. Hsu, K.L. Liou, "Design of Self-Tuning PID Power System Stabilizers for Synchronous Generators," *IEEE Trans. on Energy Conversion*, vol. 2, no. 3, pp. 343-348, 1987.
- [36] A. H. M. A. Rahim, S. G. A. Nassimi, "Synchronous Generator Damping Enhancement through Coordinated Control of Exciter and SVC," *IEE Proc. Genet. Transm. Distrib.*, vol. 143, no. 2, p. 211–218, 1996.
- [37] N. G. Hingorani, L. Gyugyi, *Understanding FACTS: Concepts and Technology of Flexible AC Transmission Systems*, New York: IEEE Press, 2000.
- [38] Hingorani, N. G., "FACTS-Flexible AC Transmission System," in *5th International Conference on AC and DC Power Transmission*, London, U.K., 1991.
- [39] Hingorani, N. G., "High Power Electronics and Flexible AC Transmission System," *IEEE Power Engineering Review*, JUL 1988.
- [40] Edris, A., "Proposed Terms and Definitions for Flexible AC Transmission System (FACTS)," *IEEE Trans Power Delivery*, vol. 12, no. 4, p. 1848–1852, 1997.
- [41] Q. Yu, P. Li, W. Liu, and X. Xie, "Overview of STATCOM technologies," in *the 2004 IEEE International Conference on Electric Utility Deregulation, Restructuring and Power Technologies*, 2004.
- [42] L. Gyugyi, "Dynamic compensation of AC transmission lines by solid-state synchronous voltage sources," *IEEE Transactions on Power Delivery*, vol. 9, no. 2, pp. 904-911, APR 1994.
- [43] T. An, M. T. Powell, H L Thanawala and N Jenkins, "Assessment of Two Different STATCOM Configurations for FACTS Application in Power Systems," in *International Conference on Power System Technology*, Beijing, China, AUG 1998.
- [44] I. A. Hamzah and J. A. Yasin, "Static var compensators (SVC) required to solve the problem of delayed voltage recovery following faults in the power system of the Saudi electricity company, western region (SEC-WR)," in *IEEE Bologna Power Tech Conference Proc*, Bologna, Italy, JUN 2003.
- [45] N. Mithulananthan, C. A. Cañizares, and J. Reeve , "Tuning, Performance and Interactions of PSS and FACTS Controllers," in *The 2002 IEEE-PES Summer Meeting*, Chicago, USA, JUL 2002.
- [46] A. Q. Huang, "4.5MVA ETO STATCOM: design and field demonstrations," in

- [47] N. G. Hingorani, "Flexible AC Transmission," *IEEE Spectrum*, p. 40–45, APR 1993.
- [48] A. E. Hammad, "Analysis of Power System Stability Enhancement by Static VAR Compensators," *IEEE Trans. PWRs*, vol. 1, no. 4, p. 222–227, 1986.
- [49] K. R. Padiyar and R. K. Varma, "Damping Torque Analysis of Static VAR System Oscillations," *IEEE Trans. PWRs*, vol. 6, no. 2, p. 458–465, 1991.
- [50] H. F. Wang, F. J. Swift, "Capability of the Static VAR Compensator in Damping Power System Oscillations," *IEE Proc. Genet. Transm. Distrib.*, vol. 143, no. 4, p. 353–358, 1996.
- [51] A. R. Messina, O. Begovich, M. Nayebzadeh, "Analytical Investigation of the Use of Static VAR Compensators to Aid Damping of Interarea Oscillations," *Electric Power Systems Research*, vol. 51, p. 199–210, 1999.
- [52] P. K. Dash, P. C. Panda, A. M. Sharaf, and E. F. Hill, "Adaptive Controller for Static Reactive Power Compensators in Power Systems," *IEE Proc. Part-C*, vol. 134, no. 3, p. 256–264, 1987.
- [53] M. Parniani, M. R. Iravani, "Optimal Robust Control Design of Static VAR Compensators," *IEE Proc. Genet. Transm. Distrib.*, vol. 145, no. 3, p. 301–307, 1998.
- [54] P. S. Rao, I. Sen, "A QFT-Based Robust SVC Controller for Improving the Dynamic Stability of Power Systems," *Electric Power Systems Research*, vol. 46, p. 213–219, 1998.
- [55] P. K. Dash, A. M. Sharaf, E. F. Hill, "An Adaptive Stabilizer for Thyristor Controlled Static VAR Compensators for Power Systems," *IEEE Trans. PWRs*, vol. 4, no. 2, p. 403–410, 1989.
- [56] M. Vidyasagar, H. Kimura, "Robust Controllers for Uncertain Linear Multivariable Systems," *Automatica*, vol. 22, no. 1, p. 85–94, 1986.
- [57] H. Kwakernaak, "Robust Control and H_∞ Optimization-Tutorial," *Automatica*, vol. 29, no. 2, p. 255–273, 1993.
- [58] P. Ju, E. Handschin, F. Reyer, "Genetic Algorithm Aided Controller Design with Application to SVC," *IEE Proc. Genet. Transm. Distrib.*, vol. 143, no. 3, p. 258–262, 1996.

- [59] G. El-Saady, M. Z. El-Sadek, M. Abo-El-Saud, "Fuzzy Adaptive Model Reference Approach-Based Power System Static VAR Stabilizer," *Electric Power Systems Research*, vol. 45, no. 1, p. 1–11, 1998.
- [60] C. S. Chang, Y. Qizhi, "Fuzzy Bang–Bang Control of Static VAR Compensators for Damping System-Wide Low-Frequency Oscillations," *Electric Power Systems Research*, vol. 49, p. 45–54, 1999.
- [61] Qun Gu, A. Pandey, S. K. Starrett, "Fuzzy Logic Control for SVC Compensator to Control System Damping Using Global Signal," *Electric Power Systems Research*, vol. 67, no. 1, p. 115–122, 2003.
- [62] K. L. Lo, M. O. Sadegh, "Systematic Method for the Design of a Full-scale Fuzzy PID Controller for SVC to Control Power System Stability," *IEE Proc. Genet. Transm. Distrib.*, vol. 150, no. 3, p. 297–304, 2003.
- [63] J. Lu, M. H. Nehrir, D. A. Pierre, "A Fuzzy Logic-Based Adaptive Damping Controller for Static VAR Compensator," *Electric Power Systems Research*, vol. 68, no. 1, p. 113–118, 2004.
- [64] A. R. Messina and E. Barocio, "Nonlinear Analysis of Interarea Oscillations: Effect of SVC Voltage Support," *Electric Power Systems Research*, vol. 64, no. 1, p. 17–26, 2003.
- [65] H. F. Wang, F. J. Swift, "A Unified Model for the Analysis of FACTS Devices in Damping Power System Oscillations Part I: Single-machine Infinite-bus Power Systems," *IEEE Trans. PWRD*, vol. 12, no. 2, pp. 941–946, 1997.
- [66] M. A. Abido, Y. L. Abdel-Magid, "Power System Stability Enhancement via coordinated design of PSS and FACTS-Based stabilizers," *Final Report of a Project Funded by FKUPM*, MAY 2002.
- [67] M. A. Abido, Y. L. Abdel-Magid, "Analysis and Design of Power System Stabilizers and FACTS Based Stabilizers Using Genetic Algorithms," in *Power System Computation Conference PSCC-2002*, Spain, JUN 2002.
- [68] X. Chen, N. Pahalawaththa, U. Annakkage, C. Kumble, "Controlled Series Compensation for Improving the Stability of Multimachine Power Systems," *IEE Proc*, vol. 142, pp. 361–366, 1995.
- [69] J. Chang, J. Chow, "Time Optimal Series Capacitor Control for Damping Inter-Area Modes in Interconnected Power Systems," *IEEE Trans. PWRD*, vol. 12, no. 1, pp. 215–221,

1997.

- [70] T. Lie, G. Shrestha, A. Ghosh, "Design and Application Of Fuzzy Logic Control Scheme For Transient Stability Enhancement In Power System," *Electric Power System Research*, pp. 17-23, 1995.
- [71] Y. Wang, Y. Tan, G. Guo, "Robust nonlinear coordinated excitation and TCSC control for power system," *IEE Proc – Gener. Trtans. Distrib.*, vol. 149, no. 3, pp. 367-372, MAY 2002.
- [72] M. A. Abido, "Genetic-based TCSC damping controller design for power system stability enhancement," in *PowerTech Budapest 99. International Conference*, Budapest, Hungary, 29 Aug.-2 Sept. 1999.
- [73] M. A. Abido, "Pole placement technique for PSS and TCSC-based stabilizer design using simulated annealing," *Electric Power System Research*, vol. 22, pp. 543-554, 2000.
- [74] Y. Wang, R. Mohler, R. Spee, W. Mittelstadt, "Variable Structure FACTS Controllers for Power System Transient Stability," *IEEE Trans. PWRS*, vol. 7, pp. 307-313, 1992.
- [75] V. Rajkumar, R. Mohler, "Bilinear Generalized Predictive Control using the Thyristor Controlled Series Capacitor," *IEEE Trans. PWRS*, vol. 9, no. 4, pp. 1987-1993, 1994.
- [76] Q. Zhao and J. Jiang, "A TCSC Damping Controller Using Robust Control Theory," *Int. J. of Electrical Power & Energy Systems*, vol. 20, no. 1, pp. 25-33, 1998.
- [77] X. Zhou and J. Liang, "Nonlinear adaptive control of TCSC to improve the performance of power systems," *IEEE Proc – Gener. Trtans. Distrib.*, vol. 146, no. 3, pp. 301-305, 1999.
- [78] R. Baker, G. Guth, W. Egli, O. Eglin, "Control Algorithm for a Static Phase Shifting Transformer to Enhance Transient and Dynamic Stability of Large Power Systems," *IEEE Trans. PAS*, vol. 101, no. 9, pp. 3532-3542, 1982.
- [79] A. Edris, "Enhancement of First-Swing Stability Using a High-Speed Phase Shifter," *IEEE Trans. PWRS*, vol. 6, no. 3, pp. 1113-1118, 1991.
- [80] F. Jiang, S. S. Choi, G. Shrestha, "Power System Stability Enhancement Using Static Phase Shifter," *IEEE Trans. PWRS*, vol. 12, no. 1, pp. 207-214, 1997.
- [81] Y. L. Tan, Y. Wang, "Nonlinear Excitation and Phase Shifter Controller for Transient Stability Enhancement of Power Systems Using Adaptive Control Law," *Int. J. Electrical Power & Energy Systems*, vol. 18, no. 6, pp. 397-403, 1996.

- [82] E. Z. Zhou, "Application of Static VAR Compensators to Increase Power System Damping," *IEEE Trans. PWRs*, vol. 8, no. 2, pp. 655-661, 1993.
- [83] S. Lee, C. C. Liu, "An output feedback static VAR controller for the damping of generator oscillations," *Electric Power System Research*, vol. 29, pp. 9-16, 1994.
- [84] Li Wang, Ming-Hsin Tsai, "Design of a H_{∞} static VAR controller for the damping of generator oscillations," in *POWERCON*, Beijing, China, AUG 1998.
- [85] M. Noroozian, M. Ghandhari, G. Andersson, J. Gronquist, I. Hiskens, "A Robust Control Strategy for Shunt and Series Reactive Compensators to Damp Electromechanical Oscillations," *IEEE Trans. On Power Delivery*, vol. 16, no. 4, pp. 812-817, OCT 2001.
- [86] M. Noroozian and G. Andersson, "Damping of Inter-Area and Local Modes by use Controllable Components," *IEEE Trans. On Power Delivery*, vol. 10, no. 4, pp. 2007-2012, OCT 1995.
- [87] M. Noroozian, G. Andersson, "Damping of Power System Oscillations by use of Controllable Components," *IEEE Trans. On Power Delivery*, vol. 9, no. 4, pp. 2046-2054, OCT 1994.
- [88] T. Luor, Y. Hsu, "Design of an Output Feedback Variable Structure Thyristor Controlled Series Compensator for Improving Power System Stability," *Electric Power Systems Research*, vol. 47, p. 71-77, 1998.
- [89] X. Dai, J. Liu, Y. Tang, N. Li, and H. Chen, "Neural Network α th-Order Inverse Control of Thyristor Controlled Series Compensator," *Electric Power Systems Research*, vol. 45, p. 19-27, 1998.
- [90] T. Senjyu, S. Yamane, Y. Morishima, K. Uezato, H. Fujita, "Improvement of Multimachine Power System Stability with Variable Series Capacitor Using On-Line Learning Neural Network," *Int. J. Electrical Power & Energy Systems*, vol. 25, no. 3, p. 403-409, 2003.
- [91] S. C. Lee and S. Moon, "Hybrid Linearization of a Power System with FACTS Devices for a Small Signal Stability Study: Concept and Application," *Electric Power Systems Research*, vol. 64, no. 1, p. 27-34, 2003.
- [92] Sidhartha Panda, N.P.Padhy, R.N.Patel, "Genetically Optimized TCSC Controller for Transient Stability Improvement," *International Journal of Computer, Information, Systems Science, and Engineering*, 2007.

- [93] R. M. Mathur, R. S. Basati, "A Thyristor Controlled Static Phase Shifter for AC Power Transmission," *IEEE Trans. PAS*, vol. 100, no. 5, p. 2650–2655, 1981.
- [94] M. Iravani, D. Maratukulam, "Review of Semiconductor-Controlled (Static) Phase Shifters for Power System Applications," *IEEE Trans. PWRD*, vol. 9, no. 4, p. 1833–1839, 1994.
- [95] Gyugyi L., "Solid-State Control of AC Power Transmission," in *International Symposium on Electric Energy Conversion in Power Systems*, Capri, Italy, 1989.
- [96] Schauder C., Gernhardt M., Stacey E., Lemak T., Gyugyi L., Cease T. W., Edris A., "Operation of ± 100 MVar TVA STATCON," *IEEE Transactions on Power Delivery*, vol. 12, no. 4, p. 1805–1811, OCT 1997.
- [97] Sen K.K., "STATCOM-STATIC Synchronous COMPensator: Theory, Modeling, and Applications," in *31 Jan-4 Feb 1999*, New York, USA, IEEE Power Engineering Society - Winter Meeting.
- [98] Wang H.F., "Phillips-Heffron Model of Power Systems Installed with STATCOM and Applications," *IEE Proceeding on Generation, Transmission and Distribution*, vol. 146, no. 5, pp. 521- 527, SEP 1999.
- [99] Wang H.F., "Application of Damping Torque Analysis to STATCOM Control," *International Journal of Electrical Power and Energy Systems*, vol. 22, no. 3, pp. 197-204, MAR 2000.
- [100] Padiyar K.R., Swayam Prakash V., "Tuning and Performance evaluation of damping controller for a STATCOM," *International Journal of Electrical Power and Energy Systems*, vol. 25, no. 2, pp. 155-166, FEB 2003.
- [101] Wang H.F., "Interaction and multivariable design of STATCOM AC and DC voltage control," *International Journal of Electrical Power and Energy Systems*, vol. 25, no. 3, pp. 387-394, MAR 2003.
- [102] Xue C., Zhang X.P, Godfrey K. R., "Design of STATCOM Damping Control with Multiple Operating Points: A Multimodal LM I Approach," *IEE Proceeding on Generation, Transmission and Distribution*, vol. 153, no. 4, pp. 375-382, JUL 2006.
- [103] Fang D.Z., Yuan S.Q., Wang. Y.J., Chung, T.S., , "Coordinated Parameter Design of STATCOM Stabilizer and PSS using MSSA Algorithm," *IEE Proceeding on Generation, Transmission and Distribution*, vol. 1, no. 4, pp. 670-678, JUL 2007.
- [104] Mohagheghi S., Venayagamoorthy G., Harley R., "Optimal Neurofuzzy External

- Controller for a STATCOM in the 12-bus Benchmark Power System," *IEEE Transaction on Power Delivery*, vol. 22, no. 4, pp. 2548-2557, OCT 2007.
- [105] Panda S., Narayana P., "Optimal Location and Controller Design of STATCOM for Power System Stability Improvement using PSO," *Journal of the Franklin Institute*, vol. 345, no. 2, pp. 166-181, MAR 2008.
- [106] L. O. Mak, Y. N., "Design of Fuzzy Logic Supplementary Controller for STATCOM using Polar Coordinate Variables," in *The IEEE Region 10 Conference*, Cheju Island, South Korea, SEP 1999.
- [107] F. F. Syed, A. H. M. A. Rahim, J. M. Ba-Khashwain, "Robust STATCOM Controller Design using PSO Based Automatic Loop-Shaping Procedure," in *2005 IEEE Conference on Control Applications*, AUG 2005.
- [108] K. K. Sen, "SSSC-Static Synchronous Series Compensator: Theory, Modeling, and Application," *IEEE Transactions on Power Delivery*, vol. 13, no. 1, pp. 241-246, JUN 1998.
- [109] L. Gyugyi, C. D. Schauder, S. L. Williams, T. R. Rietman, D. R. Torgerson, A. Edris, "The Unified Power Flow Controller: A New Approach to Power Transmission Control," *IEEE Transactions on Power Delivery*, vol. 10, no. 2, pp. 1085-1097, APR 1995.
- [110] H. Wang, "A Unified Model for the Analysis of FACTS Devices in Damping Power System Oscillations," *IEEE Transactions on Power Delivery*, vol. 15, no. 3, pp. 978-983, JUL 2000.
- [111] Chang C.T., Hsu Y.Y., "Design of UPFC Controllers and Supplementary Damping Controller for Power Transmission Control and Stability Enhancement of a Longitudinal Power System," *IEE Proc. Gener. Transm. Distrib.*, vol. 149, p. 463 – 471, 2002.
- [112] Tambey, N., Kothari, M.L., "UPFC Based Damping Controllers for Damping Low Frequency Oscillations in a Power System," *Journal of the Institution of Engineers (India) IE(I)journal-EL*, vol. 84, pp. 35-41, 2003.
- [113] Jyh Shing, Roger Jang, "ANFIS: Adaptive-Network-Based Fuzzy Inference System," *IEEE Trans. Syst. Man and Cyber*, vol. 23, no. 3, pp. 665-685, 1993.
- [114] E.V. Larsen, Juan.J. Sanchez Gasca, Chow.J.H., "Concept for Design of FACTS Controllers to Damp Power Swings," *IEEE Transactions PWRS*, vol. 10, no. 2, pp. 948-956, 1995.

- [115] Wang, H.F., "Damping Function of Unified Power Flow Controller," *IEE Proc. Gener. Transm. Distrib.*, vol. 146, no. 1, pp. 81 - 87, 1999.
- [116] Fawzi A. Rahman AL Jowder ', "Analysis of Damping Torque and Synchronizing Torque Contributed by STATCOM Considering Two Different Damping Schemes," *International Journal of Emerging Electric Power Systems*, vol. 12, no. 2, p. 1–21, APR 2011.
- [117] A. S. P.Kanojia, B. Dr.V.K.Chandrakar , "Damping of Power System Oscillations by using Coordinated Tuning of POD and PSS with STATCOM," *World Academy of Science, Engineering and Technology*, 2009.
- [118] Hung-Chi Tsai, Chia-Chi Chu, "Nonlinear STATCOM Controller using Passivity-Based Sliding Mode Control," *APCCAS 2006. IEEE Asia Pacific Conference*, p. 1996–1999, Singapore, DEC 2006.
- [119] A. Yazdani, M.L. Crow, J. Guo, , "A comparison of linear and nonlinear STATCOM control for power quality enhancement," *IEEE Power and Energy Society General Meeting - Conversion and Delivery of Electrical Energy in the 21st Century*, pp. 1-6, Pittsburgh, Pennsylvania, USA, JUL 2008.
- [120] Schauder, C. Mehta, H. , "Vector analysis and control of advanced static VAr compensators," *IEE Proceedings on Generation, Transmission and Distribution*, vol. 140, no. 4, pp. 299-306, JUL 1993.
- [121] Soto, D.; Pena, R., "Nonlinear control strategies for cascaded multilevel STATCOMs," *IEEE Transaction on Power Electronics*, vol. 19, no. 4, pp. 1919-1927, OCT 2004.
- [122] P. Petitclair, S. Bacha, and J. P. Rognon, "Averaged modeling and nonlinear control of an ASVC (advanced static VAr compensator)," *IEEE/PESC'96 Annu.. Meeting*, pp. 753-758, JUN 1996.
- [123] Petitclair, P. Bacha, S. Ferrieux, J.-P. , "Optimized linearization via feedback control law for a STATCOM," *IEEE Industry Applications Conference*, vol. 2, pp. 880 - 885, OCT 1997.
- [124] Zhichang Yuan; Qiang Song; Wenhua Liu; Qingguang Yu , "Nonlinear Controller for Cascade H-Bridge Inverter-Based STATCOM," *IEEE Transmission and Distribution Conference*, pp. 1-5, 2005.
- [125] J. E. Slotine, W. Li. , *Applied Nonlinear Control*, New Jersey: Prentice Hall, 1991.
- [126] N.C. Sahoo, B.K. Panigrahi, P.K. Dash and G. Panda, "Application of a multivariable

- feedback linearization scheme for STATCOM control," *Electric Power Syst. Res.*, vol. 62, no. 1, p. 81–91, 2002.
- [127] N. Farokhnia, R. Khoraminia and G.B. Gharehpetian, "Optimization of PI Controller Gains in Nonlinear Controller of STATCOM Using PSO and GA," *International Conference on Renewable Energies and Power Quality (ICREPQ'10)*, Granada, Spain, MAR 2010.
- [128] Goldberg D.E., *Genetic Algorithm in Search, Optimization and Machine Learning*, MA, USA: Addison Wesley, 1989.
- [129] Davis L., *Handbook of Genetic Algorithm*, New York: Van Nostrand, 1991.
- [130] Kennedy J, Eberhart R.C. , "Particle Swarm Optimization," *IEEE International Conference on Neural Networks*, vol. 4, pp. 1942-1948, Perth,Australia, 1995.
- [131] Tripathi P.K, Bandyopadhyay S, Pal S.K., "Multi-Objective Particle Swarm Optimization with time variant inertia and acceleration coefficients," *Information Sciences*, vol. 177, p. 5033–5049, 2007.
- [132] S. Morris, P. K. Dash and K. P. Basu , "A fuzzy variable structure controller for STATCOM," *Electric Power Systems Research*, vol. 65, pp. 23-34, 2003.
- [133] A. H. M. A. Rahim and M. F. Kandlawala, "Robust STATCOM voltage controller design using loop shaping technique," *Electric Power Systems Research*, vol. 68, pp. 61-74, 2004.
- [134] M.A. Abido, "Analysis and assessment of STATCOM-based damping stabilizers for power system stability enhancement," *Electric Power Systems Research*, vol. 73, no. 2, p. 177–185, 2005.
- [135] M. Aliakbar Golkar and M. Zarringhalami, "Coordinated Design of PSS and STATCOM Parameters for Power System Stability Improvement Using Genetic Algorithm," *Iranian Journal of Electrical and Computer Engineering*, vol. 8, no. 2, 2009.
- [136] Kennedy, R. Eberhart, Y. Shi, *Swarm intelligence*, San Francisco: Morgan Kaufmann Publishers, 2001.
- [137] A. Safari, R. Jahani, M. Fazli, H. Shayeghi, H. A. Shayanfar, "Optimal state feedback damping controller for the STATCOM using particle swarm optimization," *International Review of Electrical Engineering(IREE)*, vol. 5, no. 6, pp. 2779-2785, 2010.
- [138] J. Kennedy , "The particle swarm: social adaptation of knowledge," *Int. Conf on Evolutionary and Computation.* , p. 303–308, Indianapolis, USA, 1997.

- [139] R. Poli, J. Kennedy and T. Blackwell, "Particle swarm optimization: An overview, Swarm Intelligent," *IEEE Swarm Intelligence Symposium (SIS)*, vol. 1, pp. 33-57, 2007.
- [140] H. Shayeghi , H.A. Shayanfar, S. Jalilzadeh, A. Safari, "A PSO based unified power flow controller for damping of power system oscillations," *Energy Conversion and Management*, vol. 50, pp. 2583-2592, 2009.
- [141] H. Shayeghi , H.A. Shayanfar, S. Jalilzadeh, A. Safari, "Design of output feedback UPFC controllers for damping of electromechanical oscillations using PSO," *Energy Conversion and Management*, vol. 50, pp. 2554-2561, 2009.
- [142] S. L. Ho, S. Yang, G. Ni, E. W. C. Lo and H. C. Wong, "A particle swarm optimization based method for multiobjective design optimizations," *IEEE Trans on Magnetics*, vol. 41, no. 5, pp. 1756-1759, 2005.
- [143] Amin Safari, Rouzbeh Jahani, Hadi Chahkandi Nejad, "State Feedback Controller Design for a STATCOM using Quantum Particle Swarm Optimization Algorithm," *American Journal of Scientific Research*, no. 30, pp. 76-84, 2011.
- [144] A. M. A. Hamdan, "An Investigation of the Significance of Singular Value Decomposition in Power System Dynamics," *Int. Journal of Electrical Power and Energy Systems*, vol. 21, pp. 417-424, 1999.
- [145] Storn R, Price K, "Differential Evolution – a Simple and Efficient Adaptive Scheme for Global Optimization Over Continuous Spaces," *Technical Report TR*, pp. 95-012, 1996.
- [146] Storn R, Price K , "Minimizing the Real Functions of the ICEC'96 Contest By Differential Evolution," *IEEE International Conference on Evolutionary Computation*, p. 842–844, MAY 1996.
- [147] Storn, R, "On the usage of differential evolution for function optimization," *Fuzzy Information Processing Society, NAFIPS. Biennial Conference of the North American*, pp. 519 - 523, JUN 1996.
- [148] Vesterstrom J., Thomsen R., "A comparative study of differential evolution, particle swarm optimization, and evolutionary algorithms on numerical benchmark problems," *Congress on Evolutionary Computation*, vol. 2, pp. 1980-1987, JUN 2004.
- [149] O. Al-Naseem, R. W. Erickson, P. Carlin, "Prediction of Switching Loss Variation by Averaged Switch Modeling," *15th Applied Power Electronics Conference and Exposition*, vol. 1, pp. 242-248, New Orleans, LA, USA, FEB 2000.

- [150] A. D. Rajapakse, A. M. Gole, P. L. Wilson, "Electromagnetic Transients Simulation Models for Accurate Representation of Switching Losses and Thermal Performance in Power Electronic Systems," *IEEE Trans. On Power Delivery*, vol. 20, no. 1, pp. 319-327, JAN 2005.
- [151] L. Qi, S. Woodruff, M. Steurer, "Study of Power Loss of Small time-step environment Model in RTDS," in *IEEE Power Engineering General Meeting*, Tampa, FL, USA, JUN 2006.
- [152] J. Langston, L. Qi, M. Steurer, M. Sloderbeck, Y. Liu, A. Q. Huang, S. Bhattacharya, W. Litzenberger, L. Anderson, P. Sorensen, A. Sundara, "Dynamic Testing of a Controller for an ETO-Based STATCOM through Hardware-in-the-Loop Simulation," in *IEEE - Power & Energy Society General Meeting (PES '09)*, Calgary, Alberta, Canada, JUL 2009.
- [153] Chang Kang, Xue Feng, Fang Yongjie, Yu Yuehai, "Comparative Simulation of Dynamic Characteristics of Wind Turbine Doubly-Fed Induction Generator Based on RTDS and MATLAB," in *International Conference on Power System Technology*, 2010.
- [154] H. Dommel, "Digital Computer Solution of Electromagnetic Transient in Single and Multiphase Networks," *IEEE Trans. on Power Apparatus and Systems*, vol. 88, no. 4, pp. 388-399, APR 1969.
- [155] G. Rockerfeller, "Fault Protection with Digital Computer," *IEEE Trans. on PAS*, vol. 88, no. 4, pp. 438-461, APR 1969.
- [156] Z. Bo, A. Klimek, Y. Ren, J. He, "Real Time Digital Simulation System for Testing of Integrated Protection Schemes," *Power System Technology and IEEE Power India Conference, POWERCON*, pp. 1-5, 2008.
- [157] Y. Deng, S. Foo, H. Li, "Real Time Simulation of Power Flow Control Strategies for Fuel Cell Vehicle with Energy Storage by Using Real Time Digital Simulator (RTDS)," *IEEE IPEMC*, p. 2323 – 2327, MAY 2009.
- [158] Kuffel R, Giesbrecht J, Maguire T, Wierckx R P, McLaren P, "RTDS – A fully digital power system simulator operating in real time," *IEEE Catalogue No. 95TH8130*, pp. 498-503, 1995.
- [159] "RTDS Hardware Manual," *RTDS Technologies*, JAN 2009.
- [160] M. M. Farsangi, Y. H. Song, W. F. Fang, and X. F. Wang, "Robust FACTS Control Design Using the H_{∞} Loop-Shaping Method," *IEE Proc. Genet. Transm. Distrib.*, vol. 149, no. 3,

p. 352–358, 2002.

- [161] N. Mithulananthan, C. A. Canizares, J. Reeve, G. J. Rogers, "Comparison of PSS, SVC, and STATCOM Controllers for Damping Power System Oscillations," *IEEE Trans. PWRs*, vol. 18, no. 2, p. 786–792, 2003.
- [162] P. K. Dash, S. Mishra, " Damping of Multimodal Power System Oscillations by FACTS Devices Using Non-Linear Takagi–Sugeno Fuzzy Controller," *Int. Journal of Electrical Power and Energy Systems*, vol. 25, p. 481–490, 2003.
- [163] M. M. Farsangi, Y. H. Song, M. Tan, "Multi-Objective Design of Damping Controllers of FACTS Devices via Mixed H_2/H_∞ with Regional Pole Placement," *Int. Journal of Electrical Power and Energy Systems*, vol. 25, p. 339–346, 2003.
- [164] A. R. Messina, J. Arroyo, N. Evaristo, I Catillo , "Damping of Low-frequency Interarea Oscillations Using HVDC Modulation and SVC Voltage Support," *Electric Power Components and Systems*, vol. 31, no. 2, p. 389–402, 2003.
- [165] M. A. Abido, Y. L. Abdel-Magid, "Analysis and Design of Power System Stabilizers and FACTS Based Stabilizers Using Genetic Algorithms," in *The 14th Power System Computation Conference PSCC*, Spain, JUN 2002.
- [166] Ali T. Al-Awami, Y. L. Abdel-Magid, M. A. Abido, "Simultaneous Stabilization of Power Systems Equipped with Unified Power Flow Controller Using Particle Swarm," in *The 15th Power System Computation Conference - PSCC*, Liege, Belgium, AUG 2005.
- [167] R. Nelson, J. Bian, D. Ramey, T. A. Lemak, T. Rietman, J. Hill, "Transient Stability Enhancement with FACTS Controllers," in *IEEE Sixth International Conference AC and DC Transmission*, London, UK, MAY 1996.

LIST OF PUBLICATIONS

- [1] F. S. AL-Ismail, M. A. Abido, “The Impact of STATCOM Based Stabilizers on Power System Stability, Using Intelligent Computational Optimization Approach”, presented at the 2011 IEEE PES Innovative Smart Grid Technologies ISGT, Perth, Australia.
- [2] F. S. AL-Ismail, M. A. Abido, “The Impact of STATCOM Based Stabilizers on Power System Stability Enhancement”, presented at the GCC CIGRE POWER 2012 Conference & Exhibition, 12 – 14 November, 2012, Muscat, Oman.
- [3] F. S. AL-Ismail, M. A. Abido, M. A. Hassan, “RTDS Implementation of STATCOM for Power System Stability Improvement”, presented at the Saudi Arabia Smart Grid 2012 Conference & Exhibition, 08th - 11th December, 2012, Jeddah, Saudi Arabia.

Vitae

Name : Fahad Saleh Mohammad AL-Ismail

Nationality : Saudi

Date of Birth : 5/November/1985

Present Email : fsalismail@kfupm.edu.sa

Permanent Email : fahadalismail@gmail.com

Address : P.O.Box 1949, Dhahran 31261, Saudi Arabia

Telephone Number : +966 3 860 1392

Mobile Phone Number : +966 5059 61318

Academic Background : Received Bachelor of Science (B.S.) degree in Electrical Engineering from King Fahd University of Petroleum & Minerals (KFUPM), Dhahran, Saudi Arabia in 2009